Studies on Crystalline Structure and Morphology of Artificial Celluloses Synthesized by Mutant Endoglucanases as Catalyst in Solution and on Substrate

Itsuko Nakamura

2011

Studies on Crystalline Structure and Morphology of Artificial Celluloses Synthesized by Mutant Endoglucanases as Catalyst in Solution and on Substrate

Itsuko Nakamura

2011

Department of Material Chemistry

Graduate School of Engineering

Kyoto University

CONTENTS

List of Abbreviations

^{1}H HMR	proton nuclear magnetic resonance spectroscopy
ATR	attenuated total reflection
BSA	bovine serum albumin
CBB	coomassie brilliant blue
CD	circular dichroism
CED	cupriethylenediamine
CMC	carboxymethyl cellulose
DCCI	*N*,*N*-dicyclohexylcarbodiimide
DHB	dihydroxybenzoic acid
DIEA	*N*,*N*-diisopropylethylamine
DMAc	*N*,*N*-dimethylacetoamide
DMSO	dimethylsulfoxide
DMF	*N*,*N*-dimethylformamide
DNA	deoxyribonucleic acid
DP	degree of polymerization
EDTA	ethylenediaminetetraacetic acid
EDC	ethylenedichloride
EGII	endoglucanase II
FAB	fast atom bombardment
FE-SEM	field emission scanning electron microscope
FTIR	Fourier transform infrared
GH	glycoside hydrolase
Glc	glucose
GPC	gel-permeation chromatography
HCA	hydrophobic cluster analysis
HEPES	*N*-2-hydroxyethylpiperazine-*N*´-2-ethanesulfonic acid
HOSu	*N*-hydroxysuccinimide
HPLC	high performance liquid chromatography
IDA	iminodiacetic acid

IMAC	immobilized metal affinity chromatography
LB	Langmuir-Blogett
LiCl	lithium chloride
LOI	lateral order index
MALDI-TOF	matrix-assisted laser desorption ionization time of flight
MFα	prepro-α-factor leader region
MS	mass spectroscopy
NHS	*N*-hydroxysuccinimide
NMWL	nominal molecular weight limit
NTA	nitrilotriacetic acid
OBzl	benzyl ester
O^{t}Bu	*tert*-butyl ester
OSu	succinimidyl
PCR	polymerase chain reaction
PEG	polyethylene glycol
RAS	reflection absorption spectroscopy
RNA	ribonucleic acid
SAc	thioacetyl
SAM	self-assembled monolayer
SDS-PAGE	sodium dodecyl sulfate polyacrylamide gel electrophoresis
SPR	surface plasmon resonance
TC	terminal complex
TCI	total crystallinity index
TED	tris(carboxymethyl)etyhlenediamine
TEM	transmission electron microscopy
TFA	trifluoroacetic acid
TLC	thin layer chromatography
TASA	transition-state analogue substrate
UDP	uridine-5´-diphospho
UPR-ICL	5´-upstream region of the isocitrate lyase gene

List of the Measurement Instruments Used in the Present Thesis

^{1}H NMR	Bruker DPX-400 spectrometer
FAB MS	JEOL HA110 spectrometer
MALDI-TOF MS	JEOL JMS-ELITE spectrometer
	Bruker ultraflex III mass spectrometer
FTIR	Perkin-Elmer Spectrum One FTIR spectrometer
	Nicolet 6700 FT-IR spectrometer
CD	JASCO J-600 CD spectropolarimeter
UV	Shimadzu UV-2450PC spectrometer
	Hitachi U-2001 UV/Vis spectrometer
Polarization microscope	Olympus IX70
TEM	JEOL JEM-2000EXII instrument
FE-SEM	JEOL JSM-6700F instrument
SPR	BIACORE X instrument
PCR	Bio Rad Laboratories MyCycler^{TM} Thermal Cycler
DNA sequencer	Applied biosystems 3130XL genetic analyzer
Vacuum evaporation	Osaka vacuum N-KS350 instrument
Ellipsometry	MIZOJIRI DHA-OLX/S autoellipsometer
Auto fine coater	JEOL JFC-1600 iinstrument

General Introduction

Cellulose is the most abundant substance on the earth and a representative polysaccharide consisting of β-1,4-linked D-glucopyranoside (Glc) (Figure 1). Furthermore, cellulose is one of the oldest raw materials for clothing, papers, buildings, foods and so on. Cellulose has been also utilized for functional biomaterials such as membranes, filters and hollow fibers due to the excellent characteristics of biodegradability and biocompatibility. Cellulose is frequently modified at the hydroxy groups of C2, C3 and/or C6 in a Glc unit to produce a variety of cellulose derivatives; cellulose esters like cellulose acetate, cellulose ethers like carboxymethyl cellulose, which are both commercially available. These cellulose derivatives are widely utilized as materials for ink, paint, apparel, plastics, fibers, food products, biomaterials and so on. Thus, cellulose is still increasingly attractive and important materials.

Cellulose has various crystalline forms, cellulose of type I–IV, which are classified according to the orientation of the molecular chains. A cellulose chain has a direction from the reducing end to the non-reducing end (Figure 1). When the molecular chains align in parallel, the crystal structure of cellulose was designated cellulose of type I (cellulose I), which is thermodynamically metastable.[1–3] Almost all of the biologically synthesized cellulose form cellulose I. Cellulose I is further classified into two subtypes, that is, cellulose I_α and I_β.[4,5] The former is biosynthesized by acetobacter and green alga, and the crystal structure is triclinic with a single chain.[6,7] The latter, on the other hand, is monoclinic consisting of two chains, which is synthesized by higher plants.[6,8] Cellulose I_β is thermostable

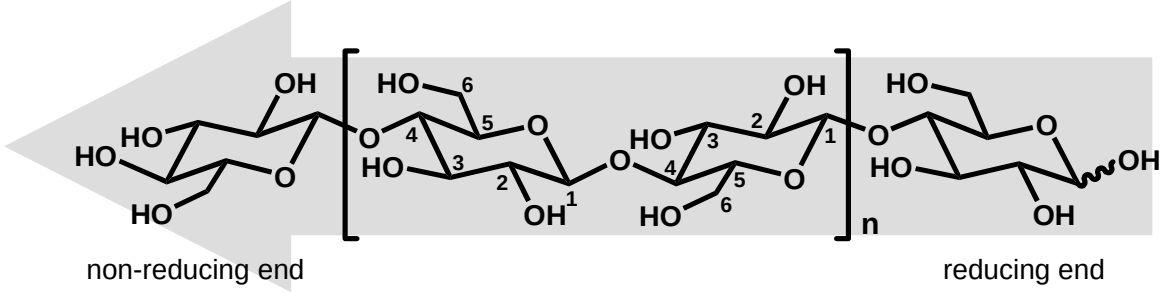

Figure 1. Chemical structure of cellulose.

more than cellulose I_α.[9] The morphology of cellulose I is a fibrous form, and its length and width depend on species derived from. A thermodynamically stable form of the crystal is cellulose of type II (cellulose II), in which the molecular chains are packed in anti-parallel order. Cellulose II is easily produced from cellulose I by two ways. One is the treatment of cellulose I with concentrated alkali solution (mercerization cellulose),[10–12] and the other is the reprecipitation from a solution of cellulose I dissolved in aqueous cuprammonium or cupriethylenediamine (CED) as solvent (regeneration cellulose). Once cellulose I is converted into cellulose II, there are no ways to restore to cellulose I because of large difference about their thermodynamic stabilities. The discriminative morphology of cellulose II is plate-like and lamellar. Cellulose of type III (cellulose III) is prepared by the treatment of cellulose I or II with liquid ammonia, in which the former crystalline form is maintained.[13,14] This structural change is reversible by hot-water treatment and cellulose III. Cellulose of type IV (cellulose IV) is obtained by heating of cellulose I or II at 280 °C in glycerol.[15,16]

Cellulose is produced by plants and microorganisms. Approximately a half amount of organic compounds on the earth is that of cellulose: about several hundred billion tons of cellulose are produced per year. Biosynthesis of cellulose is catalyzed by cellulose synthase (EC 2.4.1.12) utilizing uridine-5'-diphospho (UDP)-Glc as substrate (Figure 2). Normally, cellulose synthases are assembled on plasma membranes in particular forms designated as terminal complexes (TCs).[17,18] TCs on plasma membrane have various types of morphologies such as linear and ring (rosette) forms (Figure 2).[19–21] These TC forms enable production of cellulose I with a broad range in length and width as described above.

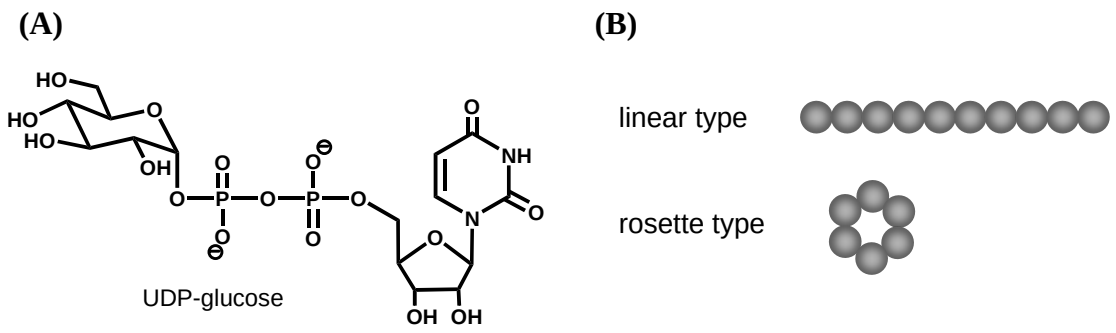

Figure 2. Chemical structure of UDP-glucose (A) and schematic illustration of various TCs (B).

In nature, degradation of cellulose occurs as well as biosynthesis, mainly via hydrolysis by enzymes derived from microorganism such as bacterium and filamentous fungus in soils and in herbivorous animals. Hydrolysis of cellulose proceeds by cooperation with several mechanisms of actions of different kinds of cellulolytic enzymes (cellulases); that is, endo-1,4-β-D-glucanase (EC 3.2.1.4), cellulose 1,4-β-cellobiosidase (EC 3.2.1.91) and β-glucosidase (EC 3.2.1.21) (Figure 3).[22] First, endo-1,4-β-D-glucanase hydrolyzes a 1,4-β-D-glucosidic linkage in a cellulose chain randomly in an amorphous region (endo-type action), resulting in production of Glc, cellobiose [Glcβ(1,4)Glc] and cellooligosaccharides. On the other hand, cellulose 1,4-β-cellobiosidase, which is an exo-type enzyme, hydrolyzes crystalline region of cellulose from the non-reducing end of cellulose to produce cellobiose. Finally, β-glucosidase hydrolyzes cellobiose and cellooligosaccharides, which are produced by the action of endo-1,4-β-D-glucanase and cellulose 1,4-β-cellobiosidase, from the non-reducing end to produce Glc. The characteristic cellulase complex was found in thermophilic anaerobe *Clostridium thermocellum*, named cellulosome.[23–25] This shows significantly high hydrolysis activity against cellulose due to its unique complex structure. Cellulase is also an important catalyst for saccharization of cellulose materials to produce bioethanol.[26]

As mentioned above, enzymes play critical roles in both biosynthesis and biodegradation of cellulose. A huge number of reactions *in vivo* are catalyzed by enzymes. Enzymes enable production of desired products in high efficiency without formation of by-products. As frequently referred to as “the lock-and-key” theory, enzymatic reactions are very specific; the enzyme and the substrate have complementary shapes with each other, leading to the specific reaction. Furthermore, enzymes decrease activation energy of the reactions by stabilizing the transition states, resulting in efficient production under mild reaction conditions.

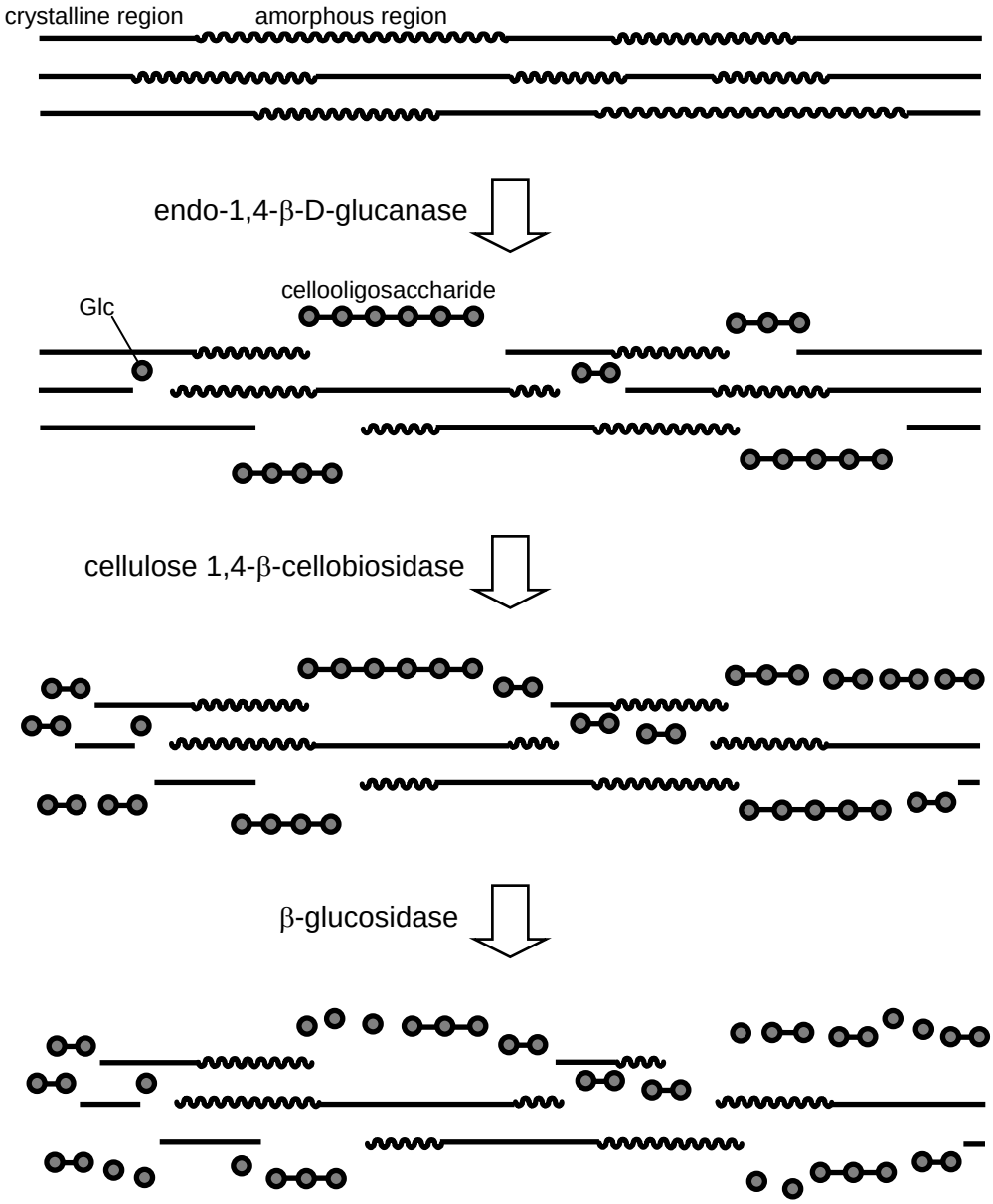

Figure 3. Schematic illustration of hydrolysis of cellulose with cooperation of cellulases.

Because of the highly controlled structures, chemical synthesis of polysaccharides is extremely difficult. Furthermore, as the structural data are not encoded, it is impossible in fact to produce targeted polysaccharides biologically. Thus, the studies on synthesis of polysaccharides are less advanced than that of the other biological polymers: nucleic acids (deoxyribonucleic acid; DNA and ribonucleic acid; RNA) and proteins.

For a long time, *in vitro* synthesis of cellulose had been challenging for a number of synthetic chemists. This was finally achieved in 1991 by "enzymatic polymerization" utilizing cellulase from filamentous fungi *Trichoderma viride* and β-cellobiosyl fluoride as catalyst and substrate, respectively (Figure 4).[27] In addition, chemical synthesis of cellulose by polymerization of tricyclic intramolecular orthoester derivatives as monomers via cationic ring-opening reaction was reported.[28] Polymerization to cellulose in LiCl/DMAc mixed solution was accomplished by using cellulase/surfactant complex and cellobiose as catalyst and substrate, respectively.[29] Cellulose with high degree of polymerization (DP) was formed in this method due to homogenous reaction system; during the polymerization in CH_3CN-buffer mixture, the chain elongation is terminated when insoluble cellulose is formed. It is also possible to synthesize cellulose using non-cellulase enzyme as catalyst.[30] In these reactions, cellulose II is exclusively formed as a product. Chemical synthesis of cellulose I was reported by using partially purified cellulase from *T. viride* as catalyst.[31] However, another study indicated that highly crystalline cellulose II was formed via enzymatic polymerization catalyzed by purified cellulase from *T. viride*.[32]

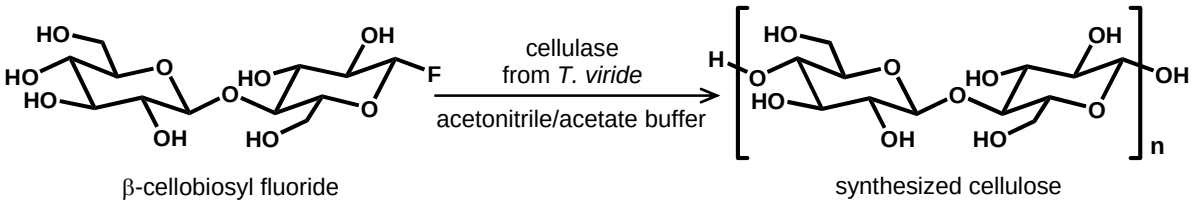

Figure 4. Enzymatic polymerization to cellulose catalyzed by cellulase from *T. viride*.

Here, a definition of "enzymatic polymerization" should be described; that is the *in vitro* polymerization of artificial substrate monomers catalyzed by an isolated enzyme via a nonbiosynthetic (nonmetabolic) pathway. This polymerization is carried out under mild reaction conditions such as ordinary temperature and pressure around neutral pH without using toxic reagents. This method therefore attracts much attention as a "green" chemical process. Enzymatic polymerization using hydrolase as catalyst has overcome difficulties in synthesis of biopolymers. Several kinds of natural-type polysaccharide such as cellulose, amylose,[33] chitin,[34,35] xylan,[36] and hyaluronan[37] are successfully synthesized by this method.

Derivatives of natural polysaccharides such as 6-*O*-methylated cellulose[38] and alternatingly *N*-sulfonated chitin,[39] can also be obtained via enzymatic polymerization of the corresponding artificial monomers.[40] Moreover, unnatural, "hybrid" polysaccharides of cellulose-chitin,[41] cellulose-xylan,[42] chitin-xylan,[43] chitin-chitosan,[44] and glycosaminoglycans were prepared by enzymatic polymerization. It is capable of producing diverse kinds of polysaccharides by using appropriate combinations of designed substrate monomers with hydrolases. Enzymatic polymerization is therefore a useful method to synthesize functionalized polysaccharides, which are potential to be applied as biomaterials and analytical materials.

The most frequently used enzyme as catalyst in enzymatic polymerization to cellulose is cellulase from *T. viride*. Endoglucanase II (EGII), which is included in cellulase from *T. viride*, is actually active for the polymerization;[31] belongs to the glycoside hydrolase family 5 (GH5).[45,46] To date, GHs are classified into 120 families based on the amino acid sequence similarities of enzymes. GH5 is formerly known as cellulose family A, which is categorized by hydrophobic cluster analysis (HCA).[47] In addition to endoglucanases, a lot of xylanases, mannanases, and cellobiohydrolases are also members of GH5. Normally, there are two types of GHs with respect to the anomeric configuration of the product after the hydrolysis reaction: retaining and inverting types. When the anomeric carbon of the product has the same stereochemistry as that of the starting substrate after the enzymatic reaction, the enzyme is classified into a retaining type. On the other hand, if the anomeric carbon has the opposite stereochemistry, the enzyme is an inverting type. EGII is a retaining type enzyme, which is composed of three domains; cellulose-binding domain, a linker region, and a catalytic core domain existing in sequence from *N* terminal. In cellulolysis, cellulose-binding domain first binds to the crystalline part of cellulose and loosens tightly packed cellulose chains, and then the hydrolysis by catalytic core domain occurs. The primary sequence of EGII from *T. viride* has already been determined; however, the three dimensional structure is still unknown.

For kinetically controlled reaction of enzymatic polymerization, it is critical for successful polymerization to design a substrate monomer for an enzyme appropriately in accordance with "transition-state analogue substrate (TSAS) monomer" theory.[34] β-Cellobiosyl fluoride is the TSAS monomer for enzymatic polymerization to cellulose.

Glycosyl fluorides are well-known as useful substrates (glycosyl donors) and inhibitors from early times.[48–50] Advantages of glycosyl fluorides for enzymatic reactions are (i) appropriate lability in their free forms as a good leaving group of fluorine atom, (ii) almost the same atomic size of fluorine atom as that of oxygen of hydroxy group (covalent radii are 0.64 and 0.66 Å, respectively) and (iii) higher stability in aqueous media due to abnormally strong C-F bond compared with those in the other glycosyl halides. Furthermore, β-cellobiose is regarded as the smallest monomer unit of cellulose recognized by cellulase.

Other useful reaction for formation of glycosidic bonds is using "glycosynthases" as catalyst.[49,51–55] Glycosynthases are genetically engineered, new types of enzymes based on GHs, which exclusively catalyze glycosidic bond formation without hydrolysis activity by replacement of the amino acid residue serving as a catalytic nucleophile (Asp or Glu) to a non-nucleophilic amino acid residue such as Ala. The donor substrate employed for glycosynthase is a glycosyl fluoride that mimics the glycosyl-enzyme intermediate during the catalysis of its corresponding wild type enzyme. To date, a variety of glycosynthases have been actively studied to generate saccharide chains. Glycosynthases based on GH5 enzymes such as EGII from *T. viride* have also been prepared.[56,57] Normally glycosynthases are designed on the basis of the catalysis mechanism of retaining-type enzymes. Recently, some glycosynthases were successfully synthesized from inverting-type GHs.[58,59] Future, it is expected that a lot of novel glycosynthases are efficiently developed because the large genomic and structural information of glycosidases will be available.

Genetic engineering technology enables the development of glycosynthases. This is one of the biotechnologies together with cell fusion and cloning technologies, in which the gene is artificially manipulated. Genetic engineering is normally carried out through the processes of separation, alternation, reintroduction, and amplification of the target DNA. This technology has been developed with the discovery of restricted enzymes,[60] DNA ligase,[61] transformation,[62] and polymerase chain reaction (PCR).[63] To multiply obtained recombinants, prokaryotic organism (e.g. *Escherichia coli*) and eukaryotic organism (e.g. yeast) are generally used as host. When eukaryotic organism is used as host in cultivation, a lot of

contaminating products are included compared with those in the case of using prokaryotic organism. Some proteins, however, expressed by prokaryotic organism are known to form inclusion body. It requires appropriate selection of host organisms on case by case. Recently, preparation of tailor-made enzymes, which possess desired properties such as substrate specificity and chemical reactivity, is actively studied by using genetic engineering. This technique enables enzyme to be utilized industrially and medically.

In addition, one of the other useful techniques in genetic engineering is insertion of small tags, which provide simple detection and purification methods without influence on enzyme activity. These are affinity tags, consisting of amino acid residues with particular sequences, introduced genetically on *N* and/or *C* terminal. One of the most useful affinity tags is His-tag, which is composed of sequential 6–10 histidine residues.[64] No further steps to truncate His-tag are required after purification of mutants, therefore it is easy to handle. His-tag displays specific binding affinity to metal ion-chelated supports via formation of strong coordinate bonds with metal ion.[65] The purification method utilizing this affinity binding is designated as the immobilized metal affinity chromatography (IMAC). Metal ion employed in this system is a member of bivalent transition metals such as Ni^{2+}, Co^{2+} and Cu^{2+}. For IMAC of the His-tag system, three major multidentate ligands are known, which are tridentate iminodiacetic acid (IDA),[66] tetradentate nitrilotriacetic acid (NTA),[67-70] and pentadentate tris(carboxymethyl)ethylenediamine (TED).[66,71] It is possible to select from

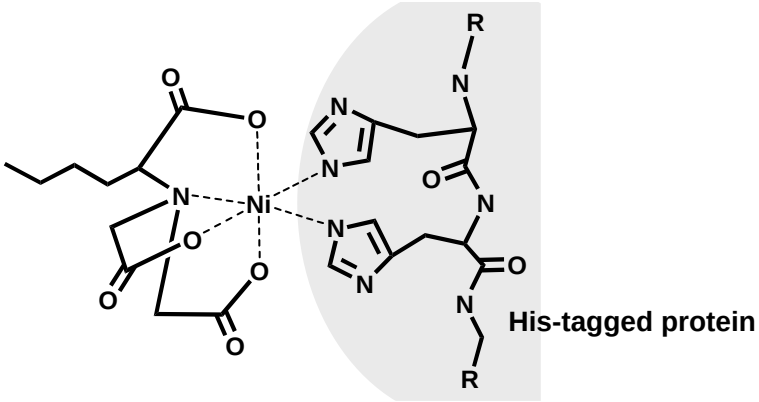

Figure 5. Interaction between His-tagged protein and Ni-chelated NTA.

these ligands in accordance with the intended use. The most frequently used combination of metal ion and a ligand is Ni^{2+} and NTA (Figure 5). Because of this superior purification system, the tagged proteins can be specifically and easily purified from cell lysates.

Recently, affinity tag is further utilized for immobilization of proteins on solid materials.[72–74] Structurally controlled and functionally modified interfaces are possible to be constructed by immobilization and arrangement of functional molecules on solid surfaces such as metals and semiconductors. This helps the mimetic studies of mimetism of vital functions[75–77] and construction of molecular devices being carried with affinity tag for immobilization.[78–80] One of the excellent scaffoldings for immobilization of biomolecules such as DNA, peptides, proteins is a self-assembled monolayer (SAM).[81] Self-assembly technique enables to form highly-oriented and highly-dense molecular layer easily,[82] and is actively applied to studies of the electrochemically functional molecular materials.[83–87] Control of surface properties of a substrate was been attempted by Langmuir-Blogett (LB) technique employing amphiphilic molecules from the first half of the 20th century.[88–90] This technique has the disadvantage of physical adsorption of amphiphiles, which is normally weak interaction. Therefore, instead of LB technique, a novel method employing covalent bond for the immobilization through silyl group to the surface hydroxy groups on solid substrate has been reported.[91] With utilization of interaction between Au and thiol, it was found that the highly oriented monolayer is obtained.[92] Constituent molecules of SAMs, anchor molecules, are generally composed of three parts; anchoring group, alkyl chain linker, and functional terminating group. The anchoring group provides a reactive site to a surface, which connects anchor molecule to the substrate. In the case of Au substrate, thiol, disulfide and sulfide groups are generally used. The alkyl chain linker is an important part, which determines the two-dimensionally ordered structure of the monolayer. Moreover, the properties of alkyl chain linker such as length and hydrophilicity affect physical properties of the SAM. The functionalized terminating group reflects the surface function.

With the background described above, novel three mutant EGIIs are synthesized by genetic engineering procedure. Their hydrolysis and polymerization activities are investigated. Furthermore, reaction behavior of these mutant EGIIs on polymerization to cellulose are also examined. Structural characteristics of cellulose obtained via the polymerization are in depth studied in addition to effect of the assembled structures of the enzymes on the polymerization in the present thesis.

Chapters 1 and 2 show the synthesis of mutant EGIIs by genetic engineering and their hydrolysis and polymerization activities are compared with each other. All mutant enzymes are expressed in yeast because of its advantages as follows: (i) heavy utilization in biochemistry and in protein engineering and (ii) to avoid the situation that the expressed enzyme formed inclusion body, and (iii) no secretion of cellulase from yeast itself.[93–95]

In Chapter 1, cellulose-binding domain deficient mutant EGII with hexameric histidine residues (His-tag) at the *N* terminal, $EGII_{core}$, is synthesized (Figure 6), and polymerization behavior is studied. Full length mutant EGII with His-tag at the *N* terminal is also synthesized and subjected to enzymatic polymerization to cellulose to investigate the effect of cellulose-binding domain on polymerization behavior. The properties of obtained product from $EGII_{core}$ are also analyzed in detail.

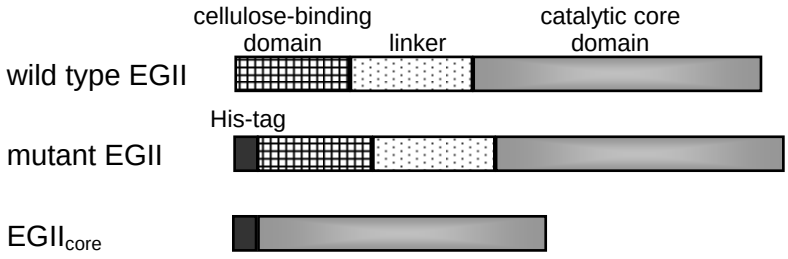

Figure 6. Schematic illustration of wild type EGII, mutant EGII, and $EGII_{core}$ from *T. viride*.

Chapter 2 deals with novel two kinds of mutants, $EGII_{core2}$ and $EGII_{core2H}$; the former has one His-tag at the *N* terminal accompanying two sequential catalytic core domains, and the latter bears two His-tags at the *N* and *C* terminals of sequentially aligned two catalytic core domains, respectively (Figure 7). Their hydrolytic and polymerization activities are compared with those of $EGII_{core}$ in terms of their conformational stabilities. Moreover,

enzymatic polymerization in a quartz optical cell is observed to obtain more information about polymerization behavior.

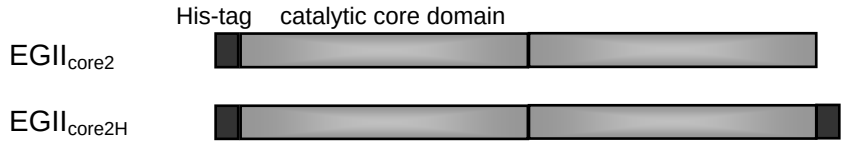

Figure 7. Schematic illustration of EGII$_{core2}$ and EGII$_{core2H}$ from *T. viride*.

Chapters 3, 4 and 5 deal with various immobilizations of EGII$_{core2}$ and EGII$_{core2H}$ utilizing affinity binding between His-tag and Ni-chelated NTA. Enzyme activities and enzymatic polymerization behaviors are investigated using obtained enzyme.

Chapter 3 describes immobilization of mutant EGII$_{core2}$ on NTA-terminated SAM surface (Figure 8). For immobilization, three kinds of anchoring molecules, which constitute of SAM with different length and hydrophilicity of chain are prepared and most suitable anchoring molecule for immobilization is determined by both kinetic and thermocynamic assessment. The hydrolytic activity of EGII$_{core2}$ onto each SAM are investigated and compared with that of free EGII$_{core2}$.

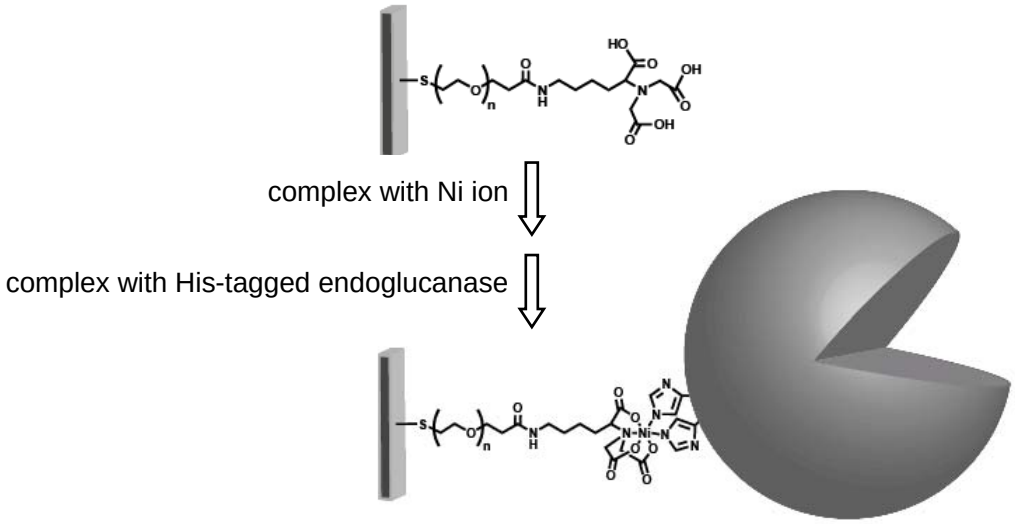

Figure 8. Schematic illustration of immobilization of His-tagged EGII on gold surface via Ni-NTA terminated SAM.

In Chapter 4, enzymatic polymerization catalyzed by immobilized $EGII_{core2}$ or $EGII_{core2H}$ on the solid surface is reported (Figure 9). The highly-ordered structure of the enzymes is similar to that of natural TC existing on the plasma membrane. Firstly, the binding properties of $EGII_{core2H}$ are investaigated. Then, the enzymatic polymerization catalyzed by immobilized $EGII_{core2}$ or $EGII_{core2H}$ is carried out. Characteristics of obtained products are studied in detail and compared to those of synthesized by using free enzyme as catalyst. This is the first study of *in vitro* synthesis of cellulose by utilizing well-ordered enzyme as catalyst.

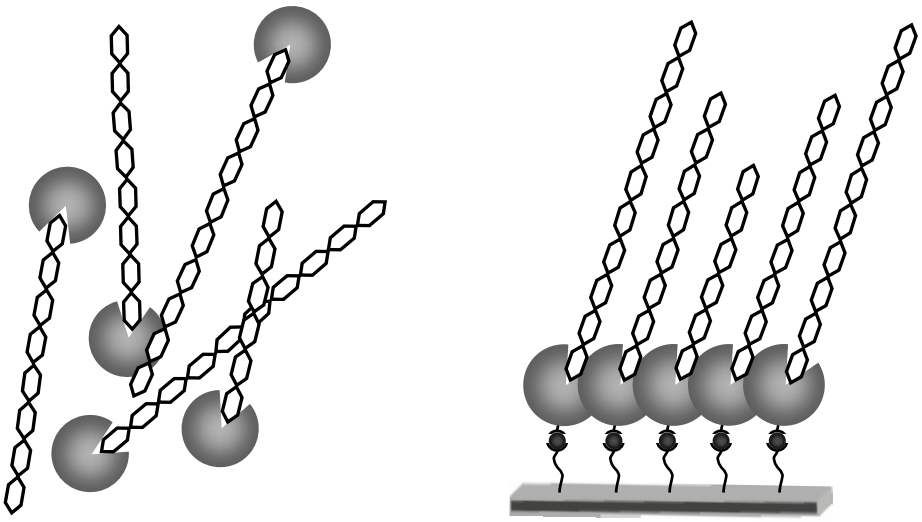

Figure 9. Schematic illustration of enzymatic polymerization using free enzyme (left) and immobilized enzyme on the substrate (right).

Chapter 5 reports the novel two assembled forms of enzyme and its activity for enzymatic polymerization: vertically stacked enzyme layers on the substrate and three-dimensionally cross-linked enzyme assemblies, both of which are constructed through His-tag–Ni-NTA binding (Figure 10). Enzymatic polymerizations catalyzed by these enzyme assemblies are carried out, and the obtained products are investigated in detail. The morphology of the products is expected to be different from that by free enzyme.

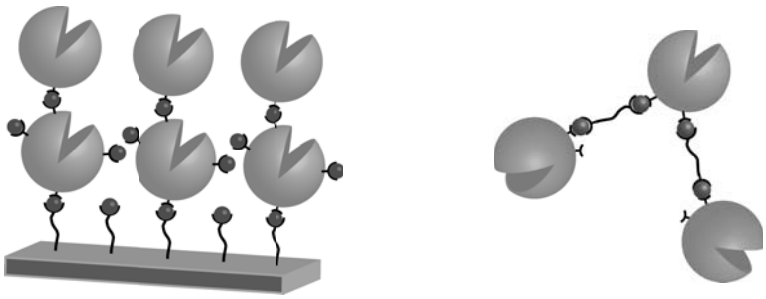

Figure 10. Schematic illustration of stacked enzyme (left) on the substrate and cross-linked enzyme (right) for enzymatic polymerization utilizing affinity between His-tag and Ni-chelated NTA.

As mentioned above, enzymatic polymerizations to cellulose catalyzed by various mutant EGIIs and by their designed assemblies are carried out, and the products from the polymerizations are studied. Reported enzymatic polymerization studies are mainly focused on monomer substrate to create novel polymer products. There are no studies of the effect of three-dimensionally assembled catalyst (enzyme) structures on the polymerization. This thesis first provides investigation of the effect of systematically constructed enzymes on the polymerization to cellulose. This attempt has potential to solve the mechanism of biosynthesis of cellulose. The detailed results are described in the following chapters.

References and Notes

(1) Chanzy, H.; Henrissat, B. *FEBS Lett.* **1985**, *184*, 285–288.

(2) Kuga, S.; Brown, R. M. *Carbohydr. Res.* **1988**, *180*, 345–350.

(3) Koyama, M.; Helbert, W.; Imai, T.; Sugiyama, J.; Henrissat, B. *Proc. Natl. Acad. Sci. U. S. A.* **1997**, *94*, 9091–9095.

(4) Atalla, R. H.; Vanderhart, D. L. *Science* **1984**, *223*, 283–285.

(5) Sugiyama, J.; Persson, J.; Chanzy, H. *Macromolecules* **1991**, *24*, 2461–2466.

(6) Wada, M.; Okano, T.; Sugiyama, J. *Cellulose* **1997**, *4*, 221–232.

(7) Imai, T.; Sugiyama, J.; Itoh, T.; Horii, F. *J. Struct. Biol.* **1999**, *127*, 248–257.

(8) Wada, M.; Sugiyama, J.; Okano, T. *J. Appl. Polym. Sci.* **1993**, *49*, 1491–1496.

(9) Yamamoto, H.; Horii, F.; Odani, H. *Macromolecules* **1989**, *22*, 4130–4132.

(10) Kolpak, F. J.; Weih, M.; Blackwell, J. *Polymer* **1978**, *19*, 123–131.

(11) Okano, T.; Sarko, A. *J. Appl. Polym. Sci.* **1984**, *29*, 4175–4182.

(12) Okano, T.; Sarko, A. *J. Appl. Polym. Sci.* **1985**, *30*, 325–332.

(13) Barry, A. J.; Peterson, F. C.; King, A. J. *J. Am. Chem. Soc.* **1936**, *58*, 333–337.

(14) Hori, R.; Wada, M. *Cellulose* **2006**, *13*, 281–290.

(15) Kulshreshtha, A. K. *J. Text. Inst.* **1979**, *70*, 13–18.

(16) Buleon, A.; Chanzy, H. *J. Polym. Sci. Pt. B-Polym. Phys.* **1980**, *18*, 1209–1217.

(17) Brown, R. M.; Montezinos, D. *Proc. Natl. Acad. Sci. U. S. A.* **1976**, *73*, 143–147.

(18) Brown, R. M.; Willison, J. H. M.; Richardson, C. L. *Proc. Natl. Acad. Sci. U. S. A.* **1976**, *73*, 4565–4569.

(19) Mueller, S. C.; Brown, R. M. *J. Cell Biol.* **1980**, *84*, 315–326.

(20) Itoh, T. *J. Cell Sci.* **1990**, *95*, 309–319.

(21) Kimura, S.; Itoh, T. *Protoplasma* **1996**, *194*, 151–163.

(22) Ryu, D. D. Y.; Kim, C.; Mandels, M. *Biotechnol. Bioeng.* **1984**, *26*, 488–496.

(23) Bayer, E. A.; Setter, E.; Lamed, R. *J. Bacteriol.* **1985**, *163*, 552–559.

(24) Lamed, R.; Bayer, E. A. *Adv. Appl. Microbiol.* **1988**, *33*, 1–46.

(25) Bayer, E. A.; Belaich, J. P.; Shoham, Y.; Lamed, R. *Annu. Rev. Microbiol.* **2004**, *58*, 521–554.

(26) Galbe, M.; Zacchi, G. In *Biofuels*; Springer-Verlag Berlin: Berlin, 2007; Vol. 108, p 41–65.

(27) Kobayashi, S.; Kashiwa, K.; Kawasaki, T.; Shoda, S. *J. Am. Chem. Soc.* **1991**, *113*, 3079–3084.

(28) Nakatsubo, F.; Kamitakahara, H.; Hori, M. *J. Am. Chem. Soc.* **1996**, *118*, 1677–1681.

(29) Egusa, S.; Kitaoka, T.; Goto, M.; Wariishi, H. *Angew. Chem.-Int. Edit.* **2007**, *46*, 2063–2065.

(30) Hiraishi, M.; Igarashi, K.; Kimura, S.; Wada, M.; Kitaoka, M.; Samejima, M. *Carbohydr. Res.* **2009**, *344*, 2468–2473.

(31) Lee, J. H.; Brown, R. M.; Kuga, S.; Shoda, S.; Kobayashi, S. *Proc. Natl. Acad. Sci. U. S. A.* **1994**, *91*, 7425–7429.

(32) Kobayashi, S.; Hobson, L. J.; Sakamoto, J.; Kimura, S.; Sugiyama, J.; Imai, T.; Itoh, T. *Biomacromolecules* **2000**, *1*, 168–173.

(33) Kobayashi, S.; Shimada, J.; Kashiwa, K.; Shoda, S. I. *Macromolecules* **1992**, *25*, 3237–3241.

(34) Kobayashi, S.; Kiyosada, T.; Shoda, S. *J. Am. Chem. Soc.* **1996**, *118*, 13113–13114.

(35) Sato, H.; Mizutani, S.; Tsuge, S.; Ohtani, H.; Aoi, K.; Takasu, A.; Okada, M.; Kobayashi, S.; Kiyosada, T.; Shoda, S. *Anal. Chem.* **1998**, *70*, 7–12.

(36) Kobayashi, S.; Wen, X.; Shoda, S. *Macromolecules* **1996**, *29*, 2698–2700.

(37) Kobayashi, S.; Morii, H.; Itoh, R.; Kimura, S.; Ohmae, M. *J. Am. Chem. Soc.* **2001**, *123*, 11825–11826.

(38) Ochiai, H.; Fujikawa, S.; Ohmae, M.; Kobayashi, S. *Biomacromolecules* **2007**, *8*, 1802–1806.

(39) Makino, A.; Nagashima, H.; Ohmae, M.; Kobayashi, S. *Biomacromolecules* **2007**, *8*, 188–195.

(40) Okamoto, E.; Kiyosada, T.; Shoda, S.; Kobayashi, S. *Cellulose* **1997**, *4*, 161–172.

(41) Kobayashi, S.; Makino, A.; Matsumoto, H.; Kunii, S.; Ohmae, M.; Kiyosada, T.; Makiguchi, K.; Matsumoto, A.; Horie, M.; Shoda, S. I. *Biomacromolecules* **2006**, *7*, 1644–1656.

(42) Fujita, M.; Shoda, S.; Kobayashi, S. *J. Am. Chem. Soc.* **1998**, *120*, 6411–6412.

(43) Kobayashi, S.; Makino, A.; Tachibana, N.; Ohmae, M. *Macromol. Rapid Commun.* **2006**, *27*, 781–786.

(44) Makino, A.; Kurosaki, K.; Ohmae, M.; Kobayashi, S. *Biomacromolecules* **2006**, *7*, 950–957.

(45) Carbohydrate Active Enzymes database. http://www.cazy.org/.

(46) Cantarel, B. L.; Coutinho, P. M.; Rancurel, C.; Bernard, T.; Lombard, V.; Henrissat, B.

Nucleic Acids Research **2009**, *37*, D233–D238.

(47) Henrissat, B.; Claeyssens, M.; Tomme, P.; Lemesle, L.; Mornon, J. P. *Gene* **1989**, *81*, 83–95.

(48) Mukaiyama, T.; Murai, Y.; Shoda, S. *Chem. Lett.* **1981**, 431–432.

(49) Williams, S. J.; Withers, S. G. *Carbohydr. Res.* **2000**, *327*, 27–46.

(50) Toshima, K. *Carbohydr. Res.* **2000**, *327*, 15–26.

(51) Mackenzie, L. F.; Wang, Q. P.; Warren, R. A. J.; Withers, S. G. *J. Am. Chem. Soc.* **1998**, *120*, 5583–5584.

(52) Malet, C.; Planas, A. *FEBS Lett.* **1998**, *440*, 208–212.

(53) Mayer, C.; Zechel, D. L.; Reid, S. P.; Warren, R. A. J.; Withers, S. G. *FEBS Lett.* **2000**, *466*, 40–44.

(54) Williams, S. J.; Withers, S. G. *Australian Journal of Chemistry* **2002**, *55*, 3–12.

(55) Perugino, G.; Trincone, A.; Rossi, M.; Moracci, M. *Trends in Biotechnology* **2004**, *22*, 31–37.

(56) Vaughan, M. D.; Johnson, K.; DeFrees, S.; Tang, X. P.; Warren, R. A. J.; Withers, S. G. *J. Am. Chem. Soc.* **2006**, *128*, 6300–6301.

(57) Tao, H. Y.; Peralta-Yahya, P.; Decatur, J.; Cornish, V. W. *ChemBioChem* **2008**, *9*, 681–684.

(58) Honda, Y.; Kitaoka, M. *J. Biol. Chem.* **2006**, *281*, 1426–1431.

(59) Kitaoka, M.; Honda, Y.; Fushinobu, S.; Hidaka, M.; Katayama, T.; Yamamoto, K. *Trends Glycosci. Glycotechnol.* **2009**, *21*, 23–39.

(60) Roberts, R. J. *Crc Critical Reviews in Biochemistry* **1976**, *4*, 123–164.

(61) Weiss, B.; Richards.Cc *Proc. Natl. Acad. Sci. U. S. A.* **1967**, *57*, 1021–&.

(62) Avery, O. T.; MacLeod, C. M.; McCarty, M. *J. Exp. Med.* **1944**, *79*, 137–158.

(63) Mullis, K.; Faloona, F.; Scharf, S.; Saiki, R.; Horn, G.; Erlich, H. *Cold Spring Harbor Symposia on Quantitative Biology* **1986**, *51*, 263–273.

(64) Knecht, S.; Ricklin, D.; Eberle, A. N.; Ernst, B. *J. Mol. Recognit.* **2009**, *22*, 270–279.

(65) Porath, J.; Carlsson, J.; Olsson, I.; Belfrage, G. *Nature* **1975**, *258*, 598–599.

(66) Sulkowski, E. *Trends in Biotechnology* **1985**, *3*, 1–7.

(67) Hochuli, E.; Dobeli, H.; Schacher, A. *Journal of Chromatography* **1987**, *411*, 177–184.

(68) Hochuli, E.; Bannwarth, W.; Dobeli, H.; Gentz, R.; Stuber, D. *Bio-Technology* **1988**, *6*, 1321–1325.

(69) Gaberc-Porekar, V.; Menart, V. *Chem. Eng. Technol.* **2005**, *28*, 1306–1314.

(70) Hochuli, E. *Genet. Eng.* **1990**, *12*, 87–98.

(71) Porath, J.; Olin, B. *Biochemistry* **1983**, *22*, 1621–1630.

(72) Sigal, G. B.; Bamdad, C.; Barberis, A.; Strominger, J.; Whitesides, G. M. *Anal. Chem.* **1996**, *68*, 490–497.

(73) Nieba, L.; NiebaAxmann, S. E.; Persson, A.; Hamalainen, M.; Edebratt, F.; Hansson, A.; Lidholm, J.; Magnusson, K.; Karlsson, A. F.; Pluckthun, A. *Anal. Biochem.* **1997**, *252*, 217–228.

(74) Kroger, D.; Liley, M.; Schiweck, W.; Skerra, A.; Vogel, H. *Biosens. Bioelectron.* **1999**, *14*, 155–161.

(75) Ko, B. S.; Babcock, B.; Jennings, G. K.; Tilden, S. G.; Peterson, R. R.; Cliffel, D.; Greenbaum, E. *Langmuir* **2004**, *20*, 4033–4038.

(76) Kincaid, H. A.; Niedringhaus, T.; Ciobanu, M.; Cliffel, D. E.; Jennings, G. K. *Langmuir* **2006**, *22*, 8114–8120.

(77) Terasaki, N.; Iwai, M.; Yamamoto, N.; Hiraga, T.; Yamada, S.; Inoue, Y. *Thin Solid Films* **2008**, *516*, 2553–2557.

(78) Choi, J. W.; Nam, Y. S.; Kong, B. S.; Choi, H. G.; Lee, W. H.; Fujihira, M. *Colloids and Surfaces B-Biointerfaces* **2002**, *23*, 263–271.

(79) Bradshaw, J. M.; Kubota, Y.; Meyer, T.; Schulman, H. *Proc. Natl. Acad. Sci. U. S. A.* **2003**, *100*, 10512–10517.

(80) Song, G. T.; Chen, M. L.; Chen, C. E.; Wang, C. Y.; Hu, D.; Ren, J. S.; Qu, X. G. *Biochimie*, *92*, 121–127.

(81) Margel, S.; Vogler, E. A.; Firment, L.; Watt, T.; Haynie, S.; Sogah, D. Y. *J. Biomed. Mater. Res.* **1993**, *27*, 1463–1476.

(82) Ulman, A. *Chem. Rev.* **1996**, *96*, 1533–1554.

(83) Morita, T.; Kimura, S.; Kobayashi, S.; Imanishi, Y. *J. Am. Chem. Soc.* **2000**, *122*,

2850–2859.

(84) Yasutomi, S.; Morita, T.; Imanishi, Y.; Kimura, S. *Science* **2004**, *304*, 1944–1947.

(85) Yasutomi, S.; Morita, T.; Kimura, S. *J. Am. Chem. Soc.* **2005**, *127*, 14564–14565.

(86) Yanagisawa, K.; Morita, T.; Kimura, S. *J. Am. Chem. Soc.* **2004**, *126*, 12780–12781.

(87) Morita, T.; Yanagisawa, K.; Kimura, S. *Polym. J.* **2008**, *40*, 700–709.

(88) Langmuir, I. *J. Chem. Phys.* **1933**, *1*, 756–776.

(89) Blodgett, K. B. *J. Am. Chem. Soc.* **1935**, *57*, 1007–1022.

(90) Blodgett, K. B.; Langmuir, I. *Physical Review* **1937**, *51*, 0964–0982.

(91) Sagiv, J. *J. Am. Chem. Soc.* **1980**, *102*, 92–98.

(92) Nuzzo, R. G.; Allara, D. L. *J. Am. Chem. Soc.* **1983**, *105*, 4481–4483.

(93) Hinnen, A.; Hicks, J. B.; Fink, G. R. *Proc. Natl. Acad. Sci. U. S. A.* **1978**, *75*, 1929–1933.

(94) Ito, H.; Fukuda, Y.; Murata, K.; Kimura, A. *J. Bacteriol.* **1983**, *153*, 163–168.

(95) Gietz, D.; Stjean, A.; Woods, R. A.; Schiestl, R. H. *Nucleic Acids Research* **1992**, *20*, 1425–1425.

Chapter 1

Enzymatic Polymerization Behavior Using

Cellulose-Binding Domain Deficient Endoglucanase II

Introduction

Polysaccharides are naturally occurring polymers and generally environmentally benign. Further, biological activities of polysaccharides are well recognized. Even though polysaccharides are highly valuable materials for our living system, synthetic problem of a specific structure from a diverse range of possible molecular structures constitutes an obstacle to be widely applied. A method to solve the problem is to use enzymes for the polysaccharide preparation because the laborious selective protection steps for the hydroxyl groups by chemical syntheses can be skipped, and the regio- and stereo-chemistry on the glycoside linkage are reliable when enzymes are used.[1,2] *In vivo* polysaccharides are produced by glycosyltransferases, but because they are transmembrane proteins with the problems related to their expression, they are not so exploited *in vitro*. For example, Kobayashi et al. have shown the enzymatic polymerization to yield artificial cellulose,[3] chitin,[4] and hyaluronic acid,[5] etc., where activated disaccharides with free hydroxyl groups are polymerized effectively by using the corresponding hydrolytic glucanases. Notably, the artificial cellulose synthesized by endoglucanase II (EGII) from *T. viride* takes the structure of the highly crystalline cellulose II.[6]

EGII is composed of three functional domains, cellulose-binding domain, linker, and catalytic core domain, which are successively arranged from the *N* terminal.[7] It is supposed that the cellulose-binding domain has an affinity only for crystalline cellulose to help the enzyme access the insoluble substrate. Upon binding of the cellulose-binding domain to crystalline cellulose, molecular packing of cellulose chains will be loosened to accelerate a following cleavage reaction by the catalytic core domain. Notably, the specific binding property of the cellulose-binding domain is used for development of functional materials.[8,9]

Since EGII hydrolyzes the crystalline substrate with the help of the binding property of the cellulose-binding domain,[10,11] deletion of this domain should make the mutant less active to the crystalline cellulose in hydrolysis. The deleted enzyme is therefore attractive for the enzymatic polymerization due to the suppression effect on the hydrolytic degradation of the crystalline product.

The molecular mechanisms for glucanases to hydrolyze the substrates have been intensively studied on the basis of the X-ray structure.[12–14] EGII is considered to follow the double displacement mechanism as endoglucanase I. Interestingly, glycosylase was successfully converted to glycosynthase by replacing Glu at the active site with Ala as a result of abolishment of the hydrolytic activity.[15–18] On the other hand, in the case of the enzymatic polymerization developed by Kobayashi et al., the activated monomer, so-called "the transition-state analog", is used.[4] The activated monomer is bound to the active site to generate an activated glycosyl enzyme intermediate, which rapidly reacts with the glycosyl acceptor. The mechanism for the chain growth is controversial; processive propagation like a chain polymerization or repeating association and dissociation between the chain and the enzyme like a condensation polymerization.[2,19,20] Further, the cellulose-binding domain may be actively involved in the polymerization process. Therefore, the enzymatic polymerization using the cellulose-binding domain deficient mutant should also provide information on the polymerization mechanism.

The mutant full length of EGII and $EGII_{core}$ were expressed in *Saccharomyces cerevisiae* to avoid the formation of inclusion body, which was the preparative problem for the expression in *Escherichia coli*. The proteins secreted by *S. cerevisiae* were purified as a single band in sodium dodecyl sulfate polyacrylamide gel electrophoresis (SDS-PAGE). The polymerization behaviors using these purified enzymes were analyzed.

Experimental section

Materials. Tryptone peptone, bacto yeast extract, bacto peptone, yeast-nitrogen base without amino acids, and casamid acids were purchased from Difco (USA) and used as received. Ampicillin was obtained from Meiji Seika Kaisya, Ltd. (Japan) and used as received. L-Leucine, L-histidine-HCl, adenine sulfate, uracil and glucose were purchased from Wako chemicals (Japan). All other reagents were purchased from commercial sources and used as received.

Strains and culture conditions. *E. coli* DH5α (F^-, *endA1*, *hsdR17*(r_K^-, m_K^-), sup E44, *thi-1*, λ^-, *recA1*, *gryA96*, *φ* 80 d*lac*ZDM15) was used as a host for recombinant DNA manipulations. *E. coli* was grown in LB (Luria-Bertani) medium (1% Tryptone Peptone, 0.5% Bacto Yeast Extract, 0.5% sodium chloride) containing 100 μl/mL ampicillin.

Yeast *S. cerevisiae* MT8-1 (*MATa*, *ade*, *his3*, *leu2*, *trp1*, *ura3*)[21] was used as the host for the protein expression, and was cultivated either in YPD (Yeast-Peptone-D-glucose) medium (1% Bacto Yeast Extract, 2% Bacto Peptone, 2% glucose) or SD−W (synthetic dextrose medium lacking tryptophan) medium (0.003% L-leucine, 0.002% L-histidine-HCl, 0.002% adenine sulfate, 0.002% uracil, 0.67% yeast-nitrogen base without amino acids, 2% glucose) containing 0.004% casamid acids.[22] For SA−W medium, 2% sodium acetate was used as a carbon source.

Construction of plasmid and transformation. The vector plasmid, pWI3+MFα, was constructed as follows. The gene encoding the prepro-α-factor leader region (MFα),[23] which achieves efficient secretion of a target protein, was amplified by the polymerase chain reaction (PCR) using the following primers; 5′-TAAATAGTCGACATGAGATTTCCTTCA-ATTTTTACTGC-3′ (*Sal* I restriction site is underlined) and 5′-GTGATGCTCGAGTCTTC-TTTTATCCAAAGATACCCCTTCTTC-3′ (*Xho* I restriction site is underlined), digested with *Sal* I/*Xho* I, and then inserted into the yeast expression vector pWI3 that has a 5′-upstream region of the isocitrate lyase gene (UPR-ICL) from the alkano-trophic yeast, *Candida tropicalis* as a promoter.[24] This PCR product was digested with *Xho*I for the following construction of pMIEG13.

The plasmid pMIEG13 encoding EGII was constructed as follows. In order to exclude the intron region in the gene encoding the egl2 region of *T. viride* genome, two DNA fragments, egl2A and egl2B, were amplified from *T. viride* genome by PCR with using the primers of 5′-CTGTTGAGTCGACCCCGCCATACACGATGAAC-3′ and 5′-CATGAA-GGTACCATCTGTGGTACATC-3′ (*Kpn* I restriction site is underlined) for 2gl2A and of 5′-ACAGTGGTACCTGCGTTACATCGAAG-3′ (*Kpn* I restriction site is underlined) and 5′-GACAACTCGAGTGCAATCGACCTC-3′ (*Xho* I restriction site is underlined) for egl2B.

The secretory signal in *T. viride* was removed from the DNA fragment encoding egl2A by PCR with using primers of 5′-GGCTCTAGAGCACAACAGAC-3′ (*Xba* I restriction site is underlined) and 5′-CATGAAGGTACCATCTGTGGTACATC-3′ (*Kpn* I restriction site is underlined) to yield egl2C. The DNA fragments, egl2C and egl2B, were digested with *Xba* I/*Kpn* I and *Kpn* I/*Xho* I, respectively, and then inserted into the plasmid pUC19X (EGpUC19X). The plasmid pUC19X possesses the *Xho* I site, which was introduced by changing the *EcoR* I site of the multi-cloning sites. His-tag (His_6) + egl2 (egl2; egl2B + egl2C) was amplified from the plasmid EGpUC19X by PCR with using primers of 5′-AAGAACTCGAG**CATCATCACCATCACCAT**GCACAACAGACTGTCTGGGGACAG-3′ (*Xho* I restriction site is underlined, His-tag coding sequence is boldface) and 5′-GACAACTCGAGTGCAATCGACCTC-3′ (*Xho* I restriction site is underlined). This PCR product was digested with *Xho* I, dephosphorylated, and then inserted into the *Xho* I site of the vector at the multi-cloning sites of pWI3 + MFα. The plasmid obtained was named as pMIEG13. The plasmid pMIEG13 was identified by sequencing.

The plasmid pWEG13 encoding $EGII_{core}$ was constructed as follows. The DNA fragment encoding His-tag and the following EGII catalytic core domain ($EGII_{core}$) from *T. viride* was amplified from the total cDNA of egl2 in the pMIEG13 plasmid by PCR using primers of 5′-CGACCCTCGAG**CATCATCACCATCACCAT**GGAGTTCGATTTGCTGG-CGTT-3′ (*Xho* I restriction site is underlined, His-tag coding sequence is boldface) and 5′-GACAACTCGAGTGCAATCGACCTC-3′ (*Xho* I restriction site is underlined). This PCR product was digested with *Xho* I, and inserted into the *Xho* I site of the vector multi-cloning sites of pWI3 + MFα. The plasmid obtained was named as pWEG13. The direction of the insert was confirmed by PCR, and the construction of pWEG13 was identified by sequencing.

The plasmid pMIEG13 and pWEG13 were transformed into *S. cerevisiae* MT8-1 by the lithium acetate method.[25] Transformants were confirmed by the colony-PCR and the Congo-red method.

Purification of secretory protein. Yeast cells carrying plasmid pMIWG13 or pWEG13 were precultivated in SD−W medium at 30 °C for 2 days, and then transferred to

YPD medium at an initial optical density of 0.01 at 600 nm, and cultivated for 5 days at 30 °C. Then yeast cells were removed by centrifugation at 4,500 g for 25 min.

All the purification steps were carried out below 4 °C. The cellulase activity and protein concentration at each purification step were evaluated b°y the Somogyi-Nelson method[26,27] and the Lowry method,[28] respectively. The substrate used for the Somogyi-Nelson method was carboxymethyl cellulose (CMC).

The crude EGII was purified by ammonium sulfate fractionation (40, 60, and 80% of $(NH_4)_2SO_4$). The 60 and 80% fractions, which showed the cellulase activity by Somogyi-Nelson method, were dialyzed (WAKO Dialysis Membrane; Size 20, Wako chemicals). The residue was purified by gel-permeation chromatography (GPC) (Sephacryl S-100 HR, GE Healthcare UK Ltd., England) eluting with 20 mM phosphate buffer (pH 7.4) containing 0.5 M NaCl. The fractions, which showed the cellulase activity, were collected and concentrated by ultrafiltration (Amicon Centriplus YM-30; NMWL 30,000, Nihon Millipore K.K., Japan). Finally, the product was purified by His-tag affinity chromatography using the His-Trap™ Kit (GE Healthcare). The fractions, which showed the cellulase activity, were collected and concentrated by ultrafiltration (Amicon Centricon YM-30, Millipore) with exchanging the buffer with 50 mM sodium acetate (pH 5.0).

$EGII_{core}$ was also purified by ammonium sulfate fractionation, and the 60% fraction was collected and dialyzed. The solution was purified by a DEAE Sepharose ion-exchange column (Amersham Biosciences). The fractions, which showed the cellulase activity, were collected and concentrated by ultrafiltration using Amicon Centriplus YM-10 (Millipore). The product was finally purified by His-tag affinity chromatography, and the solution was concentrated by ultrafiltration using Amicon Centricon YM-10 (Millipore) with exchanging the buffer with 50 mM sodium acetate (pH 5.0).

The purified enzymes were identified by SDS-PAGE on precast 10% polyacrylamide gel PAGEL NPU-10L (ATTO Corp., Japan) at 20 mA/gel for 75 min. The gel was subjected to the silver staining.

Enzymatic polymerization. Enzymatic polymerization of β-cellobiosyl fluoride (25 mM) as monomer with using these purified enzymes was carried out in a mixture of acetonitrile/acetate buffer (50 mM, pH 5.0) (3/1 v/v) at 30 °C.[3] The reactions were traced by high performance liquid chromatography (HPLC) with a COSMOSIL C18 column (Nacalai Tesque, Inc., Japan) using water/acetonitrile = 98/2 v/v as eluent. Before injection to HPLC, all the samples were heated at 100 °C for 5 min to inactivate the enzyme and freeze-dried *in vacuo*.

Fourier transform infrared spectroscopy (FTIR), electron diffraction, and mass measurements. FTIR measurement was performed on a Spectrum One FTIR spectrometer with a Universal ATR Sampling Accessory (Perkin-Elmer Japan Co., Ltd., Japan). For the electron diffraction analysis, the sample was distilled in water and charged on carbon-coated grids without any stain. On the other hand, samples for the matrix-assisted laser desorption/ionization time-of-flight mass spectrometry (MALDI-TOF/MS) were dissolved in a mixture of 1 wt% dihydroxybenzoic acid (DHB) and 1% trifluoroacetic acid (TFA), and air-dried on the sample plate prior to analysis.

Results and discussion

Synthesis of mutant EGII and $EGII_{core}$. The plasmid pMIEG13 and pWEG13 encoding mutant EGII and $EGII_{core}$ were synthesized by genetic engineering using yeast *S. cerevisiae* as host (Scheme 1). The sequences of synthesized DNA fragments were confirmed by DNA sequencing. The transformation process of yeast was examined by measuring the hydrolytic activity against CMC included in culture of the obtained transformants by the Congo-red reagent. A halo, which is the evidence for hydrolysis of the CMC, appeared around the yeast cell bearing pMIEG13 or pWEG13, but no halo occurred around the original yeast MT8-1. These results indicate EGII or $EGII_{core}$ is secreted from the transformants as designed.

Scheme 1. Construction of pMIEG13 and pWEG13.

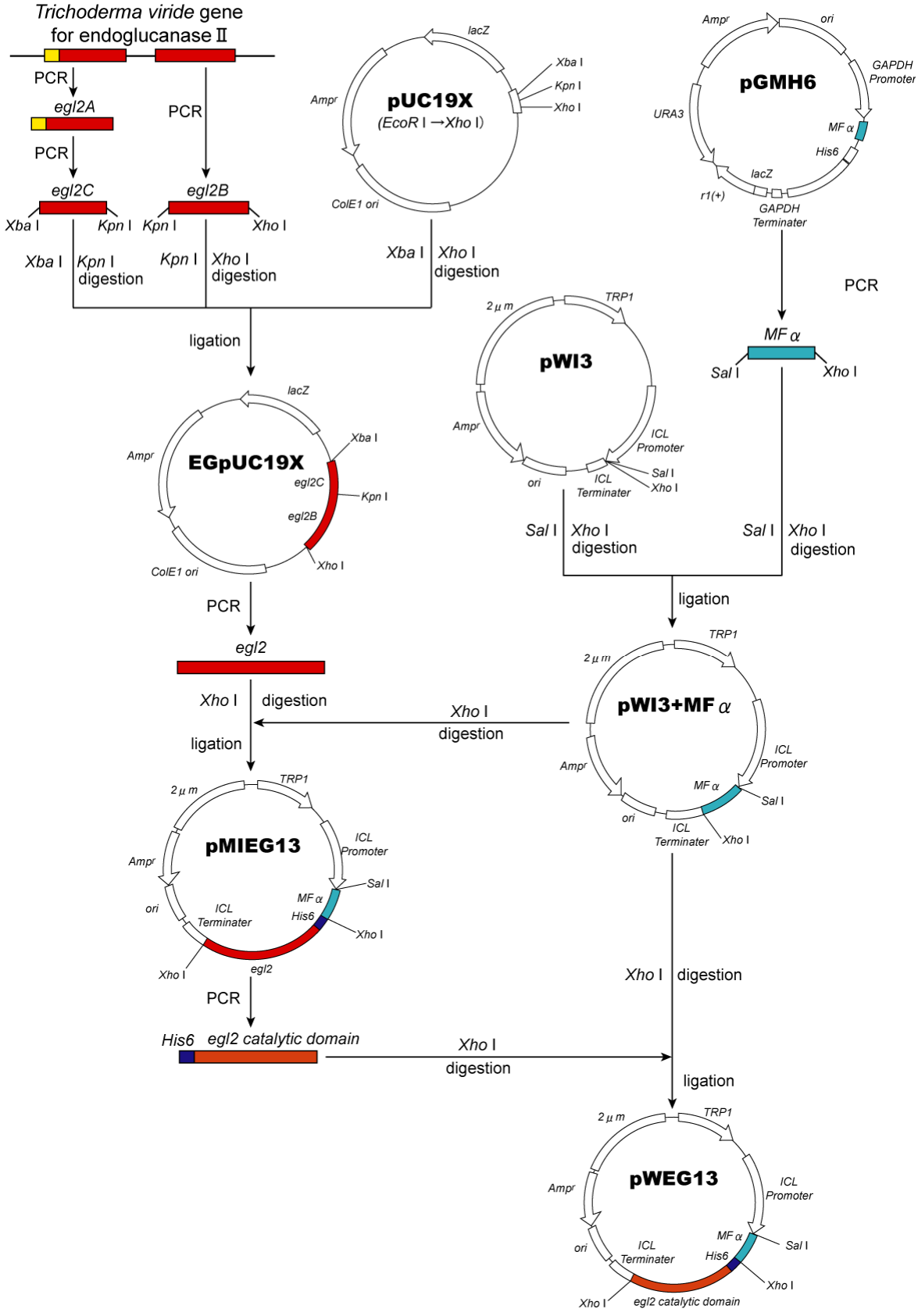

The specific activities of the secreted endoglucanases were monitored at the each purification step, which increased significantly after the His-Trap affinity chromatography, to be finally 29.5 and 5.45 U/mg for EGII and $EGII_{core}$, respectively. The specific activity of EGII was 5.4 fold larger than that of $EGII_{core}$. The constructions of pMIEG13 and pWEG13 were identified by sequencing to ensure no point mutations due to PCR during the cloning. The final products, EGII and $EGII_{core}$, showed a single band on SDS-PAGE at 50 and 38 kDa, respectively, which coincide with their calculated molecular weight (Figure 1). Since SDS-PAGE indicated the both products were highly purified, the lower specific activity of $EGII_{core}$ may be due to the removal of the cellulose-binding domain, which might have a steric effect favorably on the active site to promote the hydrolytic activity. However, the 5 fold difference remains to be solved.

Enzymatic polymerization. The purified enzymes were applied to the enzymatic polymerization of β-cellobiosyl fluoride to afford artificial cellulose. Both enzymes were able to polymerize β-cellobiosyl fluoride to yield white precipitate of artificial cellulose. It is therefore concluded that the cellulose-binding domain is not prerequisite for the enzymatic polymerization. However, the effects of the cellulose-binding domain on the enzymatic polymerization were clearly shown as follows.

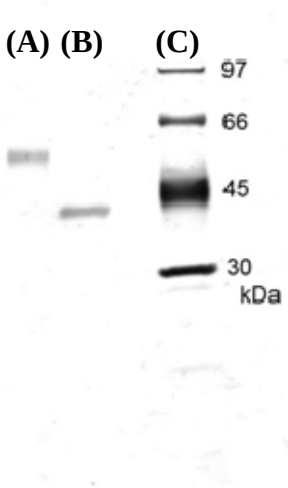

Figure 1. SDS-PAGE of the purified EGII (A), the purified $EGII_{core}$ (B) and protein molecular weight marker (C).

As the polymerization proceeded, the yield of the white precipitate, cellulose, initially increased in both cases of using EGII and $EGII_{core}$ as catalyst. However, after standing the polymerization solution at 30 °C for more than one day, the amount of the product in the solution containing EGII decreased gradually and finally disappeared from the solution. On the other hand, the product in the solution containing $EGII_{core}$ stayed as it was even after 14 days from the initiation (Figure 2). Since $EGII_{core}$ lacks the cellulose-binding domain, the hydrolytic activity of $EGII_{core}$ for crystalline cellulose should decrease drastically due to the difficult access to the crystalline cellulose. To confirm this interpretation, the products were analyzed.

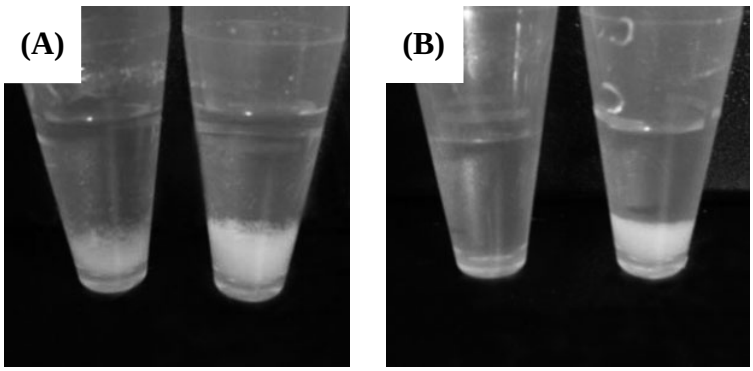

Figure 2. Enzymatic polymerization products using purified EGII (left) and $EGII_{core}$ (right) with almost equal activity after 1 day (A) and 14 days (B).

Characterization of products. The FTIR spectra of the polymerization products by using EGII and $EGII_{core}$ as catalyst exhibited the characteristic spectra of cellulose with intensive absorption at 1370cm^{-1}, which is a discriminative feature of crystalline cellulose II (Figure 3).[29,30] Further, electron diffraction of these products clearly showed three major diffraction rings that are typical equatorial spacings of cellulose II (Figure 4).[6,31] Under the present polymerization conditions, most of the precipitate therefore consists of cellulose II crystals. Interestingly, the rings in Figure 4B consist of discrete spots from the single crystal preparation of cellulose II, while the rings in Figure 4A are continuous. A rational explanation may be that the crystals produced by $EGII_{core}$ are larger or heterogeneously distributed. However, the line broadening of each Debye-Sherrer ring is similar and thus more careful

inspections are necessary to confirm without ambiguity. The stable product in the solution containing $EGII_{core}$ is therefore reasonably explained by the deficiency of the cellulose-binding domain in $EGII_{core}$. This property of $EGII_{core}$ is advantageous for the enzymatic polymerization to produce crystalline cellulose in comparison with EGII.

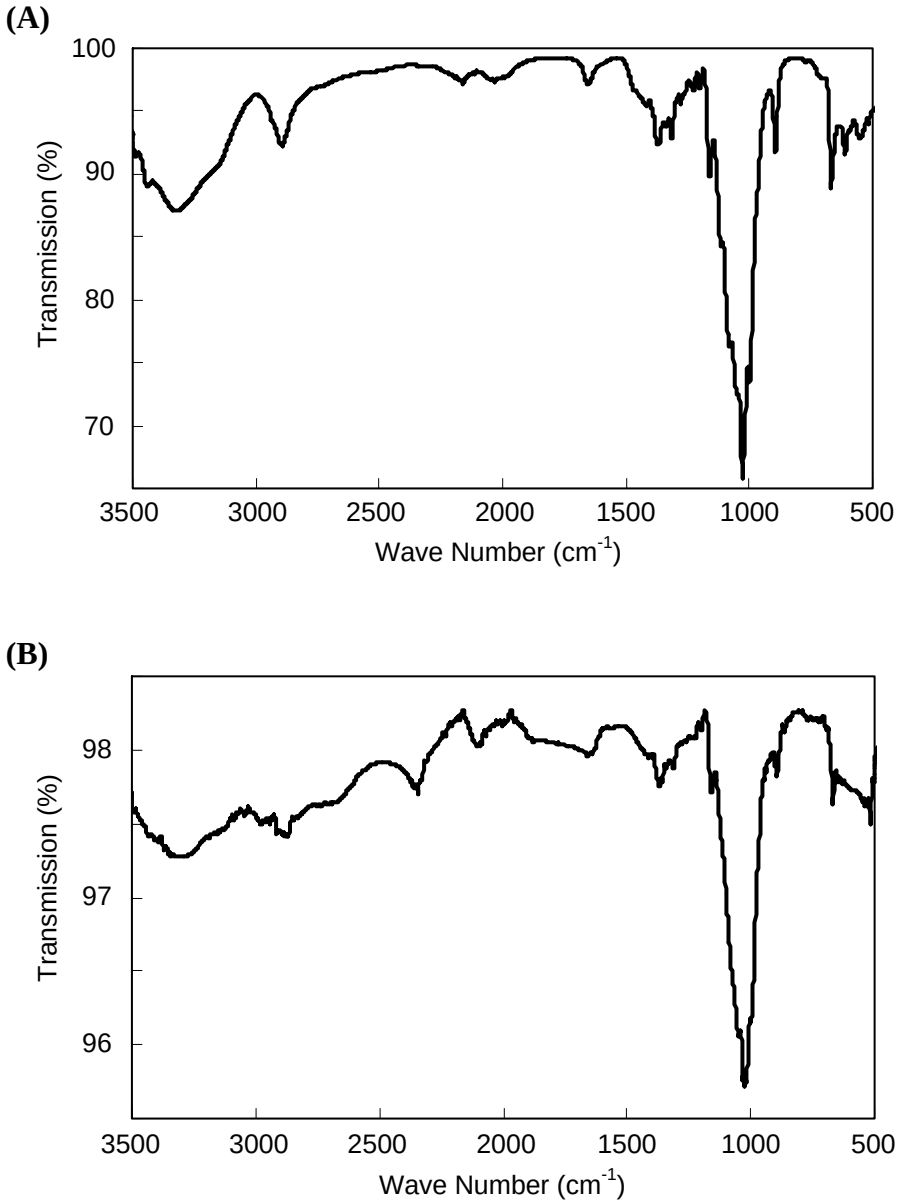

Figure 3. FTIR spectra of enzymatic polymerization products using the purified EGII (A) and the purified $EGII_{core}$ (B).

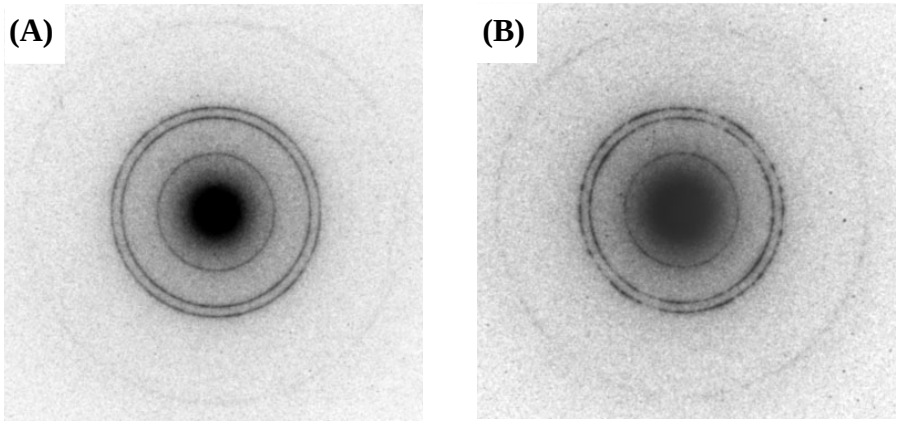

Figure 4. Electron diffraction diagrams of enzymatic polymerization products using the purified EGII (A) and the purified $EGII_{core}$ (B).

Behavior of enzymatic polymerization. Time course of the polymerization was studied by tracing the residual monomer concentration in solution by HPLC. EGII and $EGII_{core}$ clearly promoted the monomer consumption (Figure 5). The time required for complete consumption of the monomer by $EGII_{core}$ becomes similarly to that by EGII when the amount of $EGII_{core}$ was two fold larger than that of EGII on a mol basis, suggesting that EGII is more effective in the enzymatic polymerization than $EGII_{core}$. On the other hand, when the amount of EGII was nearly equal to $EGII_{core}$ on a hydrolysis-activity base, the initial monomer consumption by EGII was still as fast as that of $EGII_{core}$, but ceased out in the middle. There may be several reasons for the inactivation of EGII during the polymerization. For example, since the amount of the enzyme became less than 0.1 wt% of the substrate (in the case of EGII of 2 μg and the monomer of 5 mg), the turnover number of one enzyme should be over 10^5 to consume all monomers, which might exceed over the enzyme ability. Further, the product inhibition would occur with EGII at the low concentration through the cellulose-binding domain but would not with $EGII_{core}$.

The kinetics of polymerization using EGII shows two phases, initial fast decay and the following steady decay. It is speculated that EGII possesses higher activity than $EGII_{core}$ about the enzymatic polymerization, but in the presence of the crystalline cellulose, which is produced during the initial a few ten minutes, the apparent activity of EGII should be lowered

because of competitive adsorption of EGII to the crystalline cellulose via the cellulose-binding domain. In other words, hydrolysis reaction competes with polymerization reaction. On the other hand, the monomer consumption by $EGII_{core}$ obeyed first-order kinetics. $EGII_{core}$ may be free from the hydrolysis reaction for crystalline products due to the deficiency of the cellulose-binding domain in the present system.

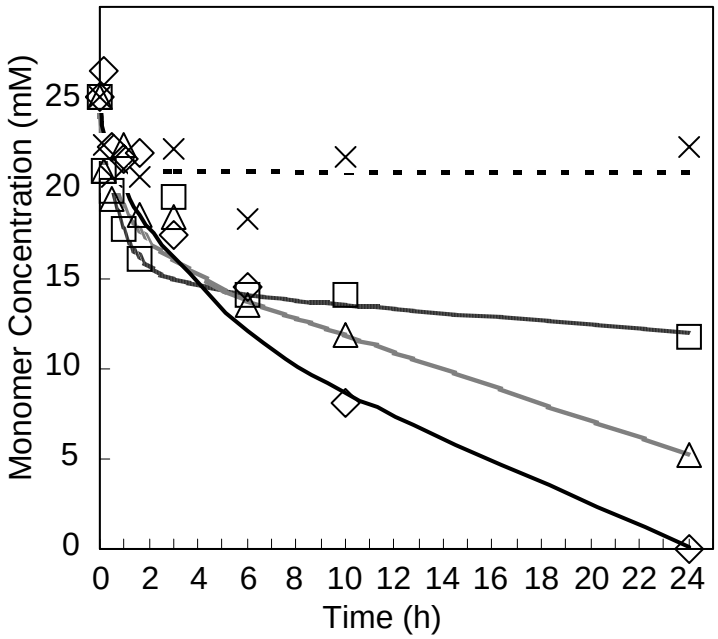

Figure 5. Time course of the monomer consumptions in the enzymatic polymerization. EGII of 2.0 μg (58 mU); □, EGII of 6.1 μg (140 mU); △, $EGII_{core}$ of 10 μg (57 mU); ◇, without enzymes; ×.

Mass measurements. The soluble part of the products by using EGII was analyzed by the MALDI-TOF/MS spectrometry. Cellulose up to 16 glucose units was identified (Figure 6). Even though cellulose of higher molecular weights is considered to be produced in the present polymerization, its detection was extremely difficult due to the tight packing of the crystalline product. The product by using $EGII_{core}$ also showed the similar mass spectrum. Notably, in either mass spectrum, cellulose with odd number of glucose units was detected, indicating occurrence of hydrolysis of the product during the reaction. $EGII_{core}$ looses the hydrolytic activity for the crystalline cellulose as described before. The observation of the odd number

glucose units in the mass spectrum suggests that the enzymatic polymerization produces the soluble oligocellulose as well as the insoluble high-molecular weight cellulose. The former should be hydrolyzed by $EGII_{core}$ to yield the cellulose with odd number of glucose units. The enzymatic polymerization using $EGII_{core}$ therefore produces artificial cellulose with a wide range of the molecular weight. Taken together, the binding and the dissociation of the polymerized product is suggested to be in equilibrium during the polymerization.

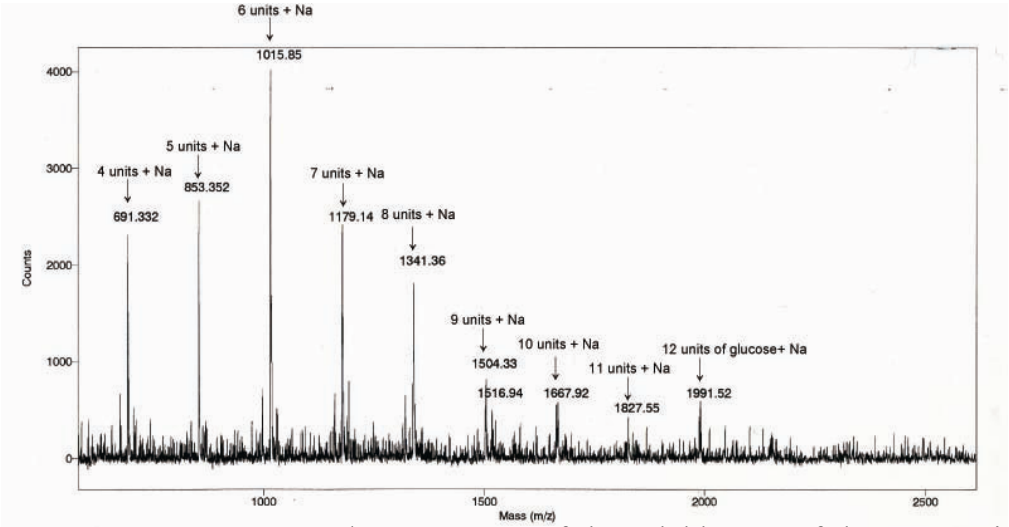

Figure 6. MALDI-TOF/MS spectrum of the soluble part of the enzymatic polymerization using the purified EGII.

References

(1) Kobayashi, S.; Uyama, H.; Kimura, S. *Chem. Rev*. **2001**, *101*, 3793–3818.

(2) Kobayashi, S.; Sakamoto, J.; Kimura, S. *Prog. Polym. Sci*. **2001**, *26*, 1525–1560.

(3) Kobayashi, S.; Kashiwa, K.; Kawasaki, T.; Shoda, S. *J. Am. Chem. Soc*. **1991**, *113*, 3079–3084.

(4) Kobayashi, S.; Kiyosada, T.; Shoda, S. *J. Am. Chem. Soc*. **1996**, *118*, 13113–13114.

(5) Kobayashi, S.; Morii, H.; Itoh, R.; Kimura, S.; Ohmae, M. *J. Am. Chem. Soc.* **2001**, *123*, 11825–11826.

(6) Kobayashi, S.; Hobson, L. J.; Sakamoto, J.; Kimura, S.; Sugiyama, J.; Imai, T.; Itoh, T. *Biomacromolecules* **2000**, *1*, 168–173.

(7) Henrissat, B. *Cellulose* **1994**, *1*, 169–196.

(8) Levy, I.; Shoseyov, O. *Biotech. Adv.* **2002**, *20*, 191–213.

(9) Nam, J. M.; Fujita, Y.; Arai, T.; Kondo, A.; Morikawa, Y.; Okada, H.; Ueda, M.; Tanaka A. *J.Mol.Catal.B:Enzymatic* **2002**, *17*, 197–202.

(10) Tomme, P.; Warren, R. A. J.; Miller, R. C.; Kilburn, D. G.; Gilkes, N. R. *ACS Symp. Ser.* **1995**, *618*, 142–163.

(11) Linder, M.; Teeri, T. T. *J. Biotechnol*. **1997**, *57*, 15–28.

(12) Chipman, D. M.; Sharon, N. *Science* **1969**, *165*, 454–458.

(13) Brameld, K. A.; Shrader, W. D.; Imperiali, B.; Goddard III, W. A. *J. Mol. Biol.* **1998**, *280*, 913–923.

(14) Brameld, K. A.; Goddard III, W. A. *Proc. Natl. Acad. Sci. U. S. A.* **1998**, *95*, 4276–4281.

(15) Fort, S.; Boyer, V.; Greffe, L.; Davies, G. J.; Moraz, O.; Christiansen, L.; Schelein, M.; Cottaz, S.; Driguez, H. *J. Am. Chem. Soc.* **2000**, *122*, 5429–5437.

(16) Zechel, D. L.; Withers, S. G. *Acc. Chem. Res*. **2000**, *33*, 11–18.

(17) Faijes, M.; Fairweather, J. K.; Driguez, H.; Planas, A. *Chem. Eur. J.* **2001**, 7, 4651–4655.

(18) Hrmova, M.; Imai, T.; Rutten, S. J.; Fairweathers, J. K.; Pelosi, L.; Bulone, V.; Driguez, H.; G. B. Fincher, G. B. *J. Biol. Chem*. **2002**, *277*, 30102–30111.

(19) Meinke, A.; Damude, H. G.; Tomme, P.; Kwan, E.; Kilburn, D. G.; Miller Jr., R. C.; Warren R. A. J.; Gilkers, N. R. *J. Biol. Chem*. **1995**, *270*, 4383–4386.

(20) Teeri, T. T. *Trends Biotechnol*. **1997**, *15*, 160–167.

(21) Tajima, M.; Nogi, N.; Fukusawa, T. *Yeast* **1985**, *1*, 67–77.

(22) Umemura, K.; Atomi, H.; Kanai, T.; Teranishi, Y.; Ueda, M.; Tanaka, A. *J. Ferm. Bioeng*. **1995**, *80*, 529–533.

(23) Kurjan, J.; Herskowitz, I. *Cell*, **1982**, *30*, 933–943.

(24) Kanai, T.; Atomi, H.; Umemura, K.; Ueno, H.; Teranishi, Y.; Ueda, M.; Tanaka, A. *Appl. Microbiol. Biotechnol*. **1996**, *44*, 759–765.

(25) Ito, H.; Fukuda, Y.; Murata, K.; Kimura, A. *J. Bacteriol*. **1983**, *153*, 163–168.

(26) Somogy, M. J. *J. Biol. Chem*. **1952**, *195*, 19–23.

(27) Nelson, N. *J. Biol. Chem*. **1944**, *153*, 375–380.

(28) Lowry, O. H.; Rosebrough, J. J.; Farr, A. L.; Randall, R. J. *J. Biol. Chem*. **1951**, *193*, 265–275.

(29) Forziati, F. H.; Rowen, J. W. *J. Res. Natl. Bur. Stand.* **1951**, *46*, 38–42.

(30) Nikonenko, N. A.; Buslov, D. K.; Sushko, N. J.; Zhbnkov, R. G. *Biopolym.* **2000**, *57*, 257–262.

(31) Buleon, A.; Chanzy, H. *J. Polym. Sci. Polym. Phys. ed.* **1978**, *16*, 833–839.

Chapter 2

Enzymatic Activities of Novel Endoglucanases

Carrying Sequential Active Sites

Introduction

Cellulose is one of the most abundant natural polysaccharides on the earth, therefore has been used in a various fields as commodity polymer. Cellulose is also potential as functional materials by chemical modification of free hydroxyl groups in the backbone. For instance, cellulose acetate is used for hollow fibers and filters,[1] nitrocellulose is suitable for coatings and films,[2] methyl and carboxymethyl cellulose is employed for cosmetics and foods.[3] To produce highly functionalized materials, however, it will become necessary to control substitution position and substitution degree more precisely at the chemical modification. Enzymatic polymerization with using cellulase as catalyst to produce artificially modified celluloses is a suitable method for this purpose because the regio- and stereo-chemistry on the glycoside linkage are reliably formed with using newly designed cellobiose derivatives.[4–7] Further, enzymatic polymerization has been extended its application widely to syntheses of artificial chitin,[8–10] hyaluronic acid,[6,11] chondroitin sulfates,[12] cellulose-chitin,[13] and cellulose-xylane hybrids.[14]

EGII from the fungus *T. viride* shows the polymerization activity for β-cellobiosyl fluoride in acetonitrile/acetate buffer (pH 5.0) = 3/1 v/v mixture to afford artificial cellulose.[15,16] EGII is composed of three functional domains; the cellulose-binding domain, the linker, and the catalytic core domain from the *N* terminal.[17] In the Chapter 1, the author synthesized a mutant EGII ($EGII_{core}$) which possessed only the catalytic core domain by genetic engineering.[18] $EGII_{core}$ polymerized β-cellobiosyl fluoride with an improvement of the enzymatic polymerization due to the suppression of the hydrolytic activity for the crystalline products because of the deletion of the cellulose-binding domain. However, the specific activity of $EGII_{core}$ was lower than that of EGII, which may be explained by large conformational fluctuation of $EGII_{core}$ because of the diminished size of $EGII_{core}$.

To improve the specific activity, the author newly designed two novel mutant EGIIs named $EGII_{core2}$ or $EGII_{core2H}$, which are composed of two sequential catalytic core domains with a His-tag at the *N* terminal or two His-tags at the both terminals, respectively. The size enlargement of these mutants will reduce the conformational fluctuation. Further, cooperative

enzymatic action of the two catalytic core domains in series is expected to enhance the hydrolytic activity of the endo-type enzyme when those mutants bind the same substrate simultaneously. Further, these mutant enzymes may influence on the morphology of the products, because the type of cellulose crystals is determined in nature by the spatial arrangement of the synthetic cellulose synthases.[19,20]

The mutant enzymes here were expressed in *S. cerevisiae* to avoid the possible formation of inclusion body.[21,22] The secretory proteins were purified by affinity chromatography to show a single band in SDS-PAGE. The specific activity and polymerization behavior of the mutant enzymes were analyzed in detail to investigate on the influence of the two sequential catalytic core domains for the enzymatic processes.

Experimental section

Materials. Ni-NTA agarose beads was purchased from QIAGEN K.K. (Japan). All other reagents were purchased from commercial sources and used as received.

Strains and culture conditions. For the recombinant DNA or the protein expression, *E.coli* DH5α or *S. cerevisiae* MT8-1 was used as the host and cultivated in LB medium or SD−W medium followed by YPD medium as well as in Chapter 1.

Construction of plasmid and transformation. The vector plasmids, pUCD1, pUCD2 and pUCD2H, were constructed as follows. The gene encoding the catalytic core domain of EGII with the His-tag at the *N* terminal was amplified by PCR using the following primers: 5′-CTCGTCGCTAGC**CATCATCACCATCACCAT**GGAGTTCG-3′ (*Nhe* I restriction site is underlined, His-tag encoding sequence is boldface) and 5′-GGAGTCCTTAAGCTTCCTG-GCGAGACACGAGCTAAC-3′ (*Bfr* I restriction site is underlined), and then was inserted into pUC19 digested with *Hinc* II (pUCD1). Similarly, the gene encoding only the catalytic core domain was amplified by PCR using the following primers: 5′-CTCGTCCTTAAGGGA-

GTTCGATTTGCTGGCGTTAACATCG-3′ (*Bfr* I restriction site is underlined) and 5′-GACAACTCGAGTGCAATCGACCTCGGTGTTACTTCCTGGC-3′ (*Xho* I restriction site is underlined), and then was inserted into pUC19 digested with *Hinc* II (pUCD2). Similarly, the gene encoding the catalytic core domain with the His-tag at the *C* terminal was amplified by PCR using the following primers: 5′-CTCGTCCTTAAGGGAGTTCGATTTGCTGGCG-TTAACATCG-3′ (*Bfr* I restriction site is underlined) and 5′-GACAACTCGAGTGCAATC-GACCTCGGTGTTA**ATGGTGATGGTGATGATG**CTTCCTG-3′ (*Xho* I restriction site is underlined, His-tag coding sequence is boldface), and then was inserted into pUC19 digested with *Hinc* II (pUCD2H). The constructions of pUCD1, pUCD2 and pUCD2H were identified by sequencing.

The plasmids of pMEGCC2 encoding $EGII_{core2}$ and pMEGCC2H encoding $EGII_{core2H}$ were constructed as follows. The vectors of pUCD1 and pMFBN were digested with *Nhe* I/*Bfr* I. The vector of pMFBN is the yeast expression vector which has two more restriction sites, *Nhe* I and *Bfr* I, than the vector pWI3. The vector of pWI3 possesses UPL-ICL as a promoter[25] and MFα[26] which completes efficient secretion of a target protein. The DNA fragment from pUCD1 was inserted into the *Nhe* I/*Bfr* I site of pMFBN (pMFBN+CD1). The construction of pMFBN+CD1 was identified by colony-PCR. Then, the vector pUCD2 or pUCD2H was digested with *Bfr* I/*Xho* I and inserted into the *Bfr* I/*Xho* I site of pMFBN+CD1 (pMEGCC2 or pMEGCC2H, respectively). The constructions of pMEGCC2 and pMEGCC2H were identified by colony-PCR and restriction enzyme cleavage.

Plasmids of pMEGCC2 and pMEGCC2H were transformed into *S. cerevisiae* MT8-1 by the lithium acetate method.[27] The transformants were confirmed by the Congo-red method measuring hydrolytic activity of CMC.[22,28]

Purification of secretory protein. Transformated yeast cells were cultivated and secretory proteins were collected by centrifugation as described in Chapter 1.

All the manipulations were carried out below 4 °C. The cellulase activity and protein concentration were evaluated by the Somogyi-Nelson method[29,30] and the Lowry method,[31] respectively. CMC was used as the substrate for the Somogyi-Nelson method.

The secreted $EGII_{core2}$ was first concentrated by stirred ultrafiltration cell (ultrafiltration membrane; NMWL 30,000, Millipore). The supernatant was incubated with Ni-NTA agarose beads on shaker over 12 h.[32–34] Beads were pre-washed with phosphate buffer (20 mM, pH 7.4, 500 mM NaCl) containing 10 mM imidazole. After the supernatant was collected by decantation, $EGII_{core2}$ was eluted with phosphate buffer containing 100 mM imidazole. The supernatant was collected, then beads were washed again with phosphate buffer containing 500 mM imidazole. Supernatants which showed cellulase activity were loaded in desalting column PD-10 (GE Healthcare) to remove imidazole. Then, the product was purified by the His-tag affinity chromatography utilizing the His-Trap™ Kit. The fractions which showed the cellulase activity were collected and concentrated by ultrafiltration (Amicon Centricon YM-30). Finally, the product was purified by GPC (Sephacryl S-100 HR) using phosphate buffer as the eluent. The fractions, which showed the cellulase activity, were collected and concentrated by ultrafiltration (Amicon Centriplus YM-30).

$EGII_{core}$ and $EGII_{core2H}$ were also secreted from yeast, then purified with Ni-NTA Agarose beads and His-trap affinity choromatography similarly to the purification method for $EGII_{core2}$. The NMWLs of the ultrafiltration membranes were 10,000 and 30,000, respectively.

The purified mutants, $EGII_{core}$, $EGII_{core2}$, and $EGII_{core2H}$, were identified by SDS-PAGE staining by silver stainning using silver stain Kit (Wako chemicals, Japan).

Circular dichroism (CD) measurement. The CD spectra with varying temperature were obtained in phosphate buffer (10 mM, pH 7.0) using an optical cell of a 0.1 cm optical path length. Wavelength scans were recorded from 300 to 190 nm with a scan rate of 20 nm/min. The accumulation number was 4. Concentration of the mutant EGIIs was set at 1 mM. Temperature intervals were 10 °C between 10 °C and 40 °C, and the samples were held at the temperature for 5 min to allow for complete thermal equilibration.

Enzymatic polymerization. Enzymatic polymerization of β-cellubiosyl fluoride (25 mM) as monomer with these purified enzymes as catalyst was carried out in a mixture of

acetonitrile/acetate buffer (50 mM, pH 5.0) = 3/1 v/v at 30 °C.[15,18] The aliquot of reaction solution was extracted to monitor monomer concentration in the reaction solution by HPLC measurements using a Tosoh LC8020 system with a COSMOSIL C_{18}-PAQ column (Nacalai tesque) eluting with a water/acetonitrile = 98/2 v/v mixed solution (flow rate, 1.0 mL/min; column temperature, 30 °C). Before injection to HPLC, all the samples were freeze-dried *in vacuo*. After 24 h, the reaction solutions were centrifuged to separate precipitates from supernatant. The supernatant was also freeze-dried *in vacuo* and injected into HPLC system using a Tosoh GPC8020 equipped with Shodex OHpac SB-802HQ column eluting with 0.1 M aqueous $NaNO_3$ (flow rate, 0.5 mL/min; column temperature, 40 °C). The precipitates were washed and subjected to various measurements.

FTIR observation. FTIR was performed on a Nicolet 6700 FT-IR (Thermo Fisher Scientific Inc., USA). The precipitates were washed with distilled water (two times) and acetone (one time), then dried in a vacuum before preparation of KBr tablets. The number of interferogram accumulations was 32.

Transmission electron microscopy (TEM), electron diffraction, and field emission-scanning electron microscopy (FE-SEM) observations. For the TEM measurements, the product was washed with ionized water and methanol to remove the enzyme. The samples were charged on carbon-coated grids and stained negatively with 2% uranyl acetate containing 1% trehalose. For electron diffraction, on the other hand, grids without staining were used. These grids were subsequently used for FE-SEM observation. Prior to FE-SEM observation, grids were coated with Pt (Auto fine coater, JFC1600, JEOL).

Optical microscopy measurement. Polymerization in the quarts cell was followed visually by polarization microscope over a 24 h period. The samples were observed between crossed nicols and also by using a sensitive color plate positioned between the polarizers.

Scheme 1. Construction of pMEGCC2 and pMEGCC2H.

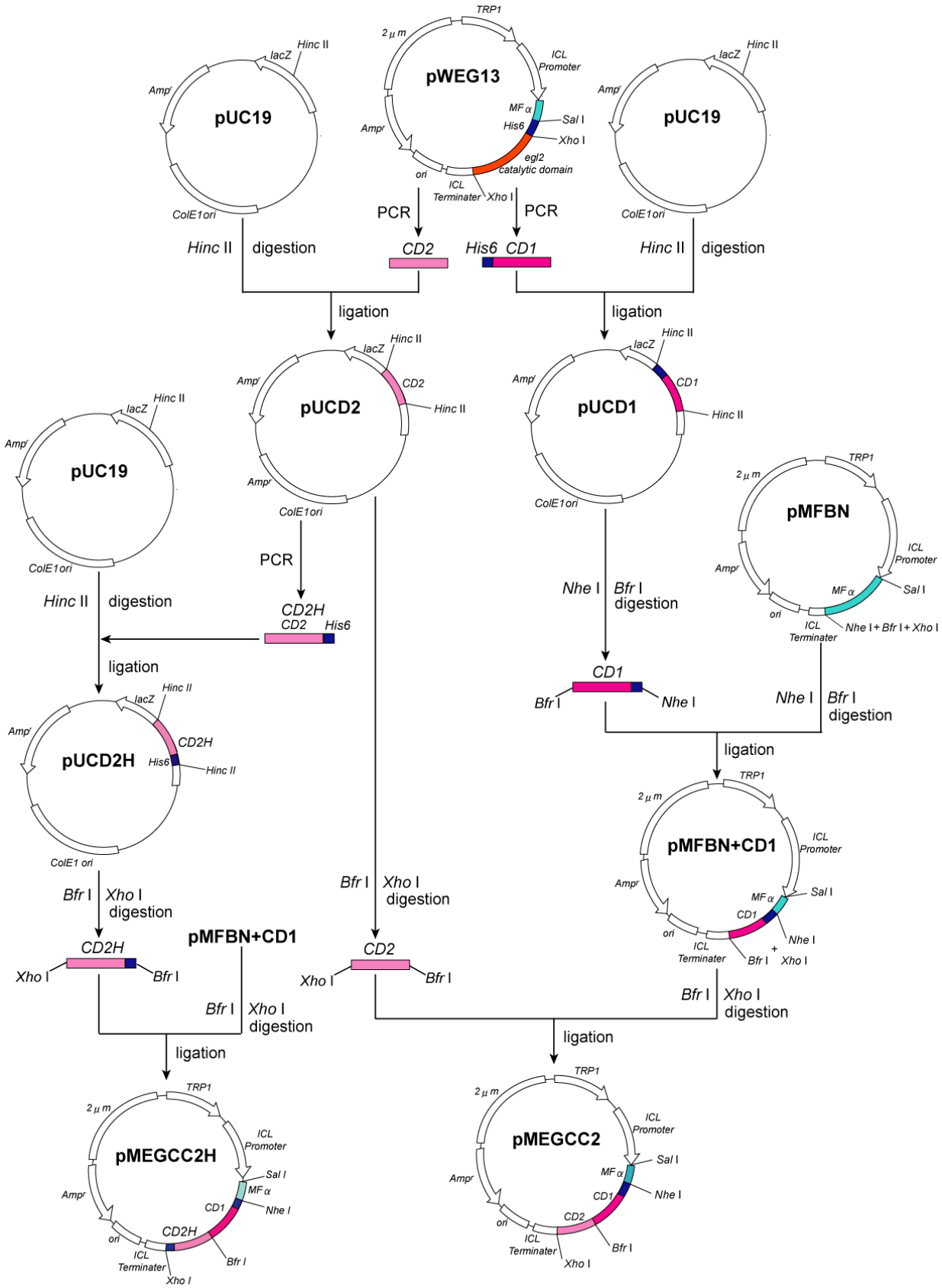

Results and discussion

Synthesis of mutant $EGII_{core2}$ and $EGII_{coreH}$. The plasmids encoding mutant $EGII_{core2}$ or $EGII_{coreH}$ were synthesized by genetic engineering as described in Scheme 1. The transformation of yeast with the plasmid was confirmed by the Congo-red method on cultivation of the transformed yeast cells, which showed a halo formation around the transformed yeast cells after 3 days incubation due to the hydrolysis of CMC included in the plate medium. The transformed *S. cerevisiae* MT8-1 cells therefore secreted $EGII_{core2}$ or $EGII_{core2H}$ without loosing the hydrolysis activity.

Hydrolytic activities of $EGII_{core2}$ and $EGII_{core2H}$. These secreted $EGII_{core2}$ and $EGII_{core2H}$ from the yeast cells were purified by the His-Tag affinity chromatography. The purified $EGII_{core2}$ and $EGII_{core2H}$ showed a single band on SDS-PAGE at about 71.5 and 72.3 kDa, respectively, which coincided with their designed molecular weights, and the purity was very high (Figure 1). The specific activity of cellulose hydrolysis was evaluated by the Somogyi-Nelson method. Notably, the specific activity of $EGII_{core2}$ and $EGII_{core2H}$ showed 25 U/mg and 27 U/mg, respectively, which were about over 3-fold larger than that of $EGII_{core}$ (7.7 U/mg). Two kinds of explanation may be possible for the enhanced hydrolytic activities of $EGII_{core2}$ and $EGII_{core2H}$ on the basis of the catalytic core concentration; i) cooperative

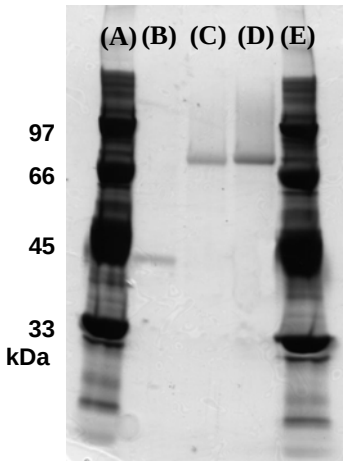

Figure 1. SDS-PAGE of protein molecular weight marker (A) and (E), the purified $EGII_{core}$ (B), $EGII_{core2}$ (C) and $EGII_{core2H}$ (D).

hydrolytic actions of the two catalytic core domains in the mutants on the same polymer substrate and ii) stably folded conformation of the mutants suitably arranged for the activity. On the other hand, the His-tag sequence at the *N* terminal or the *C* terminal did not seem to influence on the hydrolytic activity.

CD observation. Conformation of $EGII_{core2}$ and $EGII_{core2H}$ was analyzed by CD spectroscopy and was compared with that of $EGII_{core}$ (Figure 2). The double-minimum pattern at 208 and 222 nm indicates the presence of α-helical structure in $EGII_{core2}$ and $EGII_{core2H}$, but of less α-helical structure in $EGII_{core}$.[36,37] Further, the Cotton effects of $EGII_{core}$ decreased the

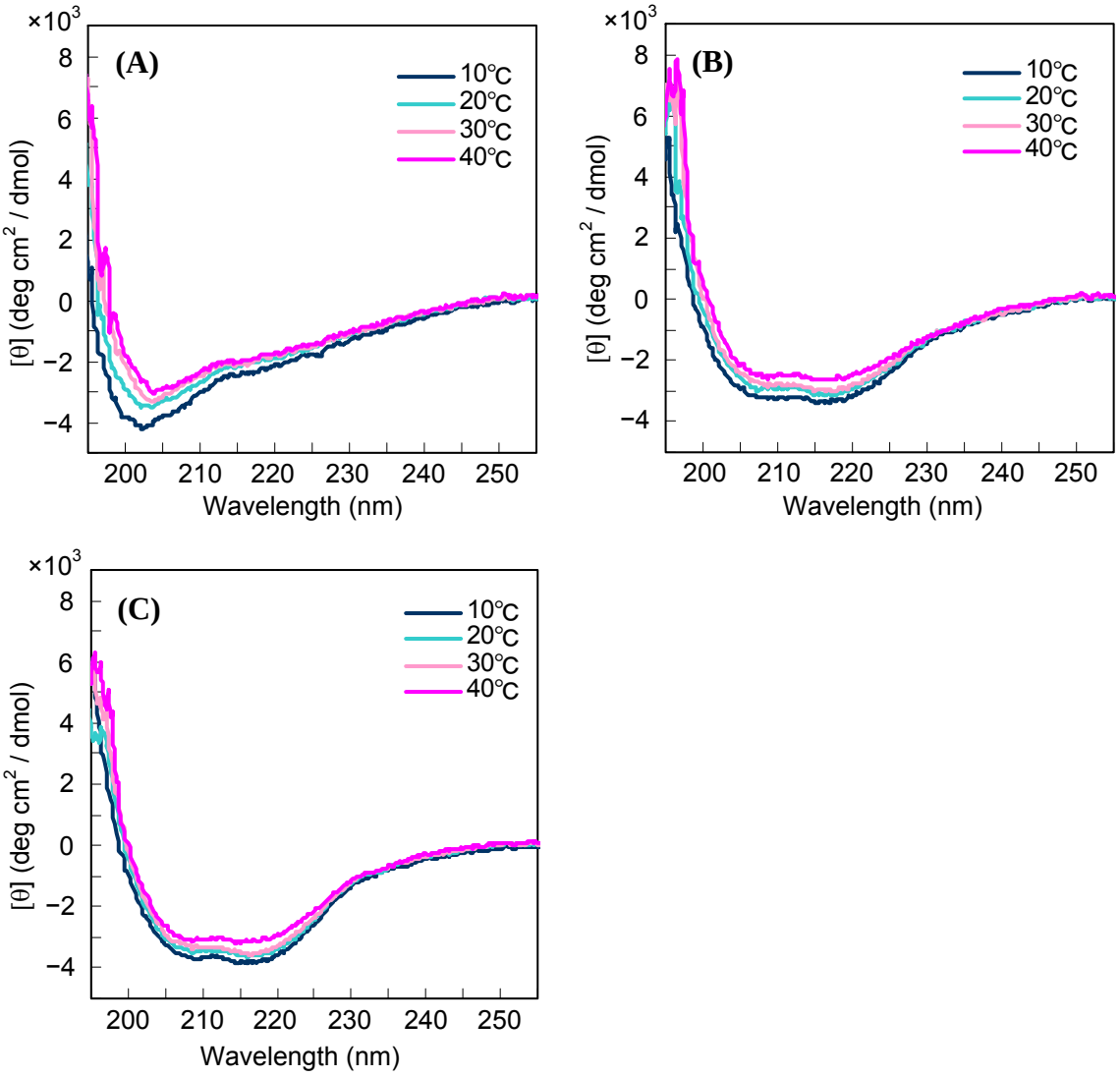

Figure 2. Temperature dependence of CD spectra of $EGII_{core}$ (A), $EGII_{core2}$ (B) and $EGII_{core2H}$ (C) in phosphate buffer (pH 7.0). Protein concentrations; 1 μM.

intensity with raising temperature (Figure 2A), whilst $EGII_{core2}$ and $EGII_{core2H}$ showed nearly temperature-independent spectra in the temperature range from 10 to 40 °C (Figures 2B and 2C). Taken together, $EGII_{core2}$ and $EGII_{core2H}$ are found to take thermally stable tertiary structure with α-helix rich content upon direct connection of two active sites in series. When the primary sequence of the connection part of the two active sites was examined by the secondary structure prediction analysis, it did not show any tendency to generate newly α-helical structure. Some parts of the two active sites in $EGII_{core2}$ and $EGII_{core2H}$ should therefore interact with each other to stabilize α-helical structure even though the two parts locate apart in the primary sequence. The stabilized conformation of $EGII_{core2}$ and $EGII_{core2H}$ is considered not to hamper the native hydrolytic activity of the active sites at lowest.

Enzymatic polymerization. The purified $EGII_{core2}$ and $EGII_{core2H}$ were applied to the enzymatic polymerization of β-cellobiosyl fluoride to afford synthetic cellulose. After 10 min incubation of the monomer and the mutants, artificial cellulose started to precipitate out from the dispersion, which was much faster than 50 min incubation in the case of using $EGII_{core}$ of the same weight. The polymerization activity of $EGII_{core2}$ and $EGII_{core2H}$ should therefore be larger than that of $EGII_{core}$.

The time course of enzymatic polymerization was analyzed by monitoring the consumption of β-cellobiosyl fluoride in the reaction solution by HPLC (Figure 3). The monomer consumption rates in the presence of $EGII_{core2}$ and $EGII_{core2H}$ were much faster than that of $EGII_{core}$ under the same amounts of enzymes were used. From the initial slop of the monomer consumption with time, polymerization rates, consumed monomer (mol)/catalytic core unit (mol) per one second, are calculated to be 1.29, 6.19 and 7.12 s^{-1} for $EGII_{core}$, $EGII_{core2}$ and $EGII_{core2H}$, respectively. The polymerization rates of $EGII_{core2}$ and $EGII_{core2H}$ were nearly the same and larger by about 4-fold than that of $EGII_{core}$ on the basis of the catalytic core concentration. This finding is consistent with the hydrolysis results showing that the specific activities of $EGII_{core2}$ and $EGII_{core2H}$ are over 2-fold higher than that of $EGII_{core}$. Enzymes are known to reduce the activation energy of the reactions in both forward

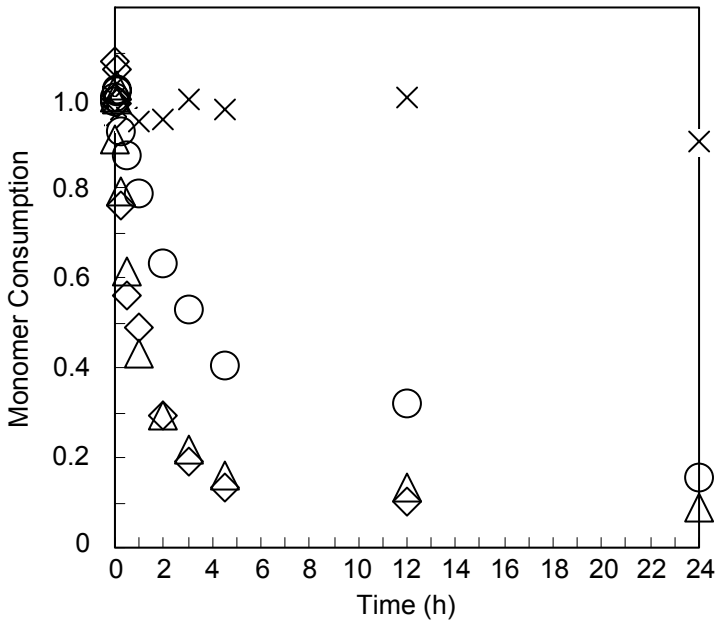

Figure 3. Time course of the monomer consumption in the enzymatic polymerization. without enzymes, ×; $EGII_{core}$, ○; $EGII_{core2}$, △; $EGII_{core2H}$, ◇.

and reverse directions. In this Chapter, hydrolysis and polymerization reactions with using the mutant enzymes are promoted similarly, which is consistent with the general comprehension on the enzymatic mechanism.

In the cases of the enzymatic polymerization using $EGII_{core2}$ and $EGII_{core2H}$, it is hard to imagine that the two catalytic sites in the mutants would cooperate to synthesize one polymer chain, because the polysaccharide chain is considered to be extended only by coupling of the monomer to the nonreducing terminal of the growing chain. Therefore, the enhanced enzymatic activities of $EGII_{core2}$ and $EGII_{core2H}$ in comparison with $EGII_{core}$ on the basis of the catalytic core concentration should be mainly due to a suitably stabilized conformation of the mutants as indicated by the CD measurements.

FTIR and TEM observations of polymerization products. The supernatants of polymerization reaction solutions after 24 h were analyzed by HPLC, which showed production of water-soluble oligosaccharides (< 6 glucose units) in the cases of all three enzymes (data not shown). However, most products were found in the insoluble fraction, and

the yield of artificial cellulose was over 70–80%. The FTIR spectra of the white precipitates obtained by $EGII_{core2}$ and $EGII_{core2H}$ exhibited a strong absorption at 1370 cm^{-1} similarly to polymerization by $EGII_{core}$, which is a characteristic of crystalline cellulose of type II (Figure 4).[38,39] Further, electron diffraction of these products by TEM clearly showed three major diffraction rings which have typical equatorial spacings of crystalline cellulose of type II (Figure 5).[40,41] Discrete spots in the diffraction rings are observed, indicating high crystallinity of the products.

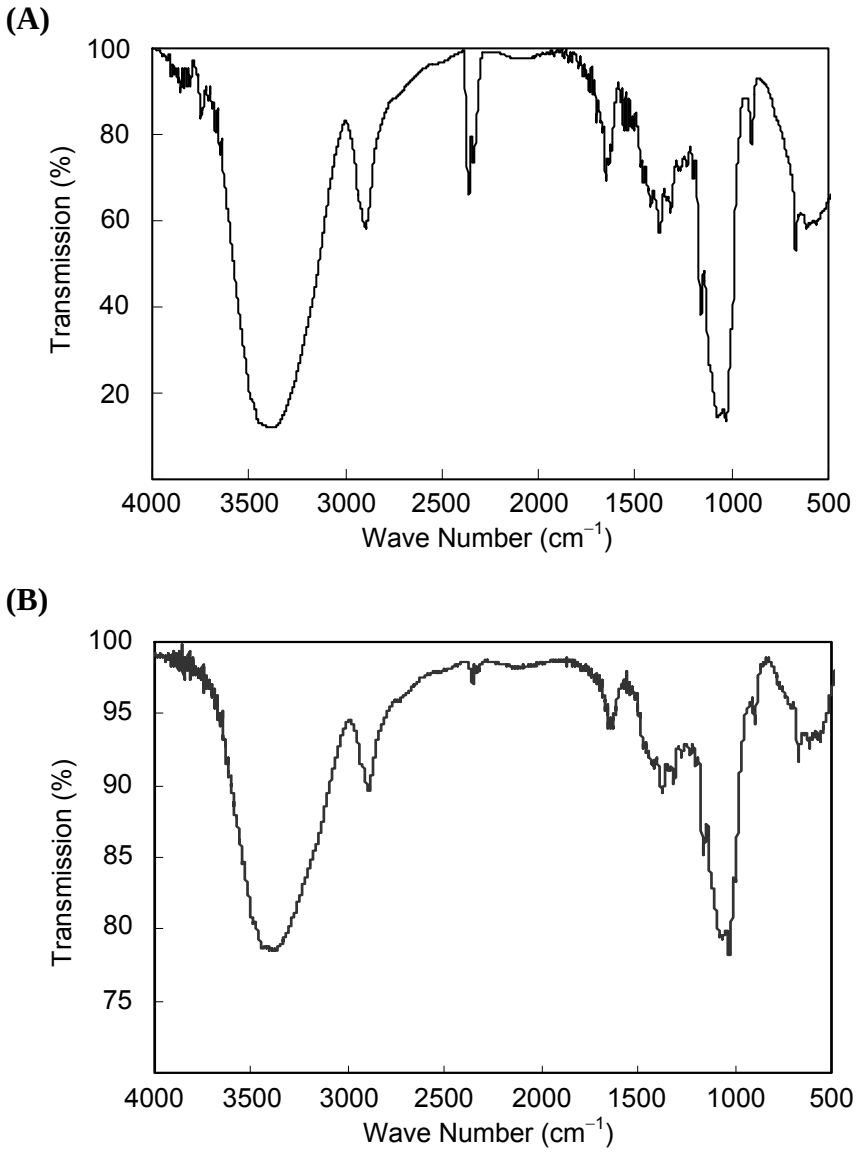

Figure 4. FT-IR spectra of enzymatic polymerization products with using $EGII_{core2}$ (A), and $EGII_{core2H}$ (B).

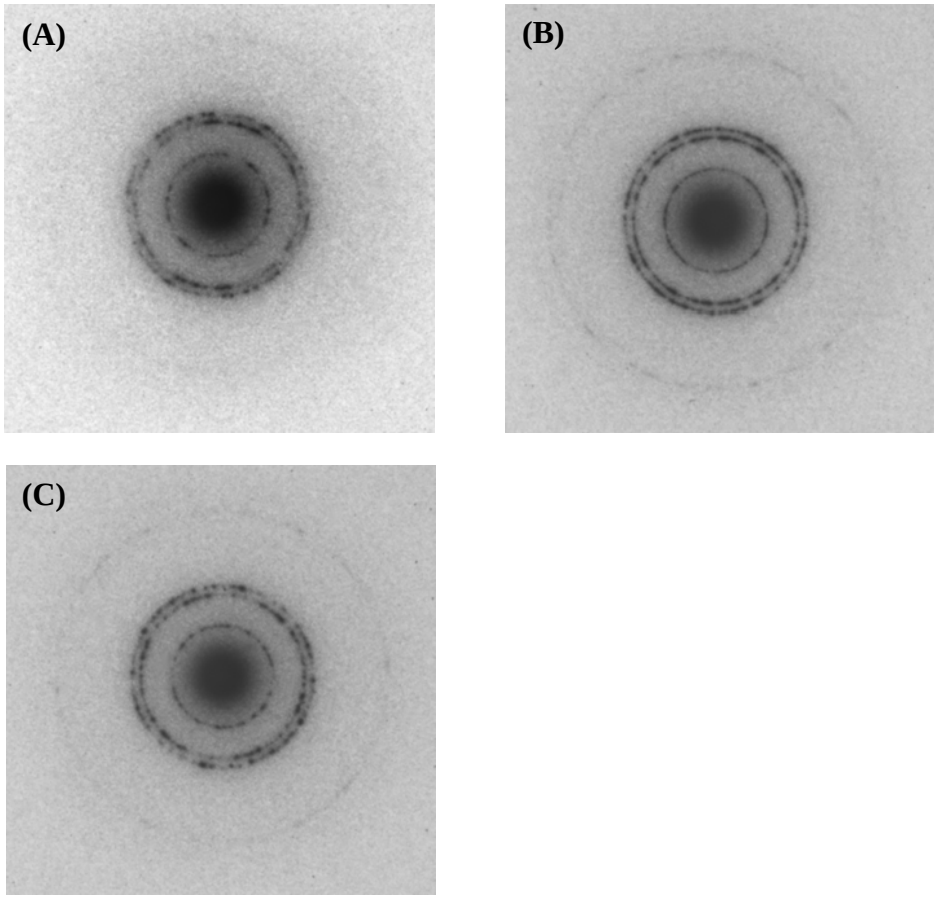

Figure 5. TEM images of the products with using $EGII_{core}$ (A), $EGII_{core2}$ (B), and $EGII_{core2H}$ (C).

Enzymatic polymerization in the quartz optical cell. Enzymatic polymerization was carried out in a quarts optical cell at room temperature, and was monitored by polarization microscopy (Figure 6). In the polymerization with using $EGII_{core2}$, a limited number of spherulites were observed in 30 min. These spherulites were identified as negative type under a polarization optical microscope with a sensitive tint plate (Figure 6D). They showed yellow at the couple of the quadrants parallel to the z' axis of the sensitive tint plate and blue at the other quadrants. Each spherulite displayed birefringence with Maltese cross under cross nicols. The spherulites grew up to be as large as about 10 μm, and the number of spherulites of this size increased with time up to 8 h. When $EGII_{core}$ was used as catalyst, spherulites of the same type were observed except the size of spherulites was about half of

that with $EGII_{core2}$ (Figure 6B). The number of spherulites reached a saturated state in 12 h. The larger size and the shorter period for the saturation of the spherulites generated by $EGII_{core2}$ than those by $EGII_{core}$ are considered to be due to the faster polymerization rate of $EGII_{core2}$ than $EGII_{core}$.

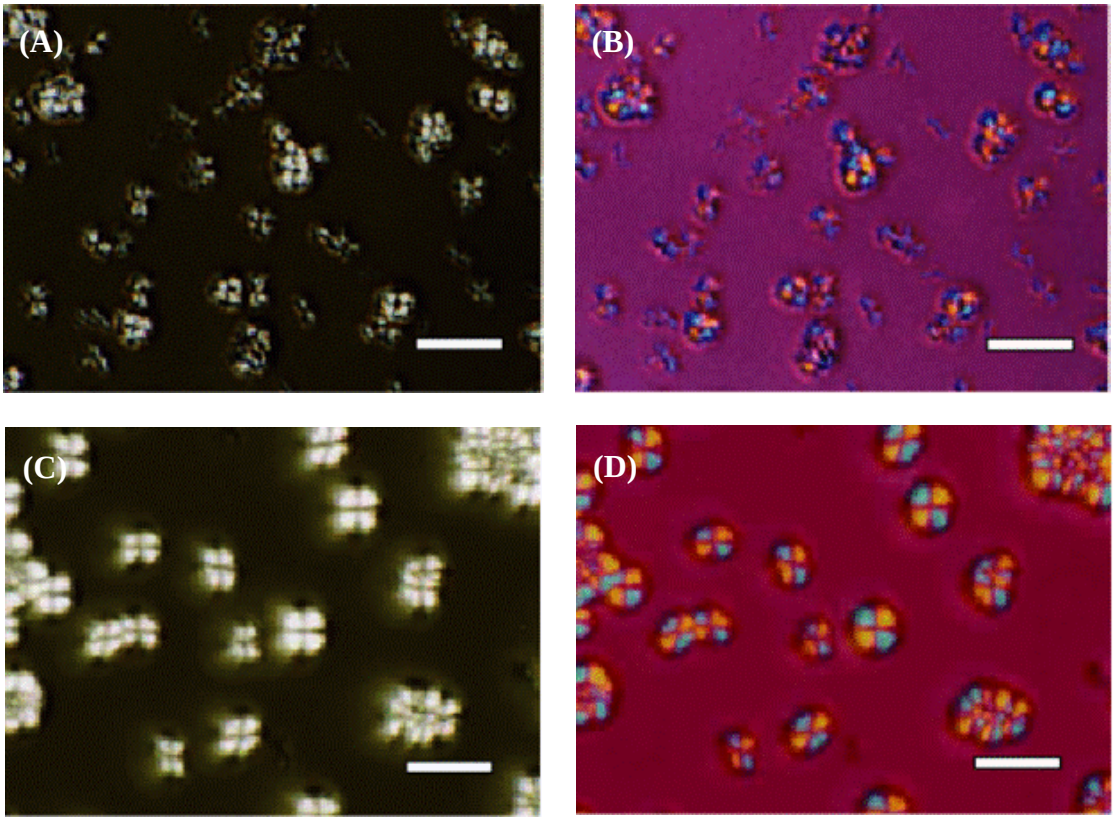

Figure 6. Polymerization optical micrographs of artificial cellulose spherulites generated by $EGII_{core}$ (A) and (B) and $EGII_{core2}$ (C) and (D). Micrographs under cross nicols, (A) and (C); under cross nicols with a sensitive tint plate (R = 530 nm, z' axis lies on the diagonal line through the first and third quadrants), (B) and (D). Bar = 20 μM.

Under the present polymerization conditions, the spherulites show only negative type structure, indicating that the orientation of cellulose chains composing the spherulite is predominantly tangential.[42] The texture of the spherulites prepared with using $EGII_{core2}$ was analyzed in detail by electron microscopy, TEM and FE-SEM. A dispersion of negative type spherulites was briefly shaken mechanically to obtain spherulite fragments. From TEM

observation, the spherulites formed thin plate-like shape and these were identified cellulose of type II by electron diffraction as described above (Figure 7A). The SEM picture of the spherulites showed a clear three-dimensional round shape (Figure 7B).[41] The diameter of each spherulite obtained from SEM observation was about 10 μm, and this is in good agreement with that obtained from the optical microscopy. Intriguingly, these spherulites were composed of accumulation of thin crystal lamella which originated radially from the center (Figure 7B).

The spherulite size generated by $EGII_{core2}$ was larger than that by $EGII_{core}$ probably due to the faster polymerization rate of the former mutant. The higher local concentration of cellulose chains should be favorable for crystalline formation to afford those spherulites. Further, $EGII_{core2}$ may have a characteristic ability to increase the local concentration of the products because the two catalytic sites are located closely in the protein.

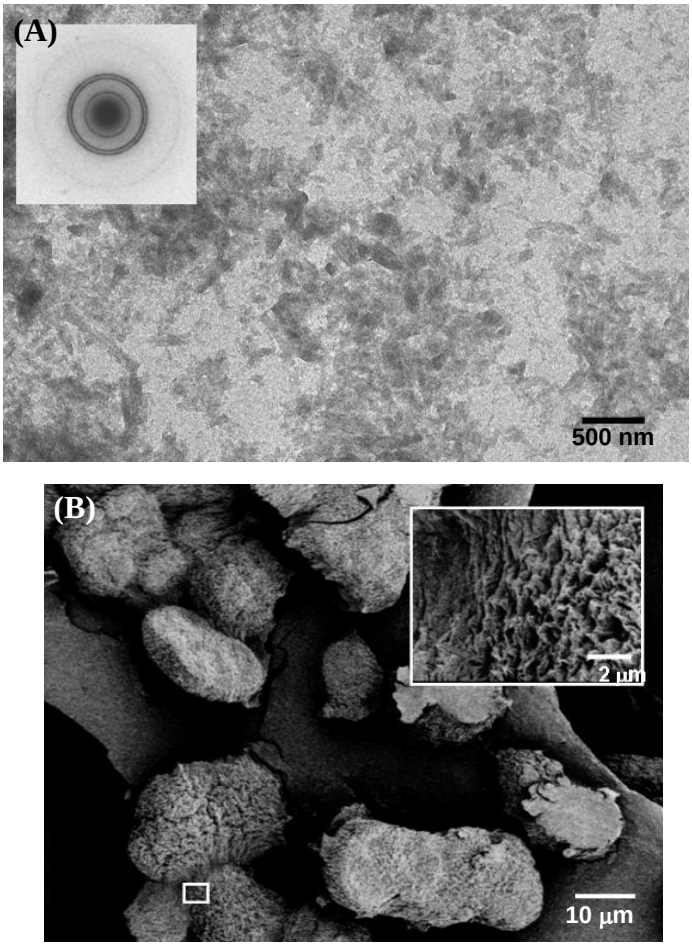

Figure 7. TEM (A) and SEM (B) images of enzymatic polymerization products in a quartz cell with using $EGII_{core2}$ as catalyst. The products were slightly deassembled by vortex.

References

(1) Liu, C. X.; Bai, R. B. *J. Membr. Sci.* **2006**, *284*, 313–322.

(2) Zhang, X. L.; Sun, F. C.; Peng, X. W.; Jin, W. R. *Anal. Chem.* **2007**, *79*, 1256–1261.

(3) Heinze, T.; Koschella, A. *Macromol. Symp.* **2005**, *223*, 13–39.

(4) Kobayashi, S.; Ohmae, M. *Adv. Polym. Sci.* **2006**, *194*, 159–210.

(5) Faijes, M.; Planas, A. *Carbohydr. Res.* **2007**, *342*, 1581–1594.

(6) Kobayashi, S.; Uyama, H.; Kimura, S. *Chem. Rev.* **2001**, *101*, 3793–818.

(7) Okamoto, E.; Kiyosada, T.; Shoda, S. I.; Kobayashi, S. *Cellulose* **1997**, *4*, 161–172.

(8) Kobayashi, S.; Kiyosada, T.; Shoda, S. *J. Am. Chem. Soc.* **1996**, *118*, 13113–13114.

(9) Sakamoto, J.; Kobayashi, S. *Chem. Lett.* **2004**, *33*, 698–699.

(10) Sakamoto, J.; Sugiyama, J.; Kimura, S.; Imai, T.; Itoh, T.; Watanabe, T.; Kobayashi, S. *Macromolecules* **2000**, *33*, 4155–4160.

(11) Ochiai, H.; Ohmae, M.; Mori, T.; Kobayashi, S. *Biomacromolecules* **2005**, *6*, 1068–84.

(12) Fujikawa, S.; Ohmae, M.; Kobayashi, S. *Biomacromolecules* **2005**, *6*, 2935–2942.

(13) Kobayashi, S.; Makino, A.; Matsumoto, H.; Kunii, S.; Ohmae, M.; Kiyosada, T.; Makiguchi, K.; Matsumoto, A.; Horie, M.; Shoda, S. I. *Biomacromolecules* **2006**, *7*, 1644–1656.

(14) Fujita, M.; Shoda, S.; Kobayashi, S. *J. Am. Chem. Soc.* **1998**, *120*, 6411–6412.

(15) Kobayashi, S.; Kashiwa, K.; Kawasaki, T.; Shoda, S. *J. Am. Chem. Soc.* **1991**, *113*, 3079–3084.

(16) Lee, J. H.; Brown, R. M.; Kuga, S.; Shoda, S.; Kobayashi, S. *Proc. Natl. Acad. Sci. U. S. A.* **1994**, *91*, 9195–9195.

(17) Henrissat, B. *Cellulose* **1994**, *1*, 169–196.

(18) Nakamura, I.; Yoneda, H.; Maeda, T.; Makino, A.; Ohmae, M.; Sugiyama, J.; Ueda, M.; Kobayashi, S.; Kimura, S. *Macromol. Biosci.* **2005**, *5*, 623–628.

(19) Okuda, K.; Tsekos, I.; Brown, R. M. *Protoplasma* **1994**, *180*, 49–58.

(20) Cousins, S. K.; Brown, R. M. *Polymer* **1995**, *36*, 3885–3888.

(21) Penttila, M. E.; Andre, L.; Saloheimo, M.; Lehtovaara, P.; Knowles, J. K. C. *Yeast* **1987**, *3*, 175–185.

(22) Skipper, N.; Sutherland, M.; Davies, R. W.; Kilburn, D.; Miller, R. C.; Warren, A.; Wong, R. *Science* **1985**, *230*, 958–961.

(25) Kanai, T.; Atomi, H.; Umemura, K.; Ueno, H.; Teranishi, Y.; Ueda, M.; Tanaka, A. *Appl. Microbiol. Biotechnol.* **1996**, *44*, 759–765.

(26) Kurjan, J.; Herskowitz, I. *Cell* **1982**, *30*, 933–943.

(27) Ito, H.; Fukuda, Y.; Murata, K.; Kimura, A. *J. Bacteriol.* **1983**, *153*, 163–168.

(28) Beguin, P. *Anal. Biochem.* **1983**, *131*, 333–336.

(29) Nelson, N. *J. Biol. Chem.* **1944**, *153*, 375–380.

(30) Somogyi, M. *J. Biol. Chem.* **1952**, *195*, 19–23.

(31) Lowry, O. H.; Rosebrough, N. J.; Farr, A. L.; Randall, R. J. *J. Biol. Chem.* **1951**, *193*, 265–275.

(32) Janknecht, R.; Demartynoff, G.; Lou, J.; Hipskind, R. A.; Nordheim, A.; Stunnenberg, H. G. *Proc. Natl. Acad. Sci. USA* **1991**, *88*, 8972–8976.

(33) Sulkowski, E. *Trends Biotechnol.* **1985**, *3*, 1–7.

(34) Porath, J.; Carlsson, J.; Olsson, I.; Belfrage, G. *Nature* **1975**, *258*, 598–599.

(35) Field, J.; Nikawa, J.; Broek, D.; Macdonald, B.; Rodgers, L.; Wilson, I. A.; Lerner, R. A.; Wigler, M. *Mol. Cell. Biol.* **1988**, *8*, 2159–2165.

(36) Yang, J. T.; Wu, C. S. C.; Martinez, H. M. *Methods Enzymol.* **1986**, *130*, 208–269.

(37) Greenfie.N; Fasman, G. D. *Biochemistry* **1969**, *8*, 4108–&.

(38) Nikonenko, N. A.; Buslov, D. K.; Sushko, N. I.; Zhbankov, R. G. *Biopolymers* **2000**, *57*, 257–262.

(39) Forziati, F. H.; Rowen, J. W. *J. Res. Nat. Bur. Stand.* **1951**, *46*, 38–42.

(40) Buleon, A.; Chanzy, H. *J. Polym. Sci. Part B-Polym. Phys.* **1978**, *16*, 833–839.

(41) Kobayashi, S.; Hobson, L. J.; Sakamoto, J.; Kimura, S.; Sugiyama, J.; Imai, T.; Itoh, T. *Biomacromol.* **2000**, *1*, 509–509.

(42) Helbert, W.; Chanzy, H.; Planchot, V.; Buleon, A.; Colonna, P. *Int. J. Biol. Macromol.* **1993**, *15*, 183–187.

Chapter 3

Immobilization of His-tagged Endoglucanase on Gold via Various Ni-NTA Self-Assembled Monolayers And Its Hydrolytic Activity

Introduction

In recent years, affinity tags have widely used for purification of genetically engineered proteins, and expression of tagged recombinant proteins have become a standard technique in molecular biology.[1,2] There are many affinity tags such as the GST tag,[3–5] the MBP tag,[6,7] the HA tag,[8,9] the myc tag,[10] the FLAG tag[11,12] and the His-tag.[4,12,13] The His-tag consists of six consecutive (or more) histidine residues, which specifically binds the Ni ion. For purification of His-tagged proteins by affinity chromatography, Ni ions are usually immobilized on the resin by multidentate chelators such as iminodiacetic acid (IDA),[14–16] nitrilotriacetic acid (NTA)[17,18] and tris-carboxymethyl ethylenediamine (TED).[14,19] The most utilized chelator is NTA.[20–22] The affinity of His-tagged proteins and Ni–NTA is reported to be as high as 10^6–10^9.[23]

The author have prepared genetically engineered endoglucanases, $EGII_{core}$ with an active site and $EGII_{core2}$ with two successive active sites, described in Chapter 1 and Chapter 2, respectively, to obtain an efficient cellulase for hydrolysis of amorphous cellulose and/or enzymatic polymerization to afford artificial celluoses.[24,25] $EGII_{core2}$ showed higher hydrolysis and polymerization activities than $EGII_{core}$ due to the stabilized conformation. In this Chapter, the author immobilized $EGII_{core2}$ on gold via three different kinds of anchor molecules having a Ni-NTA moiety, and analyzed the binding properties and hydrolytic activities on gold.

The molecular structures of anchor molecules are shown in Figure 1, which have a disulfide or a thiol group, a NTA moiety, and a spacer chain. When the spacer chain has enough molecular length to diminish the steric hindrance of gold substrate, the affinity with THE anchor and the hydrolytic activity of the His-tagged enzyme were expected to be promoted despite of immobilization.

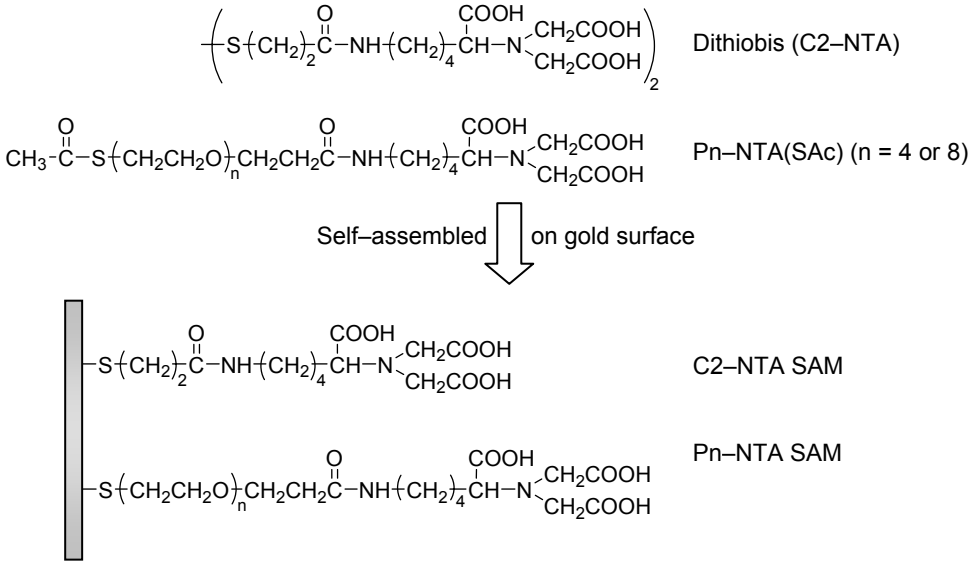

Figure 1. Chemical structure of anchor molecules used for the formation of SAMs on gold surfaces.

Experimental section

Materials. S-acetyl dPEG^{TM}4-NHS ester and S-acetyl dPEG^{TM}8 NHS ester were obtained from Quanta Biodesign, Ltd. (USA) and used as received. *N*-(5-amino-1-carboxypentyl) iminodiacetic acid (AB-NTA) and 3,3′-Dithiobis [*N*-(5-amino-5-carboxypentyl) propionamide-*N′,N′*-diacetic acid] dihydrochloride (dithiobis (C2-NTA)) were purchased from DOJINDO (Japan) and used as received. Organic reagents and solvents were used without purification except specified.

P4-NTA(SAc). A solution of S-acetyl dPEG^{TM}4-NHS ester (70 mg, 0.17 mmol) in anhydrous dimethylsulfoxide (DMSO, 1 mL) was reacted with AB-NTA (44 mg, 0.17 mmol) in DMSO (1 mL) in the presence of triethylamine (70 μL, 0.51 mmol) under Ar atmosphere at room temperature for 24 h. The reaction solution was then purified by a Sephadex LH20 column (DMSO as eluant) and condensed. The residue was dissolved in chloroform, and

hexane was added to precipitate the product. The precipitate was dissolved in deionized water, followed by lyophilization to afford P4-NTA(SAc) (63 mg, 65%). ^{1}H NMR (400 MHz, $CDCl_3$): δ(ppm) 9.53 (s, 3H, COOH), 7.17 (s, 1H, amide), 3.72–3.57 (m, 21H, SCH_2CH_2O, $(CH_2CH_2O)_3$, OCH_2CH_2CONH, $CH_2CH(COOH)$, $N(CH_2COOH)_2$), 3.21 (s, 2H, $NHCH_2$), 3.07 (t, 2H, SCH_2CH_2O), 2.49 (s, 2H, OCH_2CH_2CO), 2.30 (s, 3H, acetyl), 1.84 (s, 1H, $CH_2CH(COOH)$), 1.68 (s, 1H, $CH_2CH(COOH)$), 1.50 (s, 4H, $CONHCH_2CH_2CH_2CH_2$). MS (FAB, matrix; NBA/DTT with oxalic acid): *m/z* = 591.2 (calcd for $C_{23}H_{40}N_2O_{12}SNa$ $[(M+Na)^+]$ *m/z* = 591.2)

P8-NTA(SAc). A solution of S-acetyl dPEG^{TM}8 NHS ester (100 mg, 0.17 mmol) in anhydrous DMSO (1 mL) was treated as described above to afford P8-NTA(SAc) (94 mg, 76%). ^{1}H NMR (400 MHz, $CDCl_3$) δ(ppm): 9.49 (s, 3H, COOH), 7.15 (s, 1H, amide), 3.81–3.55 (m, 37H, SCH_2CH_2O, $(CH_2CH_2O)_7$, OCH_2CH_2CONH, $CH_2CH(COOH)$, $N(CH_2COOH)_2$), 3.19 (s, 2H, $NHCH_2$), 3.06 (t, 2H, SCH_2CH_2O), 2.47 (s, 2H, OCH_2CH_2CO), 2.31 (s, 3H, acetyl), 1.82 (s, 1H, $CH_2CH(COOH)$), 1.64 (s, 1H, $CH_2CH(COOH)$), 1.48 (s, 4H, $CONHCH_2CH_2CH_2CH_2$). MS (FAB, matrix; NBA/DTT with oxalic acid): *m/z* = 745.3 (calcd for $C_{31}H_{57}N_2O_{16}S$ $[(M+H)^+]$ *m/z* = 745.3)

Purification of secretory mutant EGII$_{core2}$. Transformed yeast cells were constructed by the method as described in Chapter 2.[25] The purification method of the secreted protein was modified slightly. Briefly, the crude enzyme solution was concentrated by stirred ultrafiltration cell (ultrafiltration membrane; NMWL 30,000, Millipore), and the supernatant was incubated with Ni-NTA agarose beads on shaker over 6 h. The bound His-tagged enzyme was recovered from the beads by using 100 mM imidazole in a phosphate buffer. The collected fractions which showed hydrolysis activity were finally purified by GPC using Sephacryl S-200 HR (GE Healthcare). The purity of the enzyme was checked by SDS-PAGE with staining by coomassie brilliant blue (CBB) (Nacalai tesque).

The solution of the purified mutant EGII was equilibrated in 10 mM *N*-2-hydroxyethylpiperazine-*N*′-2-ethanesulfonic acid (HEPES) buffer with 150 mM NaCl, 50 μM

etyhlenediaminetetraacetic acid (EDTA) and 0.005% Tween-20 (pH 7.4) or 50 mM acetate buffer (pH 5.0) before use for surface plasmon resonance (SPR) measurement or spectroscopic measurements. The protein concentrations were determined by the Bradford method[26] using bovine serum albumin (BSA) as a standard.

Preparation of NTA SAM sensor chip. The NTA SAM sensor chip was prepared onto the gold surface of Sensor Chip Au (GE Healthcare) as follows. The C2-NTA SAM chip was prepared by incubation of the gold surface with 1.5 mM dithiobis (C2-NTA) aqueous solution at room temperature. After 24 h, the surface was rinsed with Milli-Q water (three times) and dried under a N_2 stream. The P4-NTA SAM or P8-NTA SAM chip was prepared similarly except deprotection of the acetyl group, which was carried out by treatment of the anchor molecule in ethanol or methanol with dimethylamine (60 mol equivalent of the thioacetyl group). The concentration of P4-NTA(SAc) and P8-NTA(SAc) at the preparation was 0.5 and 1.2 mM, respectively.

SPR measurement. SPR experiments were performed by two flow cells system (Fc1 and Fc2), using a NTA SAM sensor chip. All binding experiments were carried out using 10 mM HEPES buffer (150 mM NaCl, 50 μM EDTA and 0.005% Tween-20, pH 7.4) as the running buffer at a flow rate of 10 μL/min at 17.5, 25.0, and 32.5 °C. The running buffer was filtered (0.45 μm) and degassed before use.

In standard SPR experiments, the Fc2 surface of NTA SAM chip was first incubated with a 500 μM $NiSO_4$ aqueous solution for 60 s to form complex between NTA and Ni ions (Ni-NTA surface). The Fc1 was a control experiment cell whose surface was absent from Ni ion. Then, the purified His-tagged enzyme solution was eluted with the running buffer at 75 nM through both Fc1 and Fc2 surfaces for 600 s, followed by a dissociation phase of 1500 s. Then, a 300 mM imidazole aqueous solution was added to the chip for 120 s to release the specifically bound enzyme. A 350 mM EDTA aqueous solution was used for regeneration of the NTA-exposing surface. Each experiment was performed in triplicate.

The kinetics parameters (association rate constant k_a, dissociation rate constant k_d equilibrium association constant K_A) were calculated by local fitting of 1:1 Langmuir binding model to each sensorgram with using the BIAevaluation Ver. 4.1 program.

The thermodynamic parameters (enthalpy ΔH, entropy ΔS and Gibbs free energy ΔG), were calculated by the van't Hoff equation (equilibrium state):

$$\ln K_A = \Delta S^o / R - \Delta H^o / RT = \Delta G^o / RT$$

or by the Eyring equation (transition state):

$$\ln k = \Delta S^{o\ddagger} / R - \Delta H^{o\ddagger} / RT + \ln k_B / \hbar$$

where R is gas constant, k_B is Boltzmann constant, and $\hbar$ is Plank's constant.

Immobilization of enzyme on gold substrate. The gold substrate for immobilization of enzyme was prepared by vacuum deposition method. Chromium (300 Å) and then gold (99.99%, 2000 Å) were deposited on a glass slide (5 mm × 76 mm). The glass slide was treated by sulfuric acid before use. The prepared gold substrate was immediately immersed in a NTA derivative solution for 24 h at room temperature followed by rinsing with ethanol or Milli-Q water for 1 min (three times) and dried under a N_2 steam. The substrate was incubated with a 500 mM $NiSO_4$ aqueous solution for 3 h at room temperature, rinsed with Milli-Q water for 1 min (three times) and dried under a N_2 steam. Finally, the substrate was incubated with a 20 nM enzyme solution (50 mM acetate buffer, pH 5.0) for 24 h at 4 °C. The substrate was rinsed with 20 mM acetate buffer (pH 5.0) for 1 min (three times) and dried under a N_2 steam.

Fourier transform infrared-reflection absorption spectroscopy (FTIR-RAS) measurement. FTIR-RAS spectra were performed with a Harrick RMA-1DG/VRA reflection attachment. The incident angle was set at 84° from the surface normal. The number of interferogram accumulations was approximately 200.

Hydrolytic activity assays of immobilized enzyme. The hydrolysis reaction was performed by immersing the immobilized enzyme in a substrate solution (50 mM acetate

buffer, pH 5.0) and incubated at 50 °C. Aliquots of the supernatant of the substrate solution were extracted after specified periods and diluted with eluant buffer of HPLC. Substrates were 1 w/v% CMC (high-molecular weight substrate) or 0.1 w/v% cellohexaose (low-molecular weight substrate). The reaction using free enzyme (1.0×10^{-3} or 5.3×10^{-4} wt% against CMC or cellohexaose, respectively) was also performed as a control experiment. HPLC measurements were performed on a BORWIN system (JASCO) consisting of a PU-980 pump, AS-950 autosumplar, and RI-930 RI detector. The chromatographic column used was a OHpak SB-802 HQ column (Tosoh) eluting with a 0.3 M $NaNO_3$ aqueous solution filtered and degassed before use. The flow rate was 0.5 mL/min and column temperature was 40 °C.

Results and discussions

Preparation of mutant enzyme and anchor molecules. The secreted mutant enzyme from the yeast cells was purified by the His-tag affinity chromatography and the GPC. The purified mutant $EGII_{core2}$ showed a single band on SDS-PAGE stained with CBB, which confirmed the molecular weight of the designed enzyme and the high purity of the obtained $EGII_{core2}$.

Pn-NTA(SAc) (n = 4 or 8) was synthesized by conventional organic chemical reaction as Scheme 1 and confirmed by ^1H NMR and mass spectroscopy.

Scheme 1. Synthetic route of Pn-NTA(SAc).

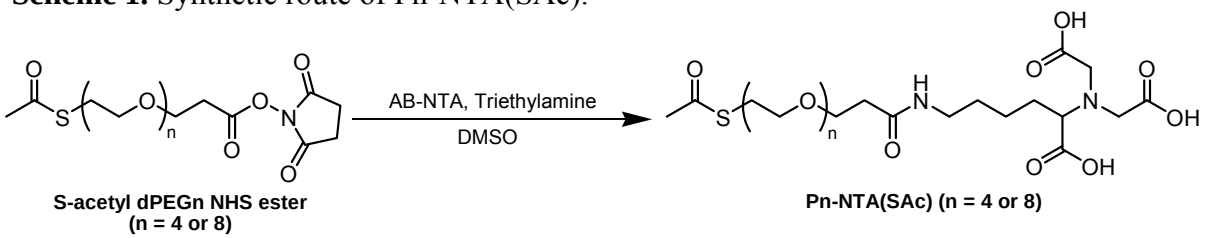

Binding of $EGII_{core2}$ with Ni-NTA surfaces. Three anchor molecules were self-assembled on Au chips for SPR measurements. Ni ions were chelated by the NTA moieties on the SAMs upon incubation in a $NiSO_4$ aqueous solution, which increased the resonance unit of 37.5 ± 8.2, 47.8 ± 3.3, and 45.7 ± 2.0 RU (corresponding 0.40, 0.50, and 0.48 pmol/mm^2 of a Ni ion with two water molecules) on the C2-NTA, P4-NTA and P8-NTA SAM chip surfaces, respectively. These densities should be equal to the amounts of the NTA sites introduced on the sensor chip surfaces. Even though there were slight differences in the amounts of the NTA sites on the surfaces, they existed on the chips excessively for immobilization of the enzyme having a large size compared with the anchor molecules.

When $EGII_{core2}$ was incubated with the C2-NTA SAM without the treatment of Ni chelation, a small amount of $EGII_{core2}$ adsorbed on the surface. This nonspecific binding of $EGII_{core2}$ was found to be about 10% of the total amount of $EGII_{core2}$ remaining on the C2-NTA-Ni surface (Figure 2A). On the other hand, the nonspecific binding of $EGII_{core2}$ on the P4-NTA-Ni or the P8-NTA-Ni surface was not observed, suggesting that the ethyleneoxide oligomers of the spacer moieties suppress the nonspecific binding due to the hydration to them.[27,28] Further, the immobilized $EGII_{core2}$ was washed away completely by treatment with the excess amount of imidazole, indicating that the association and dissociation of $EGII_{core2}$ with the surface were reversible.

The amounts of the immobilized $EGII_{core2}$ were 12, 15 and 7.6 fmol/mm^2 for the surfaces of the C2-NTA-Ni, P4-NTA-Ni and P8-NTA-Ni, respectively, at 25 °C (Figure 2B). Obviously, the P4-NTA-Ni surface shows the highest affinity for $EGII_{core2}$, because the increase of the RU value is the largest and the dissociation at the washing process is very low as shown in the sensorgrams.

Each sensorgram was curve-fitted by using a 1:1 Langmuir binding model to obtain the kinetics parameters (Table 1). The binding constants, K_A, increase in the order of surfaces of P8-NTA-Ni < C2-NTA-Ni < P4-NTA-Ni. The total amounts of the immobilized $EGII_{core2}$ at saturation (R_{max}) also increases in the same order. However, when the rate constants are compared in detail, the association constants, k_a, are large on the C2-NTA-Ni surface irrespective of the temperature. Probably, the C2-NTA-Ni surface may be more hydrophobic

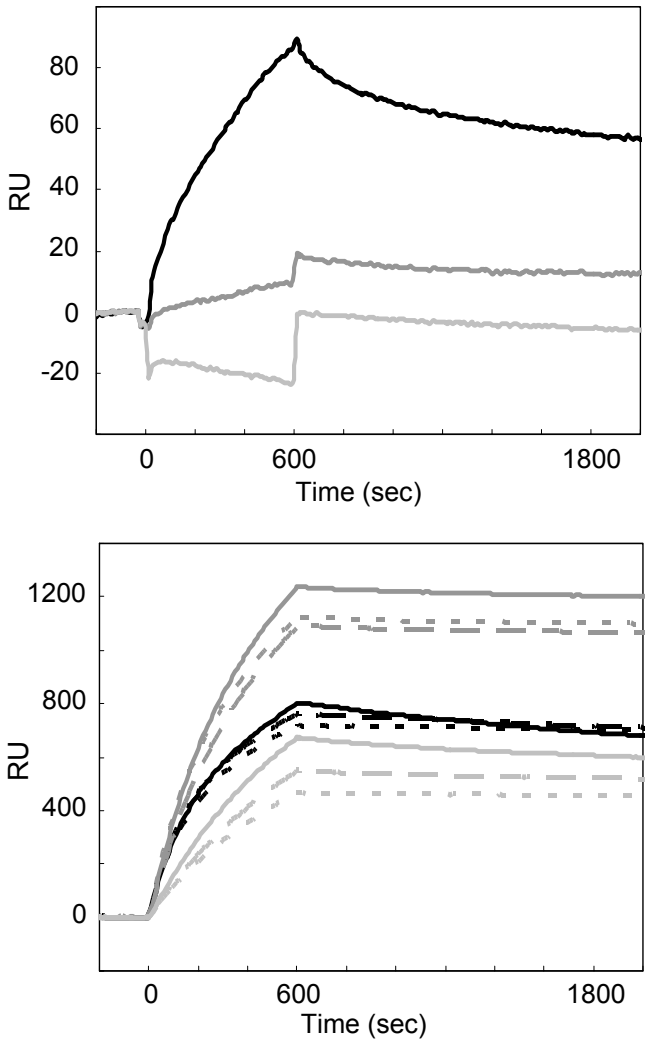

Figure 2. SPR analysis of association and dissociation of $EGII_{core2}$ on the three different surfaces of C2-NTA (black), P4-NTA (gray) and P8-NTA (light gray) SAM without Ni ions at 32.5 ^{o}C (A) and with Ni ions at three different temperatures; 17.5 (dotted line), 25.0 (broken line) and 32.5 ^{o}C (solid line) (B) at 75 nM. The enzyme was added at zero in the sensorgram, and after 600 s the running buffer without the enzyme was eluted.

than the P4-NTA-Ni and P8-NTA-Ni surfaces as shown by the nonspecific binding partially to the C2-NTA-Ni surface, which should increase the association constant. On the other hand, the dissociation constants, k_d, are small on the P4-NTA-Ni surface when they are compared with those at the corresponding temperatures, resulting in the large binding constants on the P4-NTA-Ni surface. It is therefore suggested that there is an optimum length of the anchor molecules around P4, which should counterbalance the reduction of the steric repulsion

between the immobilized $EGII_{core2}$ and the surface using a longer anchor molecule[29] and a large entropic freedom of a longer anchor molecule which is unfavorable for binding of $EGII_{core2}$.

Table 1. Summary of the kinetic parameters between His-tagged enzyme and Ni-NTA surfaces.

Anchor Molecule	Temperature (K)	k_a (1/Ms)	k_d (1/s)	K_A (M)	R_{max} (RU)
C2-NTA	290.65	5.66×10^4	1.11×10^{-5}	5.12×10^9	7.99×10^2
	298.15	5.63×10^4	4.35×10^{-5}	1.31×10^9	8.27×10^2
	305.65	4.57×10^4	1.19×10^{-4}	3.87×10^8	8.56×10^2
P4-NTA	290.65	4.42×10^4	4.75×10^{-6}	9.39×10^9	1.33×10^3
	298.15	3.37×10^4	1.51×10^{-5}	2.22×10^9	1.41×10^3
	305.65	3.25×10^4	1.91×10^{-5}	1.71×10^9	1.39×10^3
P8-NTA	285.65	2.21×10^4	9.94×10^{-6}	2.22×10^9	7.49×10^2
	298.15	1.80×10^4	4.16×10^{-5}	4.33×10^8	9.67×10^2
	305.65	1.90×10^4	8.09×10^{-5}	2.35×10^8	1.17×10^3

The thermodynamic parameters were obtained by analyzing the temperature dependence of the binding constants and the rate constants by the van't Hoff and the Eyring plots (Figure 3) and are summarized in Table 2. Since both ΔH^o and ΔS^o are negative, the association is enthalpically driven, which should be supplied partially by the interaction between Ni ion and His-tag. The largest ΔH^o is obtained with the C2-NTA-Ni surface which is related to the relatively hydrophobic surface as described before. ΔS^o is negative and the absolute value of the C2-NTA-Ni surface is the largest among the three surfaces. Since $EGII_{core2}$ is most closely immobilized to the surface, the steric effect of the surface may reduce the conformational freedom of the immobilized $EGII_{core2}$.

The Eyring plots revealed that the temperature dependence of k_d with the C2-NTA-Ni surface is larger than the others as evaluated by the large $\Delta H^{o\ddagger}$. This observation is also explainable due to the hydrophobic interaction of $EGII_{core2}$ with the surface.

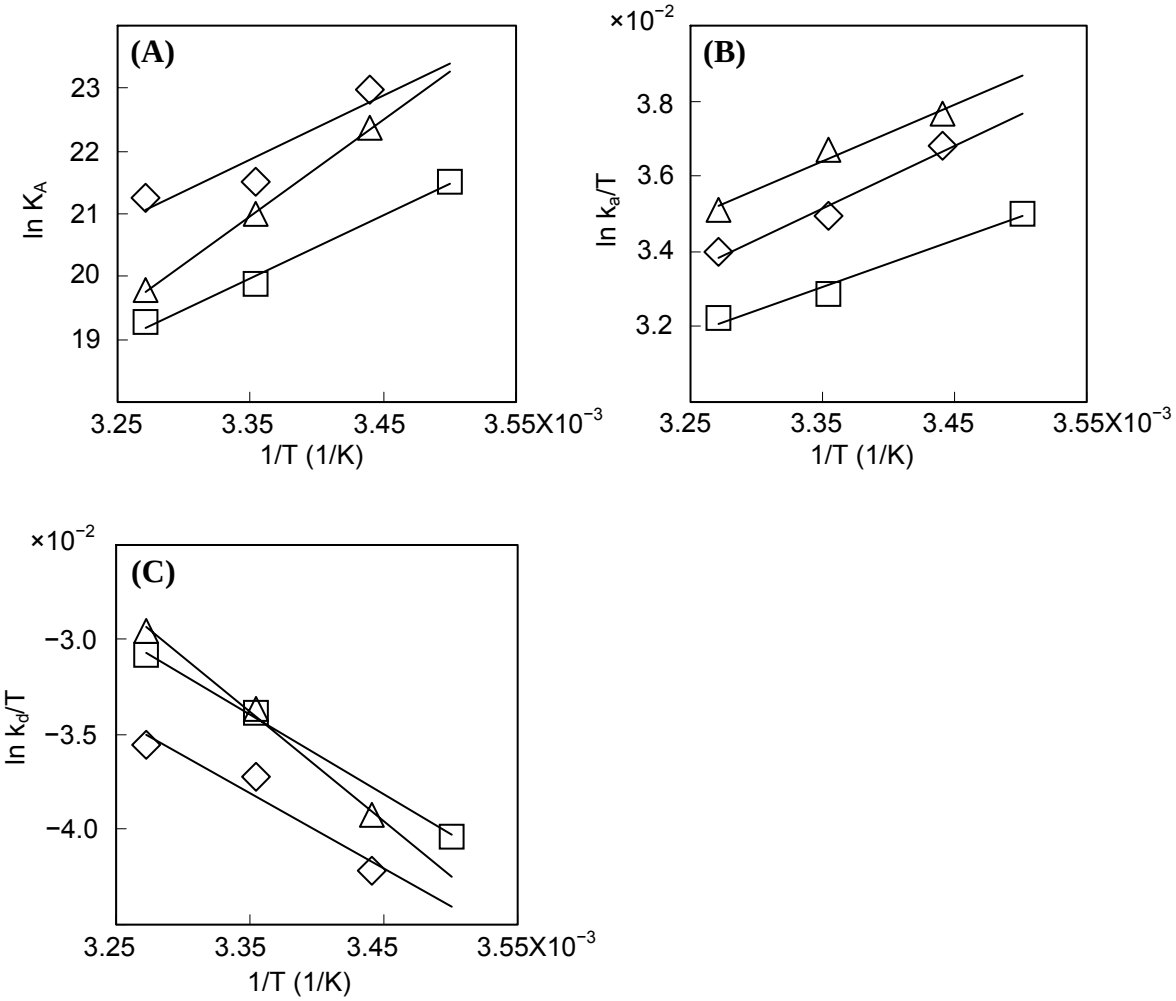

Figure 3. The van't Hoff plot (A) and the Eyring plots (B) and (C) of the association and dissociation of $EGII_{core2}$ on the C2-NTA-Ni (△), P4-NTA-Ni (◇) and P8-NTA-Ni (□) surfaces.

Table 2. Summary of the thermodynamic parameters between His-tagged enzyme and Ni-NTA surfaces.

Interaction Phase	Thermodynamic Parameter	C2-NTA-Ni	P4-NTA-Ni	P8-NTA-Ni
Equilibrium	ΔH^{o} (kJ/mol)	−127	−84.1	−82.9
	ΔS^{o} (kJ/K mol)	−0.251	−0.100	−0.112
	$*\Delta G^{o}$ (kJ/mol)	−52.0	−53.3	−49.3
Association	$\Delta H^{o\ddagger}$	−0.125	−0.139	−0.103
	$\Delta S^{o\ddagger}$	−0.213	−0.213	−0.213
	$*\Delta G^{o\ddagger}$	63.3	63.3	63.4
Dissociation	$\Delta H^{o\ddagger}$	0.477	0.328	0.348
	$\Delta S^{o\ddagger}$	−0.211	−0.212	−0.212
	$*\Delta G^{o\ddagger}$	63.5	63.5	63.5

$*\Delta G^{o} = RT\ln K_A$ or $RT\ln k$ (T = 298.15 K).

FTIR-RAS of immobilized $EGII_{core2}$. The C2-NTA, P4-NTA and P8-NTA SAMs were analyzed by FTIR-RAS. Absorption bands at 1650 and 1740 cm^{-1} are assigned to carboxylate and carboxylic groups, respectively (Figure 4A).[30,31] P4-NTA and P8-NTA showed similar spectra, but C2-NTA exhibited a weaker absorbance at 1650 cm^{-1} and an additional peak at 1710 cm^{-1}, suggesting that the immobilized state of the carboxylic groups of C2-NTA is slightly different from those of P4-NTA and P8-NTA, probably because of the short spacer of C2-NTA.[32]

After chelation of the carboxylic groups with Ni ions, the signals of the carboxyl groups disappeared and a broad signal around 1650 cm^{-1} appeared, suggesting quantitative chelation of the NTA groups with Ni ions. Upon incubation with $EGII_{core2}$, a new signal was observed around 1670 cm^{-1}, which is assigned to amide I band of $EGII_{core2}$ (Figure 4(B)). After subtraction of the Ni-chelated anchor spectrum, the densities of $EGII_{core2}$ are determined to be 5.7, 6.9 and 5.1 fmol/mm^2 for the surfaces of C2-NTA-Ni, P4-NTA-Ni and P8-NTA-Ni, respectively, with taking the molecular extinction coefficient of 9.07×10^9 cm^2/mol, which

was deduced from that of BSA after correction of the molecular weight.[33] The $EGII_{core2}$ densities increase in the order of P8-NTA-Ni < C2-NTA-Ni < P4-NTA-Ni, which agrees with that determined by SPR measurements. However, the densities determined from FTIR-RAS are lower than those from SPR measurements, because of different protein concentrations used for the preparation; 20 nM for FTIR-RAS and 75 nM for SPR measurements.

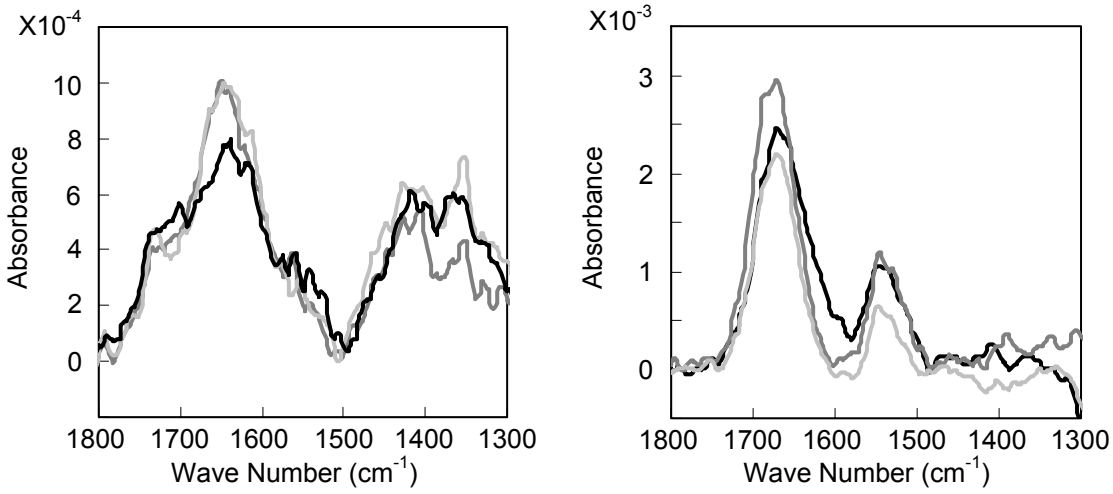

Figure 4. FTIR-RAS spectra of the NTA SAMs of C2-NTA (black), P4-NTA (gray) and P8-NTA (light gray) (A) and the immobilized $EGII_{core2}$ on the C2-NTA-Ni (black), P4-NTA-Ni (gray) and P8-NTA–Ni (light gray) (B).

Hydrolytic activity of immobilized $EGII_{core2}$. The hydrolytic activity of the immobilized $EGII_{core2}$ on the P4-NTA-Ni surface was analyzed with using CMC as a substrate. The reaction solution was analyzed by size-exclusion chromatography. Since $EGII_{core2}$ is the endo-type cellulase, the peak in the elution profile moves to longer elution time with hydrolysis of CMC. Large peak shifts were observed in a few hours after incubation with the immobilized $EGII_{core2}$, indicating that the hydrolytic activity of $EGII_{core2}$ was retained after immobilization on gold. The time course of the hydrolysis with the immobilized $EGII_{core2}$ was similar to that in a solution with free $EGII_{core2}$ (Figure 5). It should be noted that these hydrolysis data are compared under the condition that the total amounts of the immobilized $EGII_{core2}$ on the P4-NTA-Ni surface and of free $EGII_{core2}$ in solution were nearly the same, 1.0

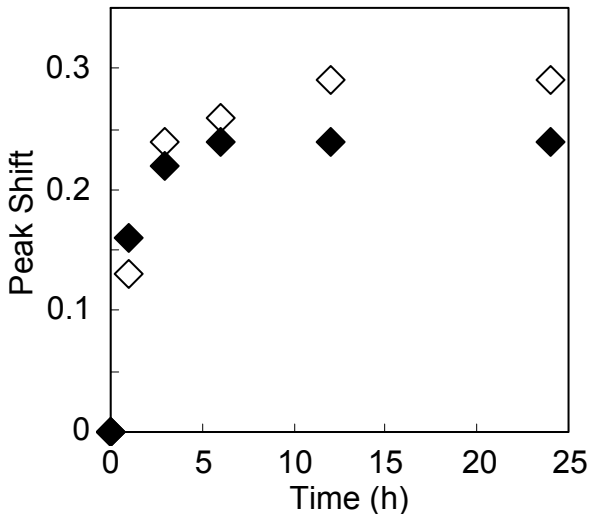

Figure 5. Peak shift of CMC in the elution profiles by HPLC at different times during hydrolysis by the immobilized $EGII_{core2}$ on the P4-NTA-Ni surface (◇) and free $EGII_{core2}$ (◆, 1.0×10^{-3} wt% of CMC).

$\times 10^{-12}$ and 1.5×10^{-12} mol, respectively. The immobilization of $EGII_{core2}$ on the P4-NTA–Ni surface therefore does not impair the hydrolytic activity apparently.

The hydrolytic reaction was analyzed in depth by using cellohexaose as substrate. Time courses of concentration changes of cellohexaose, cellotetraose, cellotriose, and cellobiose are shown in Figure 6. There are no distinct differences in the hydrolytic activities of $EGII_{core2}$ on the different three surfaces. It is thus considered that the immobilized $EGII_{core2}$ retains the hydrolytic activity despite of immobilization at different distances from the gold surface.

The hydrolytic activity of the immobilized $EGII_{core2}$ on the P4-NTA-Ni surface was compared with that of free $EGII_{core2}$ (Figure 6, inset). The total amounts of $EGII_{core2}$ on surface and in solution were set at nearly the same also in these systems as described above. The immobilized $EGII_{core2}$ hydrolyzed cellohexaose as fast as free $EGII_{core2}$, indicating that the immobilized $EGII_{core2}$ retains the inherent hydrolytic activity on the surface. However, there is some difference in the concentration change of cellotetraose between the immobilized and free $EGII_{core2}$, while any distinct difference was not observed in the concentration change

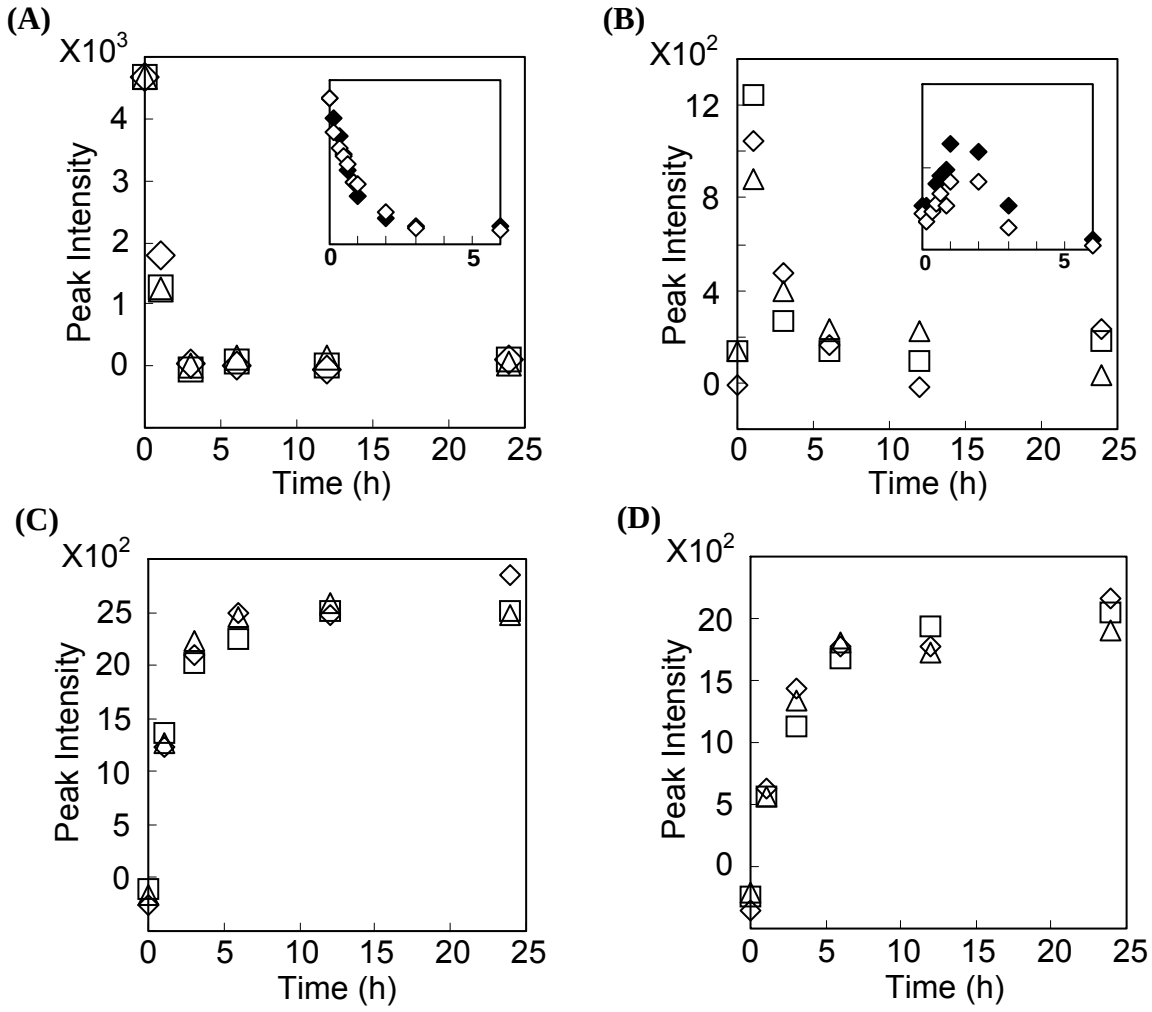

Figure 6. Hydrolysis of cellohexaose by the immobilized $EGII_{core2}$ on C2-NTA–Ni (△), P4-NTA-Ni (◇) and P8-NTA-Ni (□) at 50 °C. The time-courses of cellohexaose (A), cellotetraose (B), cellotriose (C) and cellobiose (D). The insets of (A) and (B) are the detailed time-courses of early stage using immobilized $EGII_{core2}$ on P4-NTA-Ni (◇) and free $EGII_{core2}$ (◆).

of cellotriose. The amount of cellotetraose transiently produced by the immobilized $EGII_{core2}$ is less than that by free $EGII_{core2}$ in solution (Figure 6(B), inset). Regarding cellotetraose, it is produced by hydrolysis of cellohexaose, and reduces the amount with further hydrolysis into two molecules of cellobiose. On the other hand, in the case of cellotriose, cellohexaose should be hydrolyzed into two cellotriose, because cellotriose (and cellobiose) are no longer a substrate for $EGII_{core2}$. It is therefore considered that cellotetraose generated by the

immobilized $EGII_{core2}$ should be susceptible to the following hydrolysis into cellobiose because the local concentration of the $EGII_{core2}$ on the surface is much higher than in solution. This interpretation can also explain the similar hydrolytic activity of the immobilized $EGII_{core2}$ as that of free $EGII_{core2}$.

References

(1) Terpe, K. *App. Microbiol. Biotechnol.* **2003**, *60*, 523–533.

(2) Uhlen, M. *Biotechniques* **2008**, *44*, 649–654.

(3) Smith, D. B.; Johnson, K. S. *Gene* **1988**, *67*, 31–40.

(4) Scheich, C.; Sievert, V.; Bussow, K. *BMC Biotechnol.* **2003**, *3*.

(5) Frangioni, J. V.; Neel, B. G. *Anal. Biochem.* **1993**, *210*, 179–187.

(6) Diguan, C.; Li, P.; Riggs, P. D.; Inouye, H. *Gene* **1988**, *67*, 21–30.

(7) Fox, J. D.; Routzahn, K. M.; Bucher, M. H.; Waugh, D. S. *FEBS Lett.* **2003**, *537*, 53–57.

(8) Field, J.; Nikawa, J.; Broek, D.; Macdonald, B.; Rodgers, L.; Wilson, I. A.; Lerner, R. A.; Wigler, M. *Molecular and Cellular Biology* **1988**, *8*, 2159–2165.

(9) Tyers, M.; Tokiwa, G.; Nash, R.; Futcher, B. *Embo Journal* **1992**, *11*, 1773–1784.

(10) Evan, G. I.; Lewis, G. K.; Ramsay, G.; Bishop, J. M. *Molecular and Cellular Biology* **1985**, *5*, 3610–3616.

(11) Hopp, T. P.; Prickett, K. S.; Price, V. L.; Libby, R. T.; March, C. J.; Cerretti, D. P.; Urdal, D. L.; Conlon, P. J. *Bio-Technology* **1988**, *6*, 1204–1210.

(12) Nilsson, J.; Larsson, M.; Stahl, S.; Nygren, P. A.; Uhlen, M. *J. Mol. Recognit.* **1996**, *9*, 585–594.

(13) Porath, J.; Carlsson, J.; Olsson, I.; Belfrage, G. *Nature* **1975**, *258*, 598-599.

(14) Sulkowski, E. *Trends in Biotechnology* **1985**, *3*, 1–7.

(15) Vandyke, M. W.; Sirito, M.; Sawadogo, M. *Gene* **1992**, *111*, 99–104.

(16) Lin, D. Q.; Yao, S. J.; Mei, L. H.; Zhu, Z. Q. *Chinese Journal of Chemical Engineering* **2000**, *8*, 310–314.

(17) Hochuli, E.; Dobeli, H.; Schacher, A. *J. Chromatogr.* **1987**, *411*, 177–184.

(18) Hochuli, E.; Bannwarth, W.; Dobeli, H.; Gentz, R.; Stuber, D. *Bio-Technology* **1988**, *6*, 1321–1325.

(19) McCurley, M. F.; Seitz, W. R. *Talanta* **1989**, *36*, 341–346.

(20) Janknecht, R.; Demartynoff, G.; Lou, J.; Hipskind, R. A.; Nordheim, A.; Stunnenberg, H. G. *Proc. Natl. Acad. Sci. U. S. A.* **1991**, *88*, 8972–8976.

(21) Sigal, G. B.; Bamdad, C.; Barberis, A.; Strominger, J.; Whitesides, G. M. *Anal. Chem.* **1996**, *68*, 490–497.

(22) Schmitt, J.; Hess, H.; Stunnenberg, H. G. *Molecular Biology Reports* **1993**, *18*, 223–230.

(23) Nieba, L.; NiebaAxmann, S. E.; Persson, A.; Hamalainen, M.; Edebratt, F.; Hansson, A.; Lidholm, J.; Magnusson, K.; Karlsson, A. F.; Pluckthun, A. *Anal. Biochem.* **1997**, *252*, 217–228.

(24) Nakamura, I.; Yoneda, H.; Maeda, T.; Makino, A.; Ohmae, M.; Sugiyama, J.; Ueda, M.; Kobayashi, S.; Kimura, S. *Macromol. Biosci.* **2005**, *5*, 623–628.

(25) Nakamura, I.; Makino, A.; Sugiyama, J.; Ohmae, M.; Kimura, S. *Int. J. Biol. Macromol.* **2008**, *43*, 226–231.

(26) Bradford, M. M. *Anal. Biochem.* **1976**, *72*, 248–254.

(27) McPherson, T.; Kidane, A.; Szleifer, I.; Park, K. *Langmuir* **1998**, *14*, 176–186.

(28) Lee, J. K.; Kim, Y. G.; Chi, Y. S.; Yun, W. S.; Choi, I. S. *J. Phys. Chem. B* **2004**, *108*, 7665–7673.

(29) Kroger, D.; Liley, M.; Schiweck, W.; Skerra, A.; Vogel, H. *Biosens. Bioelectron.* **1999**, *14*, 155–161.

(30) Nakamoto, K.; Morimoto, Y.; Martell, A. E. *J. Am. Chem. Soc.* **1962**, *84*, 2081–&.

(31) Rigler, P.; Ulrich, W. P.; Hoffmann, P.; Mayer, M.; Vogel, H. *ChemPhysChem* **2003**, *4*, 268–275.

(32) Valiokas, R.; Klenkar, G.; Tinazli, A.; Reichel, A.; Tampe, R.; Piehler, J.; Liedberg, B. *Langmuir* **2008**, *24*, 4959–4967.

(33) Yokoyama, Y.; Ishiguro, R.; Maeda, H.; Mukaiyama, M.; Kameyama, K.; Hiramatsu, K. *J. Colloid Interface Sci.* **2003**, *268*, 23–32.

Chapter 4

Enzymatic Polymerization Catalyzed by

Immobilized Endoglucanase on Gold

Introduction

Cellulose is the most abundant natural polymer on the earth. During the past decade, cellulose is recognized as important materials as ever in terms of green polymer and now is receiving particular attention as a new class of raw material for bioethanol.[1,2] In nature, cellulose is biosynthesized by cellulose synthase complex (EC 2.4.1.12) using uridine-5'-diphospho (UDP)-glucose as substrate monomer.[3,4] Interestingly, the spatial configuration of synthase complex decides crystalline forms of biosynthesized cellulose; synthases in a linear arrangement produce triclinic cellulose and synthases arranged in a rosette shape yield monoclinic cellulose.[5] Further, it is also shown that the thickness and the crystallinity of cellulose microfibrils were influenced by the arrangement of synthesizing complexes.[6,7] The spatial configuration of the enzyme is thus the key to regulate the physical properties of produced cellulose.

Recently, *in vitro* syntheses of cellulose catalyzed by various enzymes have been studied.[8–10] The enzyme usage in cellulose synthesis is advantageous regarding the strict regio- and stereo-selective reaction to produce highly controlled β-1, 4 structures. The author have studied enzymatic polymerization using genetically-engineered EG II (EC 3.2.1.4) from *T. viride* as catalyst.[11,12] EGII polymerizes β-cellobiosyl fluoride in acetonitrile/acetate buffer system.[8,13–15] In Chapter 3, $EGII_{core2}$, which is composed of two catalytic domains with a His-tag, was prepared by genetic engineering and immobilized on gold, and its hydrolysis activity on gold was studied. In this Chapter, the author extend the research on mutant $EGII_{core2H}$ having two His-tags at both terminals of the sequence in addition to $EGII_{core2}$ with an aim to immobilize the enzyme firmly to the surface with a defined orientation. Enzymatic polymerization by the immobilized enzymes on gold stands on the idea to mimic the natural cellulose synthases located at plasma membrane surface.[16]

The mutant EGIIs are immobilized on gold by binding of the His-tag to the NTA terminated SAM through Ni ion similarly the other reports.[17–19] The author use a NTA derivative in Figure 1, which is optimized as an anchor molecule for the His-tagged enzyme from the other and Chapter 3.[20,21] Immobilization of $EGII_{core2H}$ on gold is analyzed by SPR

method. The products which are obtained by polymerization reaction catalyzed by immobilized $EGII_{core2}$ and $EGII_{core2H}$ are investigated by FTIR-RAS measurements and electron diffraction observations. The characteristic points of the polymerization on surface are discussed.

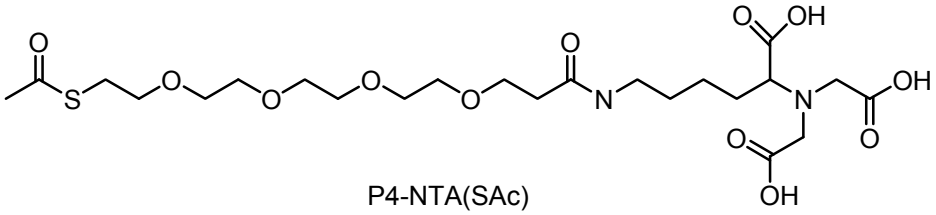

P4-NTA(SAc)

Figure 1. Chemical structure of the nitrilotriacetic acid derivative.

Experimental section

Purification of secretory mutant $EGII_{core2}$ and $EGII_{core2H}$. Mutant $EGII_{core2}$ and $EGII_{core2H}$ were purified by immobilized metal affinity chromatography (IMAC) (Ni-NTA agarose beads), followed by GPC (Sephacryl S-200) in 20 mM phosphate buffer (500 mM NaCl, pH 7.4) as described in Chapter 2.[12] The purity and molecular weight of purified enzymes were confirmed by SDS-PAGE with silver stain.

The activities and concentrations of purified enzymes were determined by the Somogyi-Nelson method[22,23] and the Bradford method,[24] respectively. The standard substances of standard curve were glucose for the Somogyi-Nelson method and BSA for the Bradford method. The substrate used for the Somogyi-Nelson method was CMC.

SPR measurement of immobilization of $EGII_{core2H}$. SPR measurement was carried out by the method described in Chapter 3.[21] Briefly, the interaction between His-tag introduced into mutant enzyme and Ni-NTA was measured eluting with 10 mM HEPES buffer (150 mM NaCl, 50 μM EDTA, and 0.005% Tween-20, pH 7.4) flowing at 10 μl/min at 25 °C. P4-NTA SAM modified sensor chip was prepared on Sensor Chip Au surface utilizing gold–thiol binding by dipping method as described below. One flow cell was activated with a

500 μM $NiSO_4$ aqueous solution to form Ni-NTA complex surface and the other was a reference cell without Ni ion. The concentration of injected enzyme was diluted at 75 nM in eluting HEPES buffer. The enzyme solution was injected at 0 s and kept flowing for 600 s. The dissociation phase was monitored for the following 1500 s. The regeneration of the P4-NTA SAM surface after immobilization of enzyme was performed by injecting of a 300 mM imidazole aqueous solution (to remove His-tagged enzymes), followed by a 350 mM EDTA aqueous solution (to remove Ni ions).

Preparation of NTA modified SAM and immobilization for FTIR-RAS. The SAM, which was a scaffold for the enzyme immobilization, was prepared on gold by the method as follows. First, the glass slide was treated by sulfuric acid, followed by depositing 300 Å chromium and then 2000 Å gold (99.99%) by the vacuum deposition method. Immediately after deposition, the P4-NTA SAM was formed by immersing the gold substrates in a 0.5 mM P4-NTA(SAc) ethanol solution with 2 M dimethylamine methanol solution (60 equiv of the thioacetyl group) at room temperature. After 24 h, the substrate was thoroughly rinsed with ethanol and Milli-Q water (three times) for 1 min and dried under a N_2 steam. Then, the coordination of Ni ion was performed by incubating P4-NTA SAM with a 500 mM $NiSO_4$ aqueous solution for 3 h at room temperature. The substrate was then rinsed with Milli-Q water for 1 min (three times) and dried under a N_2 steam (P4-NTA-Ni SAM). Finally, the immobilization of enzyme to Ni-NTA surface was carried out by incubating the obtained P4-NTA-Ni SAM substrate with a 20 nM enzyme solution in acetate buffer (50 mM, pH 5.0) for 24 h at 4 °C. The substrate was rinsed with 20 mM acetate buffer for 1 min (three times) and dried under a N_2 steam, followed by evaluation of activities of hydrolysis and polymerization. In order to quantify the amount of the immobilized endoglucanases, the substrate was washed with deuterium water for 1 min and dried under a N_2 steam before FTIR-RAS measurements to eliminate the water background from the amide I region.

FTIR-RAS measurement. FTIR-RAS measurements were carried out as described in Chapter 3. The incident angle was 84° from the surface normal. The number of interferogram

accumulations was approximately 200. The density of immobilized enzyme on substrate was calculated from the absorption of amide I of the enzyme utilizing the Lambert-Beer law. The used value of the molecular extinction coefficient of $EGII_{core2}$ and $EGII_{core2H}$ was deduced from the value of BSA with molecular weight correction.[25]

Hydrolytic activity of immobilized $EGII_{core2H}$. The hydrolytic activity of immobilized $EGII_{core2H}$ was measured by using cellohexaose as a substrate. The immobilized $EGII_{core2H}$ was incubated with 0.1 w/v% cellohexaose in a 50 mM acetate buffer (pH 5.0) at 50 °C. After specified periods, aliquots of the supernatant of the reaction solution were taken out to trace the substrate concentration by HPLC measurement with an OHpak SB-802 HQ column (Tosoh, Japan; eluent, a 0.3 M $NaNO_3$ aqueous solution; flow rate, 0.5 mL/min; column temperature, 40 °C; detection, RI). Free enzyme with an amount of 1.1×10^{-12} mol, which was nearly the same amount with immobilized $EGII_{core2H}$ in the reaction system, was also examined similarly as a reference.

Enzymatic polymerization catalyzed by immobilized $EGII_{core2}$ and $EGII_{core2H}$. Enzymatic polymerization of β-cellobiosyl fluoride catalyzed by the immobilized enzyme was carried out. The immobilized enzyme introduced on the P4-NTA-Ni SAM modified gold substrate was incubated with 25 mM β-cellobiosyl fluoride in a mixture solution of acetonitrile/acetate buffer = 3/1 v/v at 30 °C. After 5, 10, 15 and 30 min, the gold substrates were taken out from the reaction solution followed by drying under a N_2 steam without any washings to avoid dissociation of water-soluble low molecular weight products. These gold substrates were subjected to FTIR-RAS measurement.

Electron diffraction analysis of enzymatic polymerization products. The products obtained by enzymatic polymerization were analyzed by electron diffraction at an accelerating voltage of 100 kV. The sample grid was prepared by original means which was modified replica method utilizing Ni-NTA complex as follows. First, carbon thin layer was formed on the polymerization product onto gold substrate by vacuum deposition. Then the substrate was

set against petri dish and a 500 mM EDTA aqueous solution was slowly poured. Ni ions, which were intercalated between the NTA moieties and His-tags on gold, were removed by EDTA, dissociating His-tagged enzymes from NTA modified substrate surface. The deposited carbon thin layer was detached from glass slide, which was floating on the EDTA aqueous solution, was transferred on a Cu grid.

Results and discussion

Preparation of purified $EGII_{core2}$ and $EGII_{core2H}$. The crude $EGII_{core2}$ and $EGII_{core2H}$ secreted from yeast cells were purified by the His-tag affinity chromatography and GPC. Identification and purity of the purified $EGII_{core2}$ and $EGII_{core2H}$ were confirmed by SDS-PAGE. The specific hydrolysis activities of purified $EGII_{core2}$ and $EGII_{core2H}$ were evaluated to be 121 and 118 U/mg, respectively, showing nearly the same activity of these two mutants.

Affinity of $EGII_{core2H}$ for NTA-Ni surface. The binding behavior of $EGII_{core2H}$ to the P4-NTA surface was followed by SPR method. The resonance value increases gradually with injection of an $EGII_{core2H}$ solution from 0 to 600 s, suggesting the specific binding of the His-tag moieties of $EGII_{core2H}$ to P4-NTA-Ni (Figure 2). The resonance value reaches at 520 RU after 600 s from the injection, which is nearly half of 1086 RU with $EGII_{core2}$ under the same conditions. The surface densities of the immobilized $EGII_{core2}$ and $EGII_{core2H}$ was calculated to be 15.2 and 7.19 fmol/mm^2, respectively (1 RU = 1 pg/mm^2).

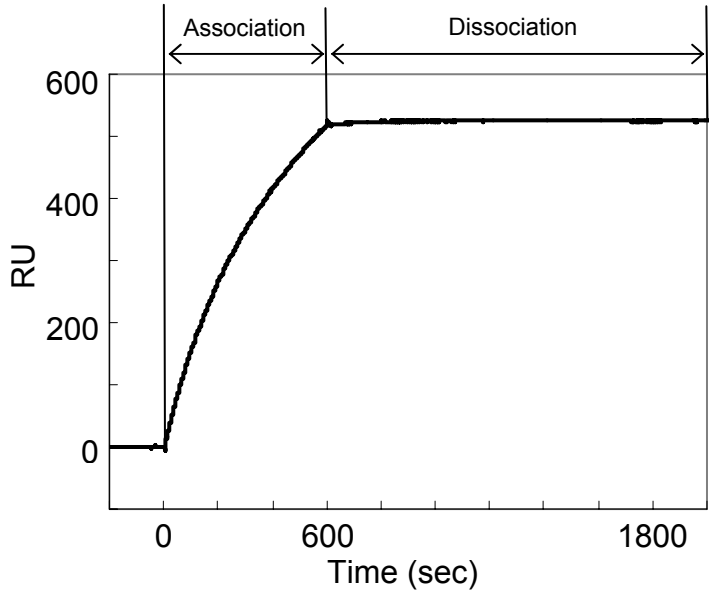

Figure 2. SPR analysis of association and dissociation of $EGII_{core2H}$ on the P4-NTA-Ni surface at 25 ^{o}C. The concentration of $EGII_{core2H}$ was 75 nM.

The dissociation of $EGII_{core2H}$ from the surface was monitored by eluting a washing buffer from 600 s to 1800 s. Only a very limited amount of $EGII_{core2H}$ is released from the surface, which is in contrast with 1.8% release of $EGII_{core2}$ under the same washing process. The dissociation constant of $EGII_{core2H}$ with the P4-NTA-Ni surface is estimated to be smaller than 10^{-9} M^{-1} but beyond the resolution limit of the present SPR apparatus. On the other hand, that of $EGII_{core2}$ was reported to be 10^{-8} M^{-1} in Chapter 3. Taken together, $EGII_{core2H}$ should be immobilized on the surface through two linkages between both His-tags at *N* and *C* terminals of $EGII_{core2H}$ and two P4-NTA-Ni groups on the surface. It is thus the molecular area occupied by $EGII_{core2H}$ should be larger than that of $EGII_{core2}$, resulting in the lower surface density of $EGII_{core2H}$ than $EGII_{core2}$. The crystal structure data of EGII from *T. viride*, which belongs to GH5, is not available, but other hydrolases of GH5 show that the both *N* and *C* terminals of the catalytic domain locates at the far ends of the domain, suggesting that the two His-tags at both terminals of $EGII_{core2H}$ can access simultaneously to the substrate surface with occupying a large area on the surface.

FTIR-RAS characterization of immobilized enzyme. Polymerization by the immobilized $EGII_{core2}$ and $EGII_{core2H}$ on gold was analyzed by FTIR-RAS, which requires a large substrate area compared with that for SPR measurements. Figure 3A illustrates the immobilization procedures with using the large substrates. The formation of P4-NTA SAM on gold substrate (Figure 3(i)) and chelation with Ni ions (Figure 3(ii)) were confirmed by carboxyl and carboxylate signals, respectively, by the FTIR-RAS spectra (data not shown).[26] Upon incubation of the P4-NTA-Ni SAM with $EGII_{core2}$ or $EGII_{core2H}$ (Figure 3(iii)), the absorption appears around 1670 cm^{-1}, which is assigned to amide I band of $EGII_{core2}$ or $EGII_{core2H}$ (Figure 4).

The author tried to immobilize $EGII_{core2}$ and $EGII_{core2H}$ on gold at a similar density, because the author can compare the data without considering the density effect of the

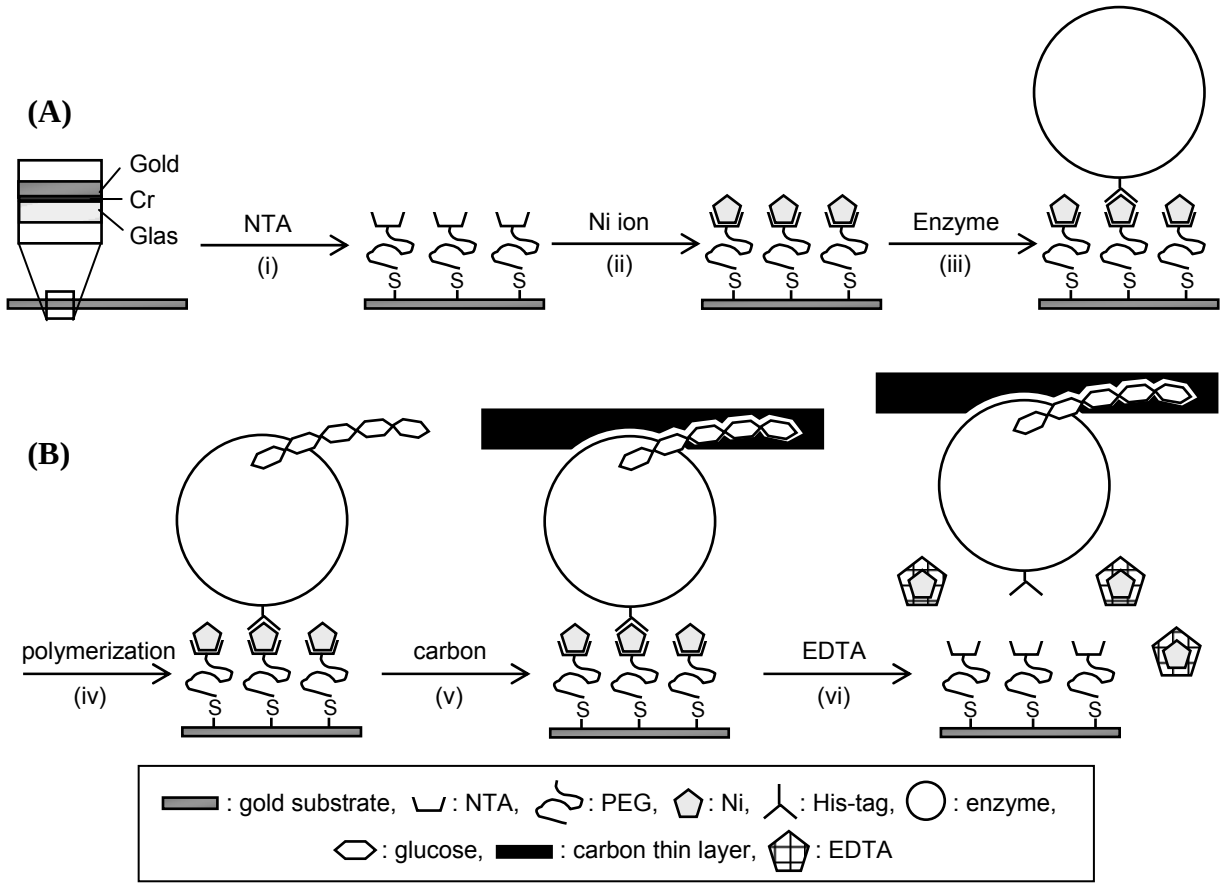

Figure 3. Schematic illustration of immobilization of His-tagged enzyme on the Ni-chelated nitrilotriacetic acid surface (A) and preparation of sample for electron diffraction observation (B).

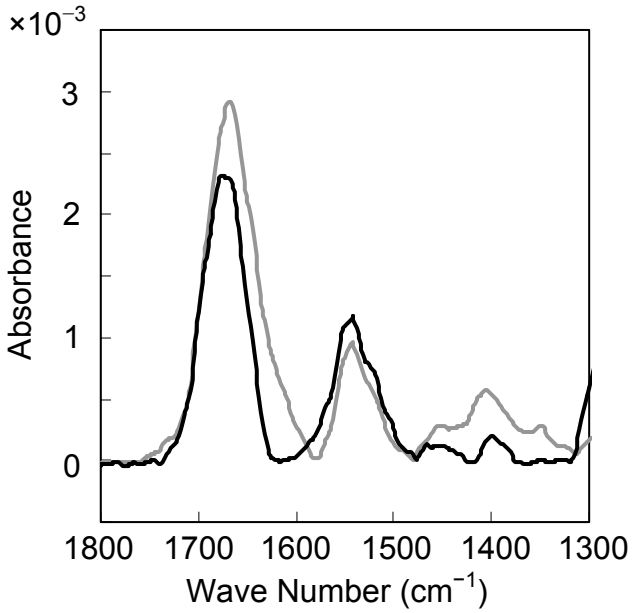

Figure 4. FTIR-RAS spectrum of the immobilized $EGII_{core2}$ (gray line) and $EGII_{core2H}$ (black line) on the P4-NTA-Ni surface.

enzyme on the polymerization behaviors by these two mutants. When the enzyme concentration of 20 nM instead of 75 nM for the SPR measurements was used, the densities of $EGII_{core2}$ and $EGII_{core2H}$ on gold, which were evaluated from the amide I intensities, were 6.9 and 5.3 fmol/mm^2, respectively, showing the similar density between these two mutants. The immobilized amount of $EGII_{core2}$ decreased with the low enzyme concentration at preparation more significantly than $EGII_{core2H}$ because of the lower binding constant of $EGII_{core2}$ than $EGII_{core2H}$.

Hydrolytic activity of immobilized $EGII_{core2H}$. The hydrolytic activity of the immobilized $EGII_{core2H}$ was studied with using cellohexaose as substrate (Figure 5). The substrate consumptions are compared between the immobilized $EGII_{core2H}$ and free $EGII_{core2H}$ as catalyst under the condition that the total amounts of the enzymes in the reaction systems are nearly equal. The hydrolytic activity of the immobilized $EGII_{core2H}$ is slightly lower than that of free $EGII_{core2H}$, which is in contrast to the case of $EGII_{core2}$, where the hydrolysis proceeded with similar rates between the immobilized $EGII_{core2}$ and free $EGII_{core2}$.[21] The

hydrolytic activity of the immobilized $EGII_{core2H}$ is considered to be impaired due to the firm immobilization to the surface via two His-tags on both terminals.

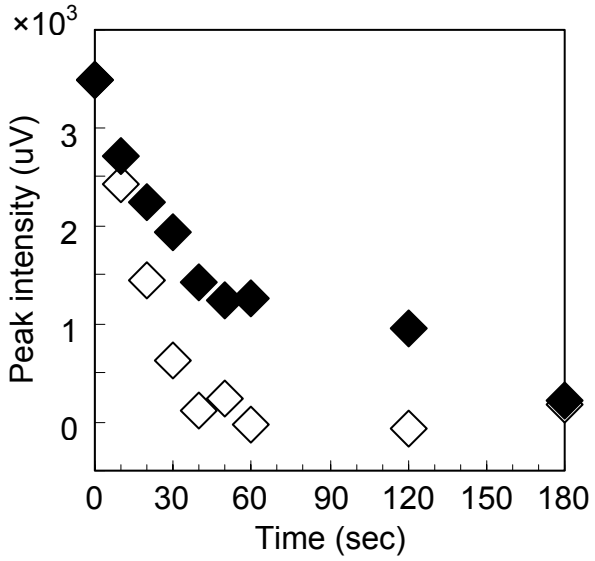

Figure 5. Hydrolysis behavior of cellohexaose by immobilized $EGII_{core2H}$ (◆) and free $EGII_{core2H}$ (◇) at 50 °C.

FTIR-RAS characterization of enzymatic polymerization products. Enzymatic polymerization of β-cellobiosyl fluoride using the immobilized $EGII_{core2}$ and $EGII_{core2H}$ as catalyst was studied by FTIR-RAS measurements. Figure 6 shows the spectra of the products on the substrate, which are obtained after subtraction of the corresponding spectrum of the immobilized $EGII_{core2}$ or $EGII_{core2H}$. The spectrum catalyzed by immobilized $EGII_{core2}$ of 30 min after initiation shows characteristic absorptions of cellulose at 3371, 1419, 1377, 1163, 1101 and 894.8 cm^{-1}, which are assigned to OH stretching of hydrogen bonds, CH_2 symmetric bending, CH bending, a skeletal vibration including the C-O-C bridge stretching parallel to the backbone, C-O stretching and C-O-C stretching at the glycosidic linkage, respectively.[27–30] On the other hand, the spectrum of 15 min after initiation by the immobilized $EGII_{core2H}$ shows the OH stretching band with the similar intensity to the spectrum after 30 min from initiation by the immobilized $EGII_{core2}$, but with shift to lower wavenumber at 3325 (-46 cm^{-1}). The shift to the lower wavenumber means formation of

hydrogen bonds. Other signals are similar between the two spectra; 1414 cm^{-1} (−5 cm^{-1}), 1377 cm^{-1} (±0 cm^{-1}), 1163 cm^{-1} (±0 cm^{-1}), 1103 cm^{-1} (+2 cm^{-1}) and 894.8 cm^{-1} (±0 cm^{-1}).

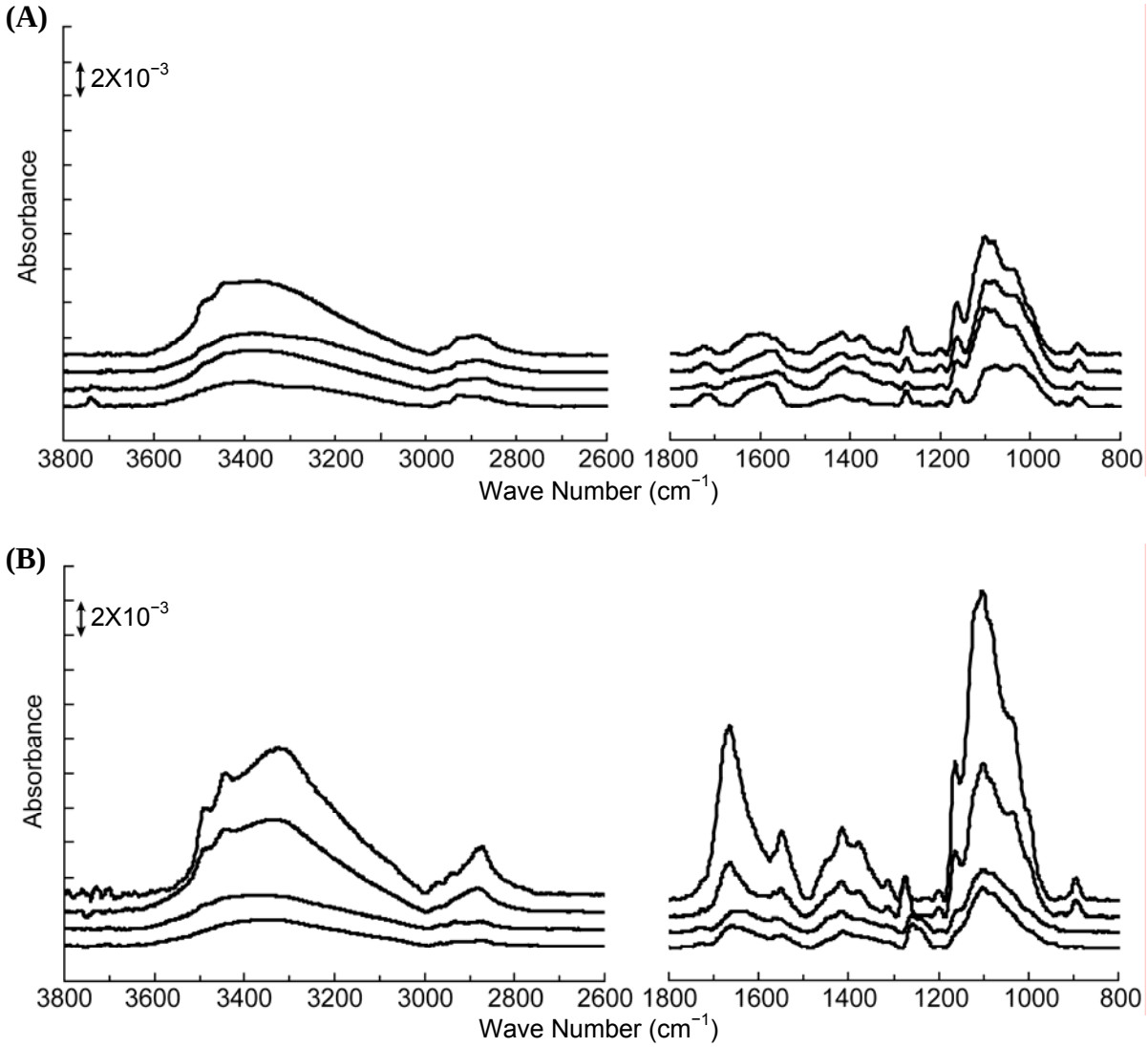

Figure 6. FTIR-RAS spectra of enzymatic polymerization products using the immobilized $EGII_{core2}$ (A) and $EGII_{coreH}$ (B) after 5, 10, 15 and 30 min from lower to upper.

Figure 7 shows the time course of maximum absorbance at OH stretching region during polymerization reaction. The time course of the polymerization catalyzed by the immobilized $EGII_{core2H}$ is two-phase; slow polymerization until 10 min followed by fast second phase. The increase is considered to be due to the progression of the crystallization of synthesized cellulose, because the wavenumber of the peak shifts to the lower wavenumber

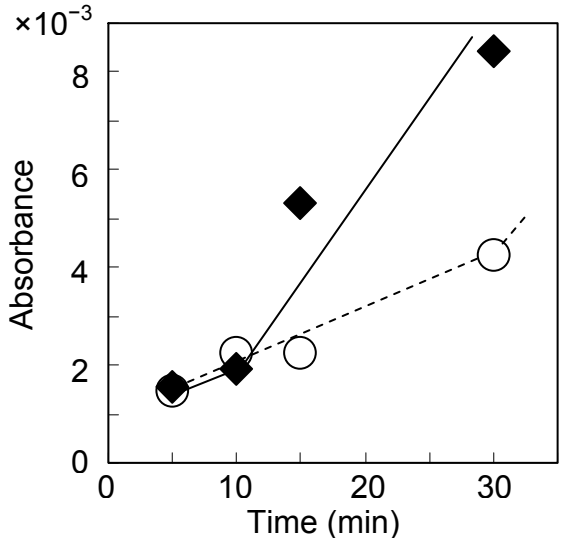

Figure 7. The maximum absorbance of OH stretching peak of synthesized cellulose catalyzed by immobilized $EGII_{core2}$ (○) and $EGII_{core2H}$ (◆) plotted against polymerization time by FTIR-RAS measurement.

significantly. The crystalline cellulose should precipitate on the surface to increase the OH absooptions. The onset time is delayed in the case of immobilized $EGII_{core2}$ as catalyst where the second phase starts after 30 nin.

The ratios lateral order index (LOI)[31] and total crystallinity index (TCI),[32] which are absorbance ratios of CH_2 symmetric bending (1420 cm^{-1})/C-O-C stretching (895 cm^{-1}) and CH bending (1377 cm^{-1})/CH stretching (2889 cm^{-1}), respectively, are known as indicatives of the degree of cellulose crystallinity. Both indexes of the produced cellulose are higher with the immobilized $EGII_{core2H}$ (LOI, 2.33; TCI, 1.14) than with the immobilized $EGII_{core2}$ (LOI, 2.11; TCI, 0.955). Further, a pair of peaks at 3488 and 3447 cm^{-1}, which is indicative of high crystalline cellulose of type II, is observed after 15 min from initiation by the immobilized $EGII_{core2H}$, which is earlier than 30 min by the immobilized $EGII_{core2}$. All the data thus indicate that the immobilized $EGII_{core2}$ and $EGII_{core2H}$ produce the high crystalline cellulose of type II, and the latter is more effective to obtain crystalline cellulose. The immobilization way of $EGII_{core2H}$ via two sites may help the two catalytic sites in the enzyme orient favorably on gold to generate the crystalline cellulose.

Electron diffraction of synthesized cellulose. The crystallization of cellulose catalyzed by the immobilized $EGII_{core2}$ was studied by electron diffraction. The samples were prepared by a modified replica method as follows. At specific periods after initiation, carbon thin layer was deposited on the substrate (Figure 3(v)). Subsequently the gold substrate was immersed in an EDTA aqueous solution, and the carbon thin layer was detached from gold substrate (Figure 3(vi)). The products after 3 min from initiation shows an electron diffraction pattern of the two typical diffraction rings of cellulose II, (110) and (020) planes (corresponding to 4.41 and 4.03 Å, respectively) (Figure 8A).[14,33] The absence of (1-10) plane (corresponding to 7.19 Å) may be due to the low crystallinity of the products. Indeed, the product after 30 min shows (1-10) plane as well (Figure 8B). The time of 30 min after initiation corresponds to the phase change of polymerization observed by FTIR-RAS measurement. After 24 h, each diffraction ring becomes strong with a pattern of the typical type II cellulose (Figure 8C). Interestingly, despite of the high crystallinity, the (004) plane (corresponding to 2.60 Å) is missing in the electron diffraction, suggesting that cellulose chains of c axial of cellulose are oriented along surface normal, which reason is remained to be solved.

Further, the diffraction rings of the product obtained by the immobilized $EGII_{core2}$ are sharper than those by $EGII_{core2}$, indicating higher crystallinity of cellulose obtained by the immobilized $EGII_{core2}$ are sharper than those by free $EGII_{core2}$, indicating higher crystallinity of cellulose obtained by the immobilized $EGII_{core2}$ than by free $EGII_{core2}$.[34] The reason may be due to the condensation effect of the catalytic core domains on gold surface.

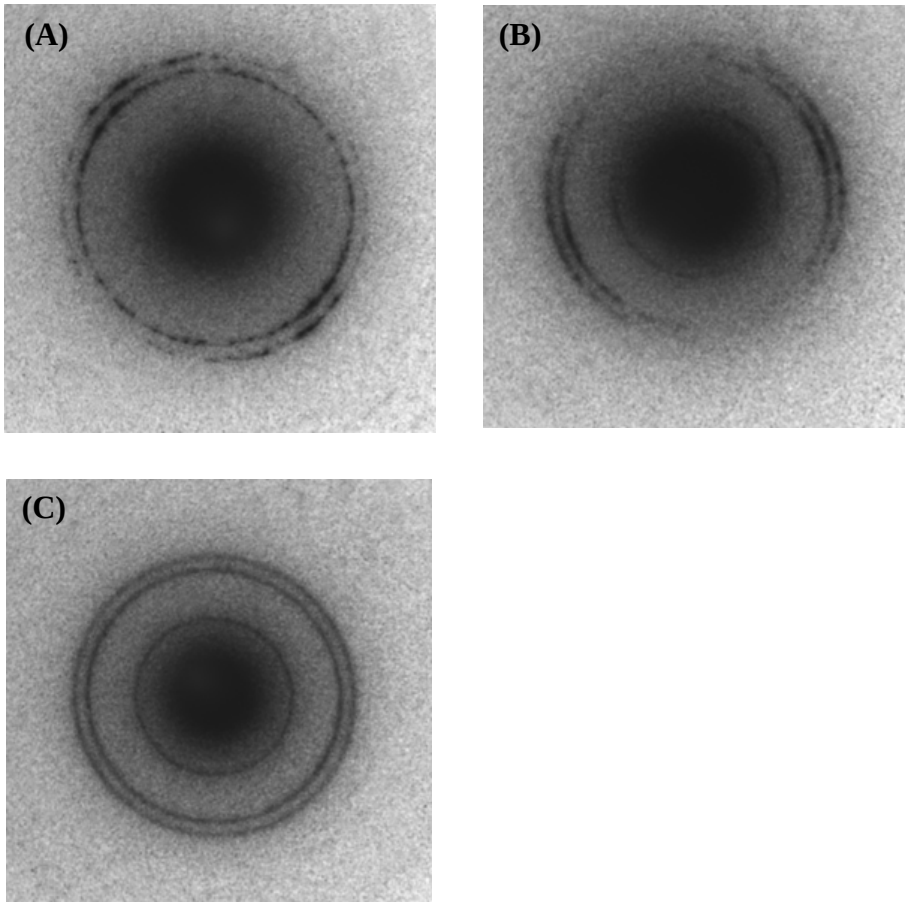

Figure 8. Electron diffraction diagrams of enzymatic polymerization products catalyzed by immobilized $EGII_{core2}$ after 3 min (A), 30 min (B) and 24 h (C).

References

(1) Balat, M.; Balat, H.; Oz, C. *Prog. Energy Combust. Sci.* **2008**, *34*, 551–573.

(2) Alvira, P.; Tomas-Pejo, E.; Ballesteros, M.; Negro, M. J. *Bioresour. Technol.* **2010**, *101*, 4851–4861.

(3) Brown, R. M.; Saxena, I. M.; Kudlicka, K. *Trends Plant Sci.* **1996**, *1*, 149–156.

(4) Delmer, D. P. *Annu. Rev. Plant Physiol. Plant Molec. Biol.* **1999**, *50*, 245–276.

(5) Sugiyama, J.; Persson, J.; Chanzy, H. *Macromolecules* **1991**, *24*, 2461–2466.

(6) Giddings, T. H.; Brower, D. L.; Staehelin, L. A. *J. Cell Biol.* **1980**, *84*, 327–339.

(7) Okuda, K.; Tsekos, I.; Brown, R. M. *Protoplasma* **1994**, *180*, 49–58.

(8) Kobayashi, S.; Kashiwa, K.; Kawasaki, T.; Shoda, S. *J. Am. Chem. Soc.* **1991**, *113*, 3079–3084.

(9) Egusa, S.; Kitaoka, T.; Goto, M.; Wariishi, H. *Angew. Chem.-Int. Edit.* **2007**, *46*, 2063–2065.

(10) Hiraishi, M.; Igarashi, K.; Kimura, S.; Wada, M.; Kitaoka, M.; Samejima, M. *Carbohydr. Res.* **2009**, *344*, 2468–2473.

(11) Nakamura, I.; Yoneda, H.; Maeda, T.; Makino, A.; Ohmae, M.; Sugiyama, J.; Ueda, M.; Kobayashi, S.; Kimura, S. *Macromol. Biosci.* **2005**, *5*, 623–628.

(12) Nakamura, I.; Makino, A.; Sugiyama, J.; Ohmae, M.; Kimura, S. *Int. J. Biol. Macromol.* **2008**, *43*, 226–231.

(13) Lee, J. H.; Brown, R. M.; Kuga, S.; Shoda, S.; Kobayashi, S. *Proc. Natl. Acad. Sci. U. S. A.* **1994**, *91*, 9195–9195.

(14) Kobayashi, S.; Hobson, L. J.; Sakamoto, J.; Kimura, S.; Sugiyama, J.; Imai, T.; Itoh, T. *Biomacromolecules* **2000**, *1*, 168–173.

(15) Kobayashi, S.; Shoda, S.; Lee, J.; Okuda, K.; Brown, R. M. *Macromol. Chem. Phys.* **1994**, *195*, 1319–1326.

(16) Brown, R. M.; Montezinos, D. *Proc. Natl. Acad. Sci. U. S. A.* **1976**, *73*, 143–147.

(17) Hochuli, E.; Dobeli, H.; Schacher, A. *J. Chromatogr.* **1987**, *411*, 177–184.

(18) Sigal, G. B.; Bamdad, C.; Barberis, A.; Strominger, J.; Whitesides, G. M. *Anal. Chem.* **1996**, *68*, 490–497.

(19) Kroger, D.; Liley, M.; Schiweck, W.; Skerra, A.; Vogel, H. *Biosens. Bioelectron.* **1999**, *14*, 155–161.

(20) McPherson, T.; Kidane, A.; Szleifer, I.; Park, K. *Langmuir* **1998**, *14*, 176–186.

(21) Nakamura, I.; Makino, A.; Ohmae, M.; Kimura, S. *Macromol. Biosci.* **2010**, *10*, 1265–1272.

(22) Somogyi, M. *J. Biol. Chem.* **1952**, *195*, 19–23.

(23) Nelson, N. *J. Biol. Chem.* **1944**, *153*, 375–380.

(24) Bradford, M. M. *Anal. Biochem.* **1976**, *72*, 248–254.

(25) Yokoyama, Y.; Ishiguro, R.; Maeda, H.; Mukaiyama, M.; Kameyama, K.; Hiramatsu, K. *J. Colloid Interface Sci.* **2003**, *268*, 23–32.

(26) Nakamoto, K.; Morimoto, Y.; Martell, A. E. *J. Am. Chem. Soc.* **1962**, *84*, 2081–&.

(27) Liang, C. Y.; Marchessault, R. H. *J. Polym. Sci.* **1959**, *37*, 385–395.

(28) Liang, C. Y.; Marchessault, R. H. *J. Polym. Sci.* **1959**, *39*, 269–278.

(29) Marechal, Y.; Chanzy, H. *J. Mol. Struct.* **2000**, *523*, 183–196.

(30) Hofstetter, K.; Hinterstoisser, B.; Salmen, L. *Cellulose* **2006**, *13*, 131–145.

(31) Hurtubise, F. G.; Krassig, H. *Anal. Chem.* **1960**, *32*, 177–181.

(32) Nelson, M. L.; O'Connor, R. T. *J. Appl. Polym. Sci.* **1964**, *8*, 1325–1341.

(33) Helbert, W.; Sugiyama, J. *Cellulose* **1998**, *5*, 113–122.

(34) Paralikar, K. M.; Betrabet, S. M. *J. Appl. Polym. Sci.* **1977**, *21*, 899–903.

Chapter 5

Fibrous Cellulose Prepared by Enzymatic Polymerization

Using Cross-linked Mutant Endoglucanase II

Introduction

Cellulose is the most abundant polysaccharide on the earth, and biosynthesized by cellulose synthase. Cellulose synthase is classified as glycosyltransferase, and forms a complex with other different enzymes.[1,2] This enzyme complex is named as TC,[3,4] which is considered to control the physical properties of cellulose depending on the enzyme arrangements in TC whether they are aligned in a linear or a cyclic way.[5–8] Cellulose produced in nature normally forms fibrils with thermodynamically metastable type I crystalline structure, where cellulose chains are aligned in parallel orientation.

The first *in vitro* cellulose synthesis by enzymatic polymerization was reported in 1991 with using cellulase from *T. viride* as a catalyst.[9] With the cellulase-catalyzed polycondensation of β-cellobiosyl fluoride monomer, synthetic cellulose having a crystalline structure of thermodynamically stable type II was obtained. Cellulose formed a spherical structure, which is a different structure from the fibrous cellulose in nature.[10] Since then, some *in vitro* syntheses of cellulose have been developed.[11] For example, in nonaqueous solution, type II cellulose was synthesized from cellobiose in stead of a β-cellobiosyl fluoride monomer with using the same catalyst of the cellulase from *T. viride* in the presence of a nonionic surfactant.[12] Further, cellodextrin phosphorylase is applied to enzymatic polymerization using α-glucose 1-phosphate as a monomer, and lamellar crystalline cellulose II was synthesized.[13] Chemical synthesis of cellulose was also accomplished by cationic ring-opening polymerization of tricyclic orthoester derivatives.[14] The obtained cellulose was identified to take a crystalline structure of type II. Most products of cellulose by *in vitro* syntheses therefore took a type II structure. There has been one report of preparation of fibrous cellulose of type I, which was obtained by enzymatic polymerization with using a partially purified cellulase as a catalyst.[15] However, with using purified cellulases no fibrous cellulose has been synthesized.[10]

The author has been studying on the crystalline structure of artificial cellulose synthesized by using the mutant enzymes having two successive active sites in the sequence.[16,17] Further, enzymatic polymerization was examined on substrate in addition to in

solution.[18] As a result, the crystallinity of synthetic cellulose was higher with using immobilized enzymes on substrate than with free enzymes in solution. It is thus expected that the physical properties of synthetic cellulose can be controlled by the arrangement and the orientation of enzymes organized in the polymerization system, which resembles to the *in vivo* synthesis of cellulose by TC.

In this Chapter, enzymes are cross-linked in several ways to fix their arrangement and orientation in the cluster of enzymes, and the activities of enzymatic polymerization to cellulose are studied on substrate and in solution. For cross-linking the enzymes, chelation of a His-tag in enzymes with a Ni ion captured by a NTA group was used.[19–22] NTA groups are introduced on enzymes and also on gold substrate. The morphology and the crystalline structure of the synthesized cellulose are examined. It is expected to obtain fibrous cellulose here, because the enzymes are fixed in a close proximity with a defined orientation, which may resemble to the *in vivo* cellulose synthesis by TC.

Experimental section

Materials. H-Glu (OBzl)-O^{t}Bu·HCl was perchased from Watanabe chemical industries (Japan) and used as received. Bis-dPEG$^{TM}_5$ acid was obtained from Quanta Biodesign Ltd. (USA) and used as received. AB-NTA free acid was perchased from DOJINDO (Japan) and used as received. All other reagents were purchased from commercial sources and used as received.

NTA (O^{t}Bu)-OBzl (3). H-Glu (OBzl)-O^{t}Bu·HCl (500 mg, 1.5 mmol) was dissolved in *N*,*N*-dimethylformamide (DMF), and t-butyl bromoacetate (887 μL, 6.0 mmol) and *N*,*N*-diisopropylethylamine (DIEA, 1.7 mL 9.8 mmol) were added. The solution was stirred at 55 °C for 17 h under N_2 atmosphere. Then, the ethyl acetate was added and washed with water, and the organic layer was dried over $MgSO_4$. This solution was purified by silica gel chromatography (cyclohexane : ethyl acetate, 3:1) to provide the pure target compound **3** (313

mg, 40%) as yellow oil. TLC (cyclohexane : ethyl acetate, 3:1): R_f = 0.6. ^{1}H NMR ($CDCl_3$, 400 MHz): δ (ppm) 7.35–7.30 (m, 5H, benzene), 5.11 (s, 2H, benzyl-C*H*$_2$), 3.44 (s, 4H, N-C*H*$_2$), 3.40–3.36 (t, 1H, N-C*H*), 2.55–2.74 (m, 2H, C*H*$_2$), 2.05–1.86 (m, 2H, C*H*$_2$), 1.45–1.43 (d, 27H, -OtBu C*H*$_3$). FAB-MS: *m*/*z* = 544.3 (calcd for $C_{28}H_{43}NO_6Na$ [(M+Na)+] *m*/*z* = 544.3).

NTA (O^{t}Bu)-COOH (4). Compound **3** (313 mg, 0.60 mmol) was dissolved in methanol, and 10% Pd/C (83 mg, 30 wt% against **3**) was added. The mixture solution was stirred at room temperature under H_2 atmosphere for 46 h. Then the Pd/C was filtered off and washed with methanol. The filtrate was evaporated and dried *in vacuo* and the residue was purified by a Sephadex LH-20 column with methanol as eluant to obtain the target deprotected compound **4** (142 mg, 55%) as colorless oil. TLC (chloroform : methanol : ammonia, 13:5:1): R_f = 0.7. ^{1}H NMR ($CDCl_3$, 400 MHz): δ (ppm) 3.45 (s, 4H, N-C*H*$_2$), 3.38–3.34 (t, 1H, N-C*H*), 2.72–2.56 (m, 2H, C*H*$_2$), 2.05–1.86 (m, 2H, C*H*$_2$), 1.44 (d, 27H, -O^{t}Bu C*H*$_3$). FAB-MS: *m*/*z* = 454.2 (calcd for $C_{21}H_{37}NO_8Na$ [(M+Na)+] *m*/*z* = 454.3).

NTA (O^{t}Bu)-OSu (5). *N*-hydroxy succinimide (HOSu, 19 mg, 0.16 mmol) was added to Compound **4** (69 mg, 0.16 mmol) and dissolved in dichloromethane (2 mL). Then ethylenedichloride (EDC, 46 mg, 0.24 mmol) was added and stirred for 4 h under dried air by calcium chloride tube. Then the solution was evaporated. The residue was washed with NaCl, saturated $NaHCO_3$, and saturated NaCl (two times), and the organic layer was dried over $MgSO_4$. The solvent was evaporated and dried *in vacuo* to obtain the product **5** (65 mg, 76%) as colorless oil. ^{1}H NMR ($CDCl_3$, 400 MHz): δ (ppm) 3.45 (s, 4H, N-C*H*$_2$), 3.43–3.38 (t, 1H, N-C*H*), 3.12–2.88 (mm, 2H, C*H*$_2$), 2.82 (s, 4H, C*H*$_2$), 2.13–1.94 (m, 2H, C*H*$_2$), 1.44 (d, 27H, -O^{t}Bu C*H*$_3$). IR (cm^{-1}): 1814, 1785 (CO-N-CO). FAB-MS: *m*/*z* = 551.4 (calcd for $C_{25}H_{40}N_2O_{10}Na$ [(M+Na)+] *m*/*z* = 551.3)

NTA-OSu (1). Compound **5** was dissolved in trifluoroacetic acid (TFA, 100 μL). After 1 h, dimethyl ether was added to the solution to obtain the slurry. The precipitation was collected by centrifugation, and dried *in vacuo* to obtain the deprotected product **1**.

BisOSu (6). To the DMF (0.8 mL) solution of bis-dPEG$^{TM}_5$ acid (30 mg, 0.089 mmol), *N*,*N*-dicyclohexyl carbodiimide (DCCI, 38 mg, 0.18 mmol) was added. After 15 min stirring of the reaction mixture at room temperature under Ar atmosphere, HOSu (41 mg, 0.36 mmol) dissolved in DMF (0.2 mL) was dropwised, and stirred more 36 h, the reaction mixture was concentrated. The crude product **6** was dissolved into ethyl acetate, and dicyclohexylurea was removed by filtration. Crude compound **6** was obtained after evaporation of the solvent.

BisNTA (2). To the solution of crude compound **6** in DMSO (5 mL), AB-NTA free acid (47 mg, 0.18 mmol) and triethylamine (74 μL, 0.53 mmol) mixed DMSO solution (2 mL) was added, and the mixture was stirred at room temperature under Ar atmosphere for 6 h. The reaction mixture was purified by Sephadex LH-20 column chromatography using DMF as an eluent to afford pure **2** as colorless syrup (60 mg, 2 steps: 82%). ^{1}H NMR (DMF-d_7, 400 MHz) δ (ppm): 7.95 (s, 2H, N*H*CO), 3.90–3.70 (m, 28H, -CH_2COOH, -O-CH_2-), 3.65 (dd, 2H, C*H* (C-1) of 5-amino-1-carboxypentyl), 3.33 (m, 4H, CH_2 (C-5) of 5-amino-1-carboxypentyl), 2.59 (t, 4H, -CH_2CONH), 1.96 (m, 2H, C*H* (C-2a) of 5-amino-1-carboxypentyl), 1.83 (m, 2H, C*H* (C-2a) of 5-amino-1- carboxypentyl), 1.77–1.56 (m, 8H, CH_2 (C-3, 4) of 5-amino-1-carboxypetyl).

Enzyme immobilization on SPR gold chip. In the flow channel of SPR system, enzyme was immobilized on the gold sensor chip surface (BIAcore X; running buffer, 10 mM HEPES buffer with 150 mM NaCl, 50 μM EDTA, and 0.005% Tween-20, pH 7.4; flow rate, 10 μl/min; Temperature, 25 °C). On to the commercial Sensor chip Au, P4-NTA was immobilized as described in Chapter 3.[23] P4-NTA immobilized surfaces of both flow cells were activated by 500 μM $NiSO_4$ solution.

Enzyme immobilization was performed following two methods. On the first method, 20 nM $EGII_{core2H}$ solution was injected to Ni-chelated P4-NTA immobilized surface for 10 min. Then, excess NTA-OSu in HEPES buffer (pH 9.0) was flowed for 10 min to introduce NTA moiety on $EGII_{core2H}$, followed by 500 μM $NiSO_4$ solution incubation for 1 min to activate NTA moieties bound on $EGII_{core2H}$. $EGII_{core2H}$ solution was injected to construct second enzyme layer via His-tag–Ni-NTA linkage on the first $EGII_{core2H}$ layer. These immobilization cycles were repeated for ten times. The reference sample was prepared by sequential injection of the enzyme solution without NTA-OSu and Ni solutions. In another method, NTA introduced $EGII_{core2H}$ was used for immobilization. To the excess NTA-OSu in HEPES buffer (pH 9.0), $EGII_{core2H}$ was added and incubated for 4 h at 4 °C. NTA introduced $EGII_{core2H}$ was purified by ultrafiltration (NMWL; 30,000), to remove excess amount of NTA-OSu. NTA introduced $EGII_{core2H}$ solution (20 nM) was injected to Ni-chelated P4-NTA chip surface for 10 min. After 500 μM $NiSO_4$ solution was flowed for 1 min, NTA introduced $EGII_{core2H}$ solution was again injected to the surface for 10 min to form second enzyme layer via Ni ion binding. These cycles were repeated for ten times. Reference sample was prepared in the manner without Ni ion incubation.

Enzyme multi-layer formation on gold substrate. $EGII_{core2H}$ immobilized substrate for enzymatic polymerization was prepared as follows. Ni ion chelated P4-NTA SAM was formed on glass slide (76 mm × 5 mm) as described in Chapter 3.[23] Subsequently, enzyme immobilization was carried out onto the Ni chelated P4-NTA SAM. To the solution of $EGII_{core2H}$ (20 nM) in 20 mM phosphate buffer (500 mM NaCl, pH 7.4), P4-NTA SAM was immersed for 3 h. The enzyme immobilized substrate was rinsed with 20 mM phosphate buffer (pH 7.4) for 1 min (three times), followed by drying under a N_2 steam. Next, the substrate was incubated into excess NTA-OSu in phosphate buffer (pH 9.0) for 1 h, and then 100 mM $NiSO_4$ aqueous solution for 30 min, sequentially. After every incubation processes, the obtained substrate was rinsed with 20 mM phosphate buffer (pH 7.4) for 1 min (three times), followed by drying under a N_2 steam. This immobilization process was carried out at 4 °C, and repeated for 1–4 times. In the case of using NTA introduced $EGII_{core2H}$,

immobilization of the enzyme was carried out as in the case of using $EGII_{core2H}$, but no need of incubation with a NTA-OSu solution.

Enzymatic polymerization using the immobilized enzyme. Enzyme immobilized gold substrate was incubated with 25 mM β-cellobiosyl fluoride in acetonitrile/acetate buffer (pH 5.0) = 3/1 v/v mixed solution at 30 °C. Polymerization was terminated by taking out the substrate from the reaction solution, followed by drying under a N_2 steam.

Cross-linking of enzyme using a bifunctional cross-linking molecule (bisNTA) in the solution. Ni-chelated bisNTA (bisNTA-Ni) was prepared as follows. To the bisNTA aqueous solution, $NiSO_4$ aqueous solution was added and the reaction mixture was incubated for 24 h at room temperature. Unreacted Ni ion was removed by Sephadex G-10 column chromatography with water as eluent. Construction of bisNTA-Ni was confirmed by ultraviolet-visible spectroscopic analysis at 280 and 395 nm (derived from bisNTA and Ni ion, respectively). Then, $EGII_{core2}$ or $EGII_{core2H}$ solution was added to the bisNTA-Ni solution (excess amount against enzyme). The reaction mixture was incubated at 4 °C and bisNTA-Ni–His-tag mediated linkage was formed. After 24 h, excessive amount of bisNTA-Ni was removed by ultrafiltration (NMWL; 30,000) and bisNTA-Ni bound enzyme was collected. Then, $EGII_{core2}$ or $EGII_{core2H}$ was additionally added to the solution. After 24 h, the solution was analyzed by Sephacryl S-200 column. The fractions which showed absorption at both 280 and 395 nm were collected and concentrated by ultrafiltration (NMWL; 30,000).

Enzymatic polymerization using bisNTA-Ni–His-tag mediated cross-linked enzyme. Enzymatic polymerization of β-cellobiosyl fluoride (25 mM) was carried out in the acetonitrile/acetate buffer (pH 5.0) = 3/1 v/v mixture solution with obtained cross-linked enzyme as catalyst at 30 °C. After 48 h, the solution was centrifuged to separate water-soluble part and water-insoluble part. The obtained precipitate was washed by acetonitrile/acetate buffer = 3/1 v/v solution for two times, and dispersed in acetonitrile.

Characterization of the immobilized enzyme using FTIR-RAS and ellipsometry. FTIR-RAS spectra were measured as described in Chapter 3.[23] Ellipsometry was performed by a MIZOJIRI DHA-OLX/S autoellipsometer at room temperature. A helium-neon laser with 632.8 nm wavelength was used as the incident light with 65° of incident angle. The thicknesses were measured on five different points on the surface, and the data were averaged.

TEM observation and MALDI-TOF MS measurement. TEM images were taken as described in Chapter 1. Samples were dispersed into acetonitrile and putted on the carbon-coated grid without any staining.

MALDI-TOF MS spectra was taken as described in Chapter 1.

Results and discussions

EGII originated from *T. viride* has been used for enzymatic polymerization to cellulose. Two mutated enzymes, $EGII_{core2}$ and $EGII_{core2H}$, were prepared by genetic engineering, which are composed of two sequentially aligned catalytic core domains with one His-tag on *N* terminal and two His-tags on both terminals, respectively. These enzymes were purified by metal immobilized affinity chromatography (Ni-NTA agarose beads) and GPC (Sephacryl S-200). Molecular weight and purity of the obtained enzyme were confirmed by SDS-PAGE.

Figure 1 shows two bifunctional molecules, heterobifunctional molecules composed of NTA and OSu (NTA-OSu) and homobifunctional molecule having two NTA moieties (bisNTA). They were synthesized by conventional organic chemical reactions as Figure 2 and 3, respectively, and confirmed by ^{1}H NMR and mass spectroscopy.

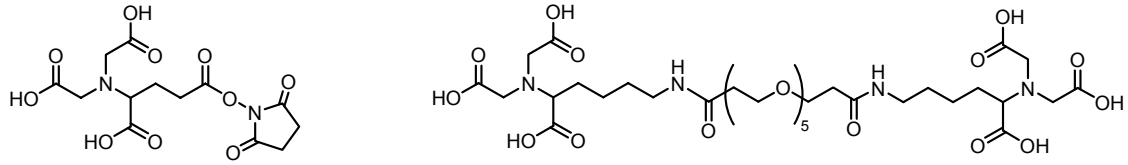

Figure 1. Chemical structures of NTA-OSu (left) and bisNTA (right).

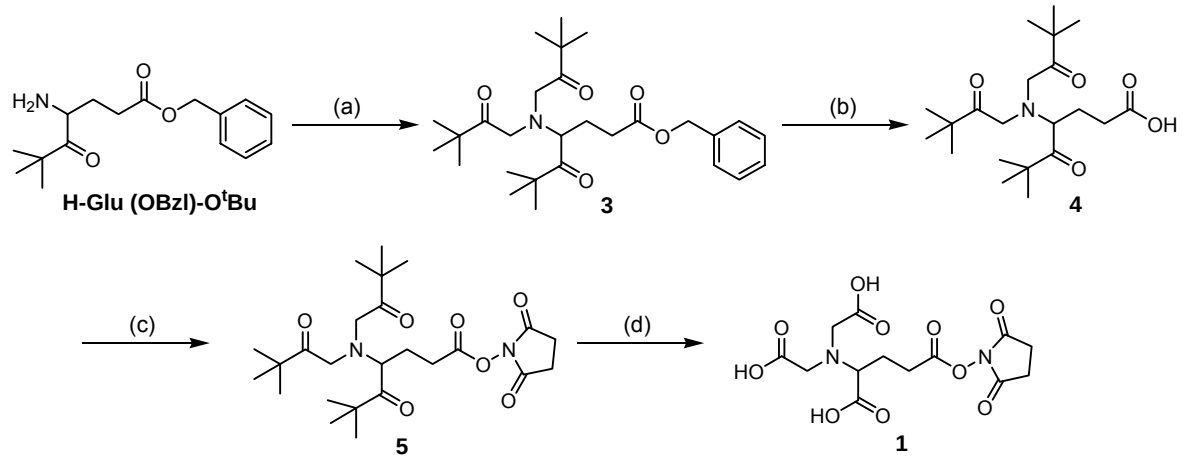

(a) tert-buthyl bromoacetate, DIEA/DMF; (b) Pd/C, H_2/methanol; (c) HOSu, EDC/CH_2Cl_2; (d) deprotection in TFA.

Figure 2. Synthetic route of NTA-OSu.

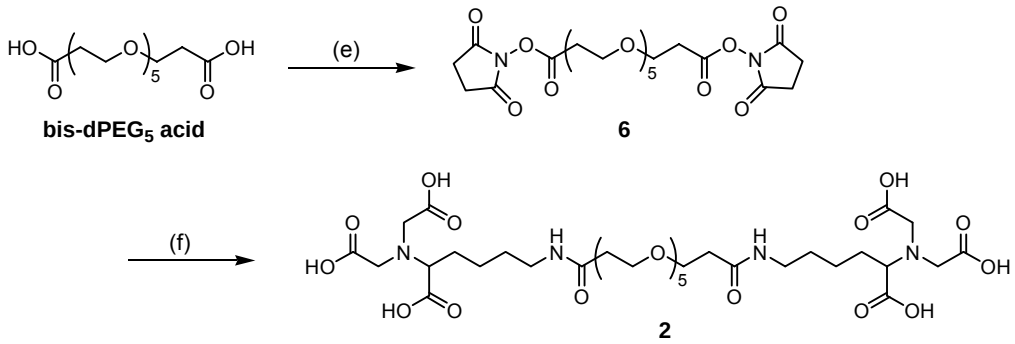

(e) HOSu, DCCI/DMF; (f) AB-NTA, triethylamine/DMSO.

Figure 3. Synthetic route of bisNTA.

Immobilization of enzymes on gold monitored by SPR. Immobilization of $EGII_{core2H}$ on gold substrate was performed in the following two ways as schematically shown in Figure 2A and 2B. Ni-chelated P4-NTA SAM was prepared on gold as described in Chapter 3.[23] A solution of $EGII_{core2H}$ was flowed over the sensor chip coated with the SAM (Figure 4(i)), followed by reaction of NTA-OSu with Lys residues on molecular surface of the immobilized $EGII_{core2H}$ (Figure 4(ii)).[24,25] Ni ions were bound to the introduced NTA moiety (Figure 4(iii)), and a solution of $EGII_{core2H}$ was flowed over the surface to construct the second layer of the enzyme (Figure 4(iv)). These processes were repeated for ten times to obtain stacked layers of $EGII_{core2H}$ on substrate. In another way, $EGII_{core2H}$ was in advance chemically modified by NTA-OSu to obtain NTA introduced $EGII_{core2H}$ instead of reaction of

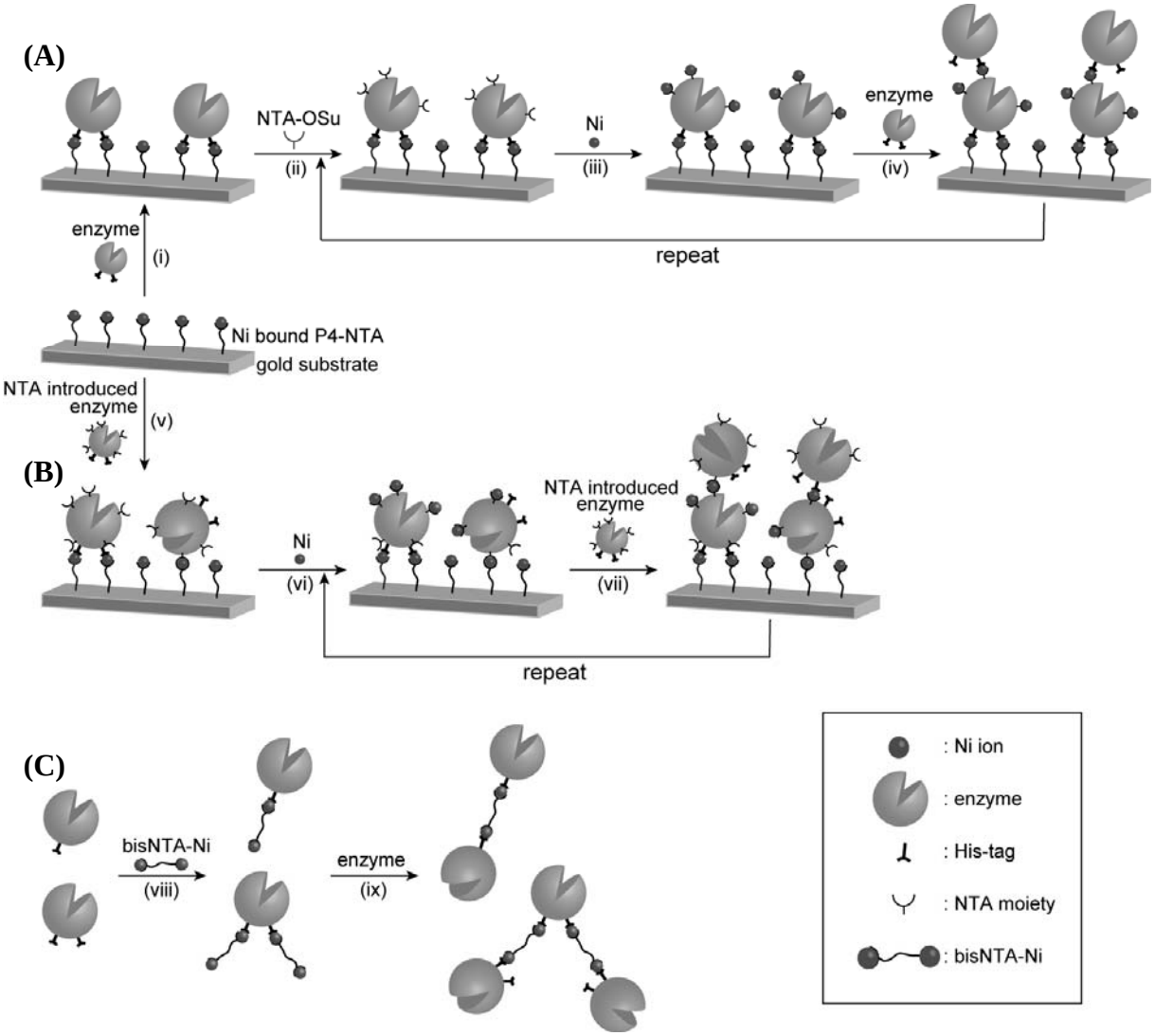

Figure 4. Schematic illustration of immobilized of $EGII_{core2H}$ (A), and NTA introduced $EGII_{core2H}$ (B), and cross-linked of $EGII_{core2H}$ (C).

$EGII_{core2H}$ with NTA-OSu on substrate surface described above. The immobilized layers of $EGII_{core2H}$ were prepared similarly except using NTA introduced $EGII_{core2H}$.

Figure 5A shows the process of $EGII_{core2H}$ immobilization on the Ni-chelated P4-NTA SAM monitored by SPR measurement. The amounts of immobilized $EGII_{core2H}$ increase with repetitions of the enzyme treatment on the substrate surface. On the other hand, the reference trace of $EGII_{core2H}$ immobilization, where treatments of the surface with NTA-OSu and Ni ions were skipped, shows very small increase of RU units after 5 repetitions of the

immobilization cycle. It is therefore concluded that $EGII_{core2H}$ stacks over one another on the surface via NTA-Ni–His-tag linking with this preparative method.

Figure 5B shows immobilization of the NTA introduced $EGII_{core2H}$ on the Ni-chelated P4-NTA SAM. In this case, the total amount of the NTA introduced $EGII_{core2H}$ immobilized on gold is less than that of the reference, where treatment of the surface with Ni ions was skipped. It is considered that the NTA introduced $EGII_{core2H}$ may compete with the Ni-chelated P4-NTA binding to His-tag of NTA introduced $EGII_{core2H}$ under the present condition of excess presence of the NTA introduced $EGII_{core2H}$, even though the association

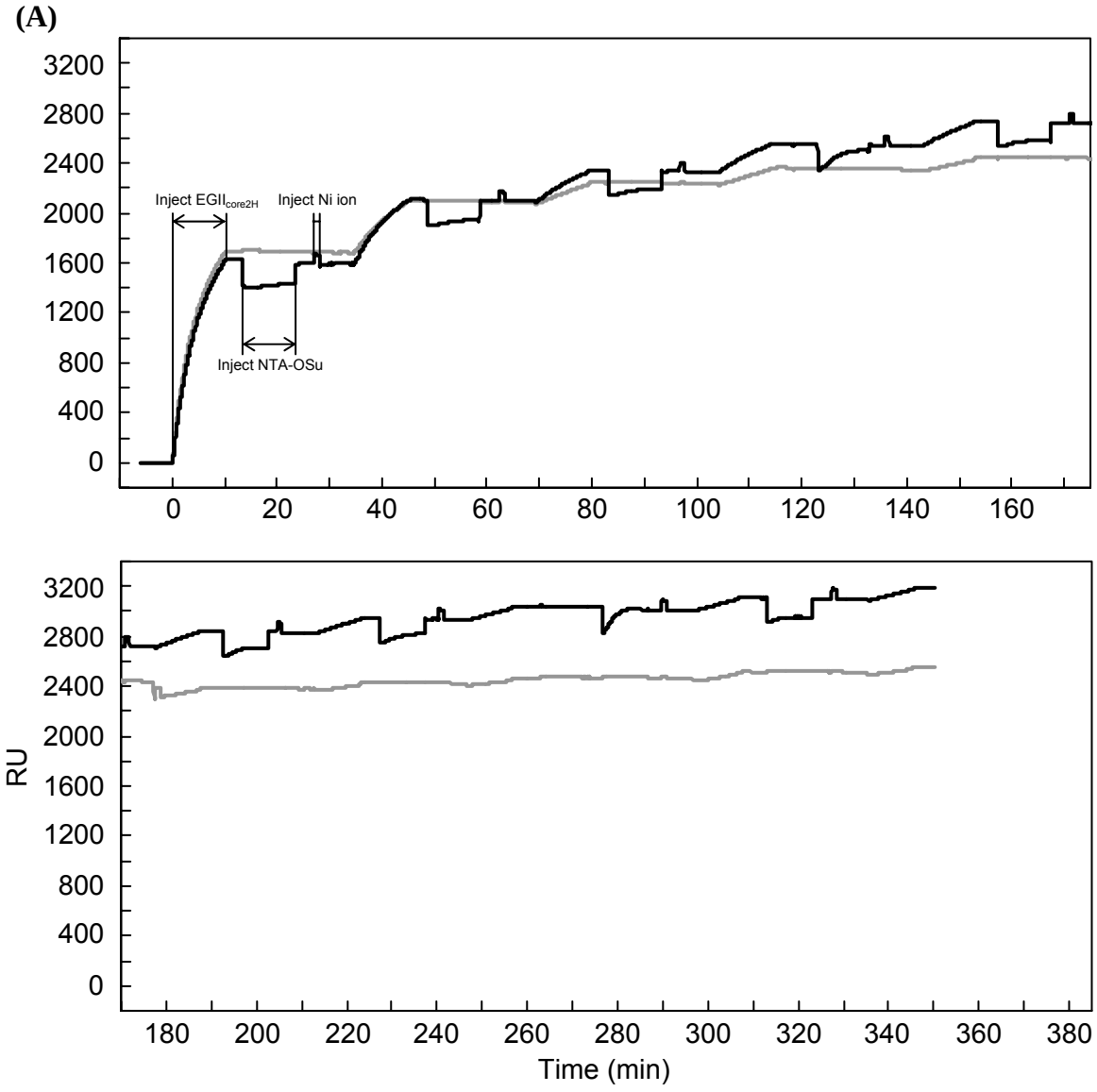

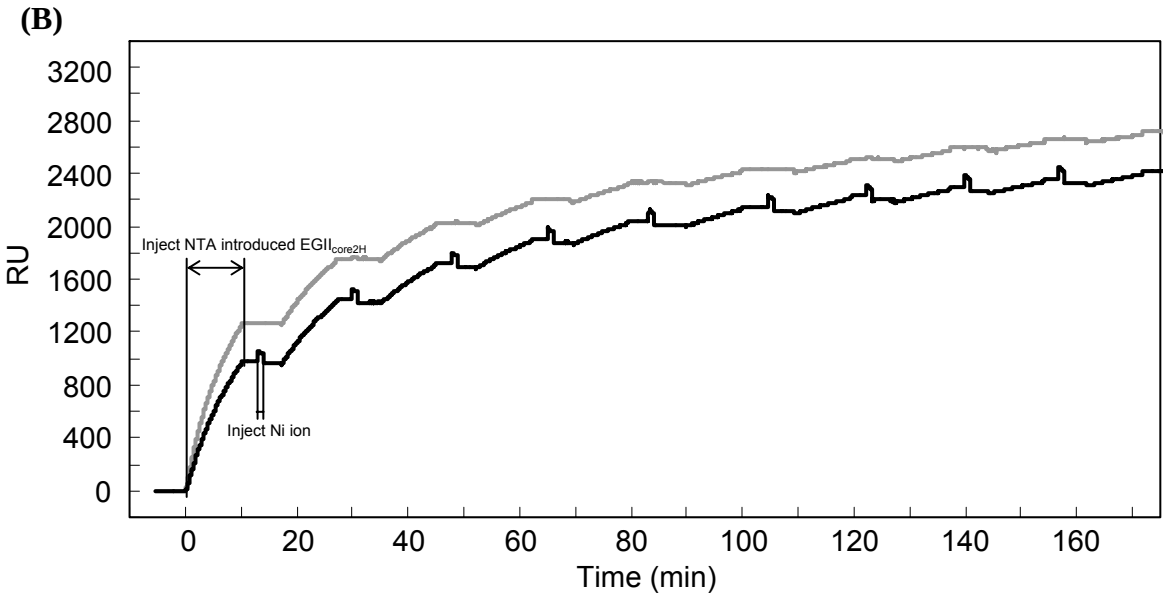

Figure 5. Results of SPR analysis of stacking behavior of ten cycles of $EGII_{core2H}$ (A) and NTA introduced $EGII_{core2H}$ (B). The concentration of enzyme was 20 nM. The start time of first cycle of enzyme was set at 0 s. The gray line is the result of reference measurement.

constant between His-tag and Ni ion is more than ten times higher than that between NTA and Ni ion.

Immobilization of enzymes on gold monitored by FTIR-RAS. Immobilization of enzymes on the P4-NTA SAM was carried out as illustrated in Figures 4A and 4B with using large gold substrates for FTIR-RAS measurements. The repetition of the enzyme treatment was four times for 3 h incubation instead of 10 times for 10 min incubation in the case of SPR measurements. As the reference samples, treatments of the surface with NTA-OSu and Ni ions were skipped for enzyme immobilization.

In the case of $EGII_{core2H}$, FTIR-RAS spectra show nearly no change in absorption intensity of amide I with the repetition time of the enzyme treatment (Figure 6A). Compared with the reference, the amount of the enzyme after four repetitions is similar between these two preparations. It is therefore considered that the treatment of the surface with NTA-OSu may partially dissociate the immobilized enzyme due to the competition of NTA-OSu to the binding of His-tag to Ni-NTA SAM. The amounts of the enzyme immobilized on gold

happens to be similar between these two preparations due to the competing dissociation process. On the other hand, the thickness of the immobilized $EGII_{core2H}$ layer determined by ellipsometry increases with the immobilization repetition time, and the thickness after four repetitions becomes larger than that of the reference (Figure 7). The different results between IR and ellipsometry measurements remain to be solved, but in the case of IR, amide I band may be overlapped with other absorptions of water and carboxylates which disturb quantitative evaluation of the enzyme immobilized on gold.

In the case of the NTA introduced $EGII_{core2H}$, amide I intensity after four repetitions becomes weaker than that of the reference (Figure 6B). The thicknesses of the immobilized enzyme layers determined by ellipsometry show nearly the same between the two preparations (Figure 7). As describe before, the introduced NTA on the NTA introduced

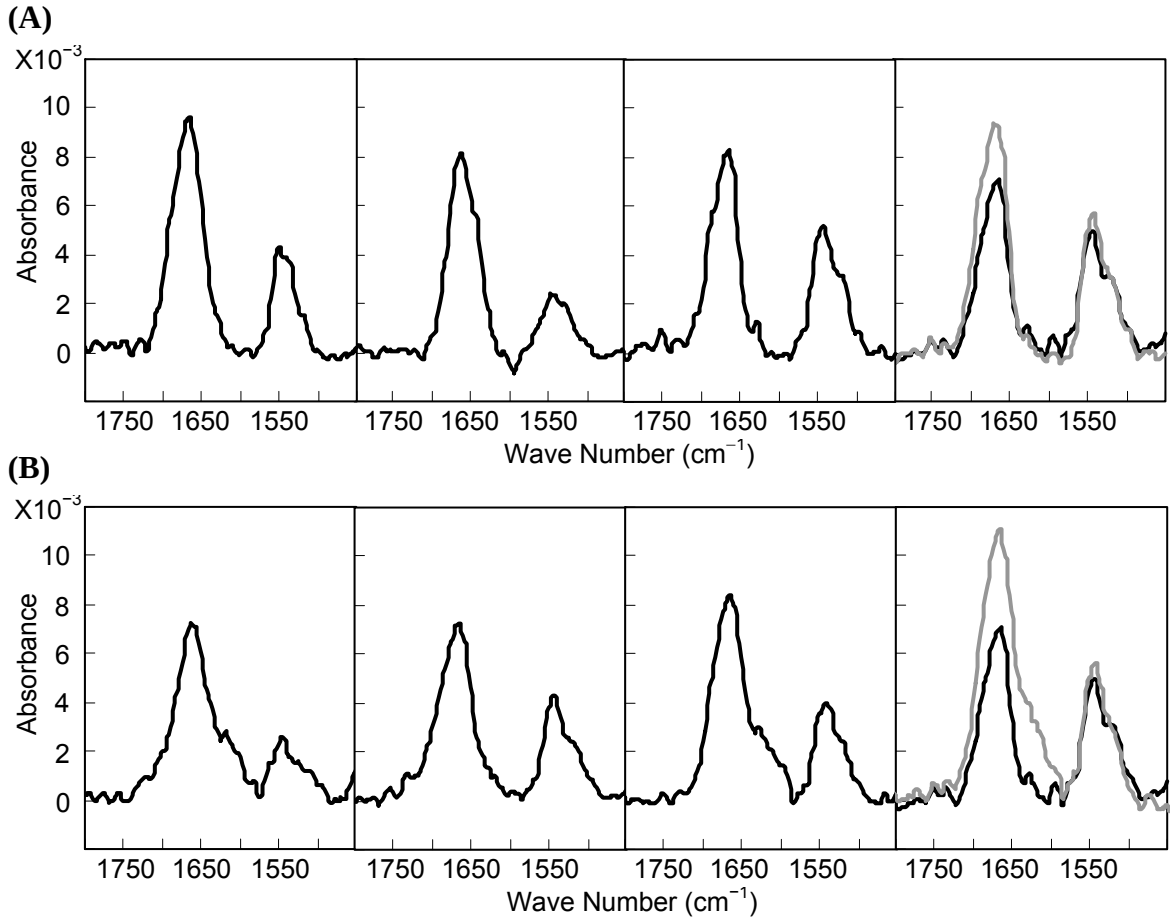

Figure 6. FTIR-RAS spectra of the immobilized $EGII_{core2H}$ (A) and NTA introduced $EGII_{core2H}$ (B) after first, second, third and fourth cycles of immobilized from left to right. Gray line is the result of reference measurement.

$EGII_{core2H}$ may dissociate partially the binding of His-tag to Ni-NTA SAM to disturb accumulation of the enzyme on the surface in total.

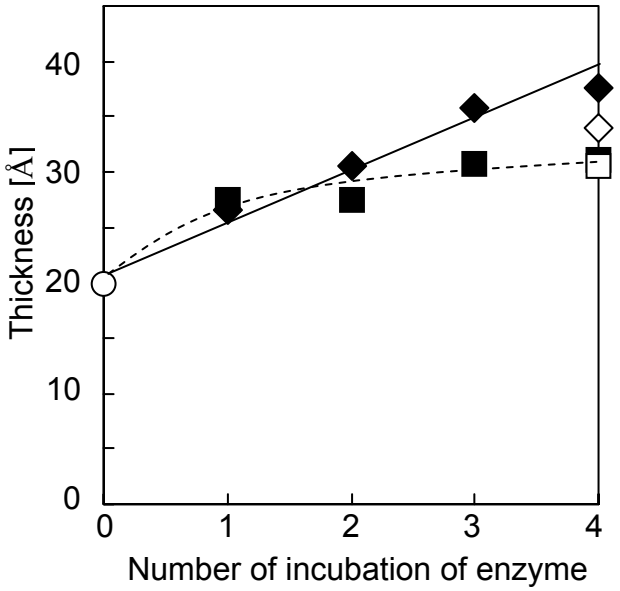

Figure 7. Thicknesses of immobilized $EGII_{core2H}$ layer (◆) and NTA introduced $EGII_{core2H}$ layer (■). Opened signals represent the result of reference measurement. At 0 times is the thickness of Ni-bound P4-NTA SAM.

Enzymatic polymerization catalyzed by immobilized $EGII_{core2H}$. Enzymatic polymerization was performed with using the $EGII_{core2H}$ immobilized on gold, which was prepared by the method shown in Figure 4A under the conditions of four repetitions of enzyme treatment for 3 h per one treatment. Figure 8 shows differential FTIR-RAS spectra after and before the polymerization, which indicate formation of cellulose by the immobilized $EGII_{core2H}$.[26–28] The FTIR-RAS spectra of cellulose obtained by the immobilized $EGII_{core2H}$ with two and three repetitions of the enzyme treatment show two characteristic peaks at 3446 and 3490 cm^{-1} (Figure 8A), which are assigned to high crystalline cellulose of type II. On the basis of comparing the absorption intensities of the hydroxyl group, the amount of cellulose on the substrate produced by the immobilized enzyme after three repetitions of the enzyme treatment becomes much larger than that produced by the immobilized enzyme after two repetitions of the enzyme treatment. The yield of cellulose is therefore very sensitive to the

surface density of $EGII_{core2H}$, suggesting that synthesized oligosaccharides may be recruited easily by the neighboring enzymes for further chain elongation due to the high density.

Utilizing the immobilized $EGII_{core2H}$ with four repetitions of enzyme treatment, enzymatic polymerization was performed and the product obtained after 10 min polymerization was investigated. All peaks of the FTIR-RAS spectrum were assigned to characteristic peaks of cellulose (Figure 8B). The yield of cellulose after 10 min

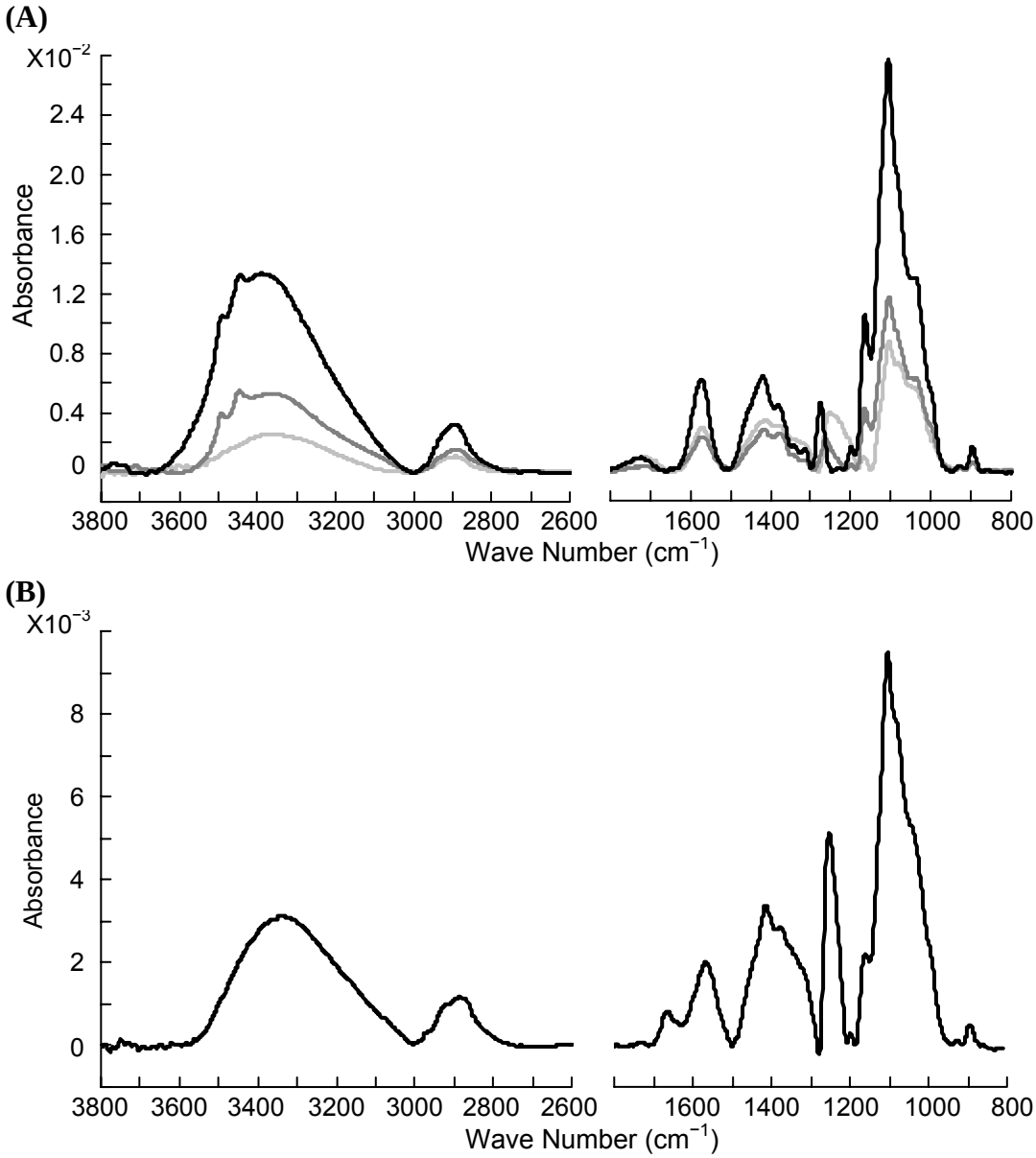

Figure 8. FTIR-RAS spectra of enzymatic polymerization products using the immobilized $EGII_{core2H}$ of first (light gray), second (gray) and third layers after 30 min polymerization (A) and fourth layers after 10 min polymerization (B).

polymerization was higher than that after 10 min polymerization catalyzed by the single layer of $EGII_{core2H}$ as described in Chapter 4, even though the total amount of $EGII_{core2H}$ immobilized on gold was one third of that of the case of Chapter 4.[18] Crystallinity of cellulose can be determined by calculation of the LOI (absorbance ratio of CH_2 symmetric bending (1415 cm^{-1})/C-O-C stretching (895 cm^{-1}))[29] and the TCI (CH bending (1379 cm^{-1})/CH stretching (2883 cm^{-1})).[30] The spectrum of 10 min polymerization by the immobilized $EGII_{core2H}$ was compared with that of 15 min polymerization by the single layer of $EGII_{core2H}$, where the amounts of cellulose produced on the substrate were similar. Both crystallinity indexes of cellulose obtained by the immobilized $EGII_{core2H}$ (10 min) (LOI, 6.11; TCI, 2.62) were much higher than those from the single layer of $EGII_{core2H}$ (15 min) (LOI, 2.33; TCI, 1.14).[18] Cellulose prepared from the immobilized $EGII_{core2H}$ shows higher crystallinity therefore due to the cross-linking structure of $EGII_{core2H}$ on substrate in the present case.

Importantly, two typical signal peaks for type II cellulose at 3446 and 3490 cm^{-1}, which appear in FTIR-RAS spectra of cellulose prepared by the immobilized $EGII_{core2H}$ of two and three repetitions of enzyme treatment after 30 min polymerization (Figure 8A), disappear (Figure 8B). Since the crystallinity indexes show high crystallinity of cellulose, the crystalline structure should be different from the typical cellulose II. Cross-linking of $EGII_{core2H}$ should change the crystalline structure of the product, but the structural analysis remains to be solved.

Cross-linking of enzymes in solution and their catalytic behaviors. Mutated enzymes of $EGII_{core2}$ and $EGII_{core2H}$ were cross-linked by bisNTA in phosphate buffer (500 mM NaCl, pH 7.4) (Figure 4C). Elution profiles of the products by GPC (Sephacryl S-200) are shown in Figure 9. In either case of $EGII_{core2}$ or $EGII_{core2H}$, new peaks appear at molecular weights higher than the corresponding monomer (molecular weights of $EGII_{core2}$ and $EGII_{core2H}$ are 71.5 kDa and 72.3 kDa (Figure 9C), respectively) and catalase (molecular weight is 232 kDa)[31] as a reference (Figure 9D), indicating that these enzymes are cross-linked under the present conditions. $EGII_{core2}$ has one His-tag region, and the number of the cross-linkable enzyme is theoretically limited to two. However, in the GPC profile, peaks at

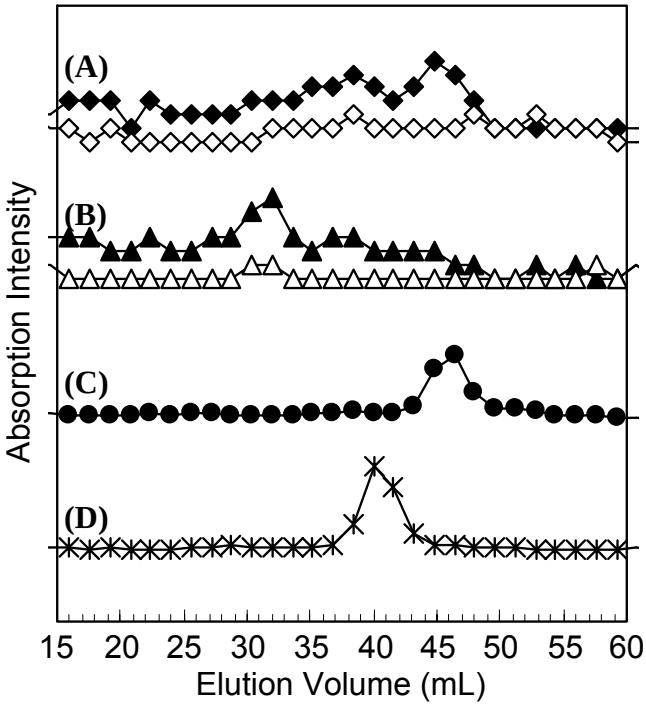

Figure 9. Elution prifiles of GPC of cross-linked $EGII_{core2H}$ (A), cross-linked $EGII_{core2}$ (B), $EGII_{core2H}$ (C) and catalase from bovine liver (D). Opened signals of (A) and (B) are observed at 395 nm. Others are at 280 nm.

molecular weights higher than dimer are observed. The reason is unknown at the present moment, but the mutant may have some affinity sites for Ni ions. On the other hand, $EGII_{core2H}$ may form an enzyme network utilizing two His-tags in one molecule.

Enzymatic polymerization catalyzed by cross-linked $EGII_{core2}$ or $EGII_{core2H}$ was carried out. After 0.5 h polymerization, white precipitate was produced in both cases. The precipitates remained in solution, which were collected at 48 h and washed with acetonitirile/acetate buffer = 3/1 v/v and acetonitrile. The obtained white precipitate was analyzed by MALDI-TOF MS. Mass spectra showed peaks with an equal interval of *m/z* 324 which corresponds to molecular weight of a cellobiose unit. The peak up to heptamer (equal to 14 glucose units) was observed in both cases. Therefore, the obtained white precipitates were identified as cellulose.

Chapter 1 explained that in the case of the cellulase-catalyzed polymerization of β-cellobiosyl fluoride, the synthesized cellulose was composed of $(\beta\text{-glucosyl})_n$ where n is odd numbers as well as even numbers. Cellulose with odd numbers of the glucose unit indicates

that the synthesized cellulose should be hydrolyzed by the endoglucanase during the reaction. On the other hand, in the present case, cellulose with odd numbers of the glucose units were not detected, indicating that cellulose was not hydrolyzed by the enzymes during the polymerization period of 48 h. Mutated $EGII_{core2}$ and $EGII_{core2H}$ lack cellulose-binding domain, which is essential for hydrolysis of the crystalline cellulose. Taken together, polymerization by the cross-linked enzymes should proceed quickly to generate crystalline cellulose, which is hardly hydrolyzed by these enzymes. The interpretation is supported by the observation that no oligosaccharides were obtained from the polymerization solution by size exclusion chromatography analysis (column, Shodex OHpak SB-802 HQ; data not shown)

Figure 10 shows the TEM images of the product catalyzed by the cross-linked $EGII_{core2}$ and $EGII_{core2H}$. In the both cases, morphology of the synthetic cellulose is fibril over μm length. The fibril width prepared from the cross-linked $EGII_{core2}$ and $EGII_{core2H}$ is in the range of 50–120 nm. Thin fibril having the width of 8.5 nm is also observed (Figure 10A, inset). Diffraction rings of these fibrils were weak, indicating that the crystallinity of synthesized fibrous cellulose was low. To our best knowledge, fibril formation by pure cellulase is firstly reported in this Chapter.

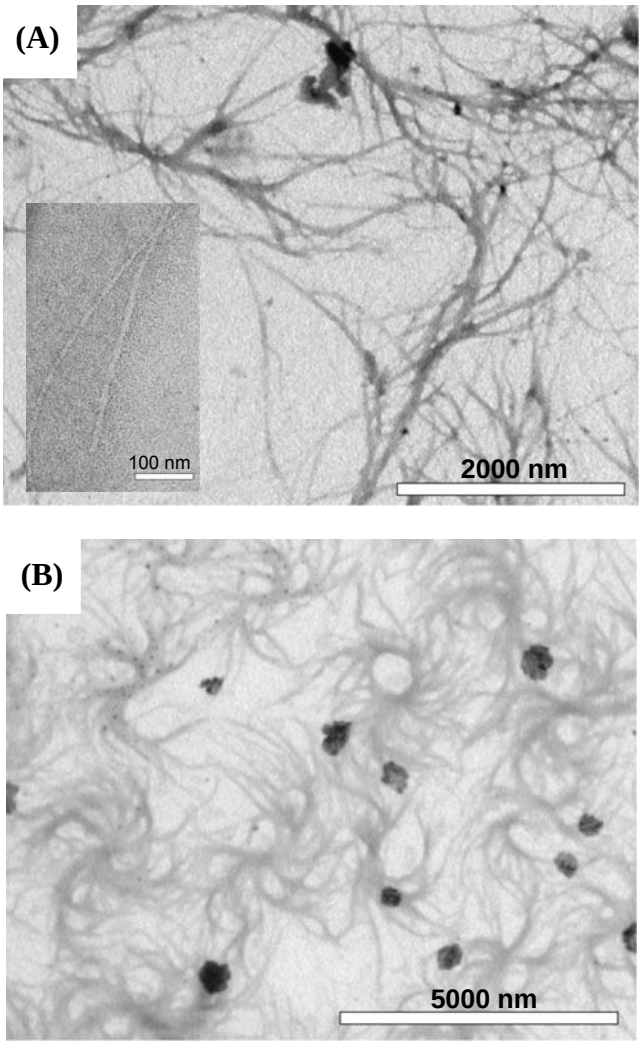

Figure 10. TEM images of products from cross-linked $EGII_{core2}$ (A) and $EGII_{core2H}$ (B). The inset of (A) is extended figure.

References

(1) Scheible, W. R.; Eshed, R.; Richmond, T.; Delmer, D.; Somerville, C. *Proc. Natl. Acad. Sci. U. S. A.* **2001**, *98*, 10079–10084.

(2) Taylor, N. G.; Howells, R. M.; Huttly, A. K.; Vickers, K.; Turner, S. R. *Proc. Natl. Acad. Sci. U. S. A.* **2003**, *100*, 1450–1455.

(3) Brown, R. M.; Montezinos, D. *Proc. Natl. Acad. Sci. U. S. A.* **1976**, *73*, 143–147.

(4) Brown, R. M.; Willison, J. H. M.; Richardson, C. L. *Proc. Natl. Acad. Sci. U. S. A.* **1976**, *73*, 4565–4569.

(5) Okuda, K.; Brown, R. M. *Protoplasma* **1992**, *168*, 51–63.

(6) Okuda, K.; Tsekos, I.; Brown, R. M. *Protoplasma* **1994**, *180*, 49–58.

(7) Kimura, S.; Itoh, T. *Protoplasma* **1996**, *194*, 151–163.

(8) Tsekos, I. *Journal of Phycology* **1999**, *35*, 635–655.

(9) Kobayashi, S.; Kashiwa, K.; Kawasaki, T.; Shoda, S. *J. Am. Chem. Soc.* **1991**, *113*, 3079–3084.

(10) Kobayashi, S.; Hobson, L. J.; Sakamoto, J.; Kimura, S.; Sugiyama, J.; Imai, T.; Itoh, T. *Biomacromolecules* **2000**, *1*, 168–173.

(11) Kobayashi, S.; Makino, A. *Chem. Rev.* **2009**, *109*, 5288–5353.

(12) Egusa, S.; Kitaoka, T.; Goto, M.; Wariishi, H. *Angew. Chem.-Int. Edit.* **2007**, *46*, 2063–2065.

(13) Hiraishi, M.; Igarashi, K.; Kimura, S.; Wada, M.; Kitaoka, M.; Samejima, M. *Carbohydr. Res.* **2009**, *344*, 2468–2473.

(14) Nakatsubo, F.; Kamitakahara, H.; Hori, M. *J. Am. Chem. Soc.* **1996**, *118*, 1677–1681.

(15) Lee, J. H.; Brown, R. M.; Kuga, S.; Shoda, S.; Kobayashi, S. *Proc. Natl. Acad. Sci. U. S. A.* **1994**, *91*, 7425–7429.

(16) Nakamura, I.; Yoneda, H.; Maeda, T.; Makino, A.; Ohmae, M.; Sugiyama, J.; Ueda, M.; Kobayashi, S.; Kimura, S. *Macromol. Biosci.* **2005**, *5*, 623–628.

(17) Nakamura, I.; Makino, A.; Sugiyama, J.; Ohmae, M.; Kimura, S. *Int. J. Biol. Macromol.* **2008**, *43*, 226–231.

(18) Nakamura, I.; Horikawa, Y.; Makino, A.; Sugiyama, J.; Kimura, S. *Biomacromolecules* **2010**, *accepted*.

(19) Hochuli, E.; Dobeli, H.; Schacher, A. *J. Chromatogr.* **1987**, *411*, 177–184.

(20) Kroger, D.; Liley, M.; Schiweck, W.; Skerra, A.; Vogel, H. *Biosens. Bioelectron.* **1999**, *14*, 155–161.

(21) Tinazli, A.; Tang, J. L.; Valiokas, R.; Picuric, S.; Lata, S.; Piehler, J.; Liedberg, B.; Tampe, R. *Chem.-Eur. J.* **2005**, *11*, 5249–5259.

(22) Chen, L.; Kopecek, J.; Stewart, R. J. *Bioconjugate Chem.* **2000**, *11*, 734–740.

(23) Nakamura, I.; Makino, A.; Ohmae, M.; Kimura, S. *Macromol. Biosci.* **2010**, *10*, 1265–1272.

(24) Lindsay, D. G.; Shall, S. *Biochem. J.* **1971**, *121*, 737–&.

(25) Deng, S. X.; Bharat, N.; Fischman, M. C.; Landry, D. W. *Proc. Natl. Acad. Sci. U. S. A.* **2002**, *99*, 3412–3416.

(26) Liang, C. Y.; Marchessault, R. H. *J. Polym. Sci.* **1959**, *37*, 385–395.

(27) Liang, C. Y.; Marchessault, R. H. *J. Polym. Sci.* **1959**, *39*, 269–278.

(28) Kondo, T.; Sawatari, C. *Polymer* **1996**, *37*, 393–399.

(29) Hurtubise, F. G.; Krassig, H. *Anal. Chem.* **1960**, *32*, 177–181.

(30) Nelson, M. L.; O'Connor, R. T. *J. Appl. Polym. Sci.* **1964**, *8*, 1325–1341.

(31) Takeda, A.; Hachimori, A.; Murai, M.; Sato, K.; Samejima, T. *J. Biochem.* **1975**, *78*, 911–924.

Concluding Remarks

This section briefly summarizes the results of synthesis of mutant enzyme, preparation of immobilized enzymes, and investigation of enzymatic polymerization product catalyzed by obtained various enzymes.

Chapter 1 demonstrates that the cellulose-binding domain deficient endoglucanase II (EGII) from *Trichoderma viride*, $EGII_{core}$, is more suitable for enzymatic polymerization compared with full length EGII. These mutant EGIIs have hexameric histidine residues (His-tag) at *N* terminal, and they become possible to prepare as high purified enzymes. In both cases, crystalline cellulose II is synthesized as white precipitation. Obtained cellulose from $EGII_{core}$ stably exists in the reaction solution more than 14 days, on the other hand, cellulose from EGII is disappeared. $EGII_{core}$ shows less hydrolytic activity against obtained crystalline cellulose because of deletion of cellulose-binding domain, and this is results in increase of polymerization activity.

Chapter 2 reports the enzymatic polymerization catalyzed by two novel mutant EGIIs, $EGII_{core2}$ and $EGII_{core2H}$, which are composed of two sequential catalytic core domains with one or two His-tag on *N* or both terminal. These mutant enzymes are synthesized by genetic engineering. The specific activities of purified $EGII_{core2}$ and $EGII_{core2H}$ are three-times higher than that of purified $EGII_{core}$. Moreover, in early phase, the monomer consumption using $EGII_{core2}$ or $EGII_{core2H}$ as catalyst is four times as fast as $EGII_{core}$. These are due to the stabilized conformation of $EGII_{core2}$ and $EGII_{core2H}$ compared with $EGII_{core}$. The products from both $EGII_{core2}$ and $EGII_{core2H}$ are identified as crystalline cellulose II. When enzymatic polymerization is carried out in quartz cell, the morphology of the synthesized cellulose is spherulite and the crystalline form is type II.

Chapter 3 investigates the immobilization of $EGII_{core2}$ on self-assembled monolayer (SAM) utilizing affinity binding between His-tag and Ni-chelated nitrilotriacetic acid (NTA). Three NTA derivative anchor molecules with different chain length which have zero or four or eight poloyethylene glycol moieties in their chain are prepared. It is confirmed that $EGII_{core2}$

is immobilized on Ni-chelated NTA SAM via His-tag. The most suitable anchor molecule for immobilization is identified as having four polyethylene glycol moieties due to an appropriate chain length and hydrophilicity. The hydrolysis activity of immobilized enzyme is retained on the gold surface showing similar value with that of nearly the same amount of free enzyme. No effect of anchor molecule on hydrolysis activity of immobilized enzyme is confirmed.

Chapter 4 shows enzymatic polymerization catalyzed by immobilized $EGII_{core2}$ and $EGII_{core2H}$ on substrate. First, the binding property of $EGII_{core2H}$ is studied, suggesting that it possess larger binding strength compared with $EGII_{core2}$ due to two binding sites. Enzymatic polymerization catalyzed by immobilized $EGII_{core2}$ or $EGII_{core2H}$ proceeds with producing highly crystalline cellulose in comparison with free enzyme. The immobilized $EGII_{core2H}$ shows higher polymerization activity than immobilized $EGII_{core2}$. Further, the crystallinity of synthesized cellulose is also higher in the case of immobilized $EGII_{core2H}$. It is indicated that the well-oriented enzyme is the key to synthesize cellulose.

Chapter 5 presents the synthesis of fibril cellulose using high oriented and concentrated enzyme as catalyst. Objective enzyme is prepared by cross-linking each other on the substrate or in the solution utilizing NTA-Ni–His-tag complex: immobilized enzyme layer and cross-linked enzyme. In the case of immobilized enzyme layer, the highest crystalline cellulose is synthesized compared with all previous works. The morphology of obtained cellulose by cross-linked enzyme is fibril, demonstrating that the orientation and concentration are important factors to synthesize fibril cellulose. In contrast to previous, the repeating unit of the synthesized fibrous cellulose shows cellobiose unit, indicating that the obtained fibrous cellulose is not hydrolyzed by catalyst of polymerization. The polymerization using cross-linked enzyme is kinetically high advantageous.

As demonstrated in the present thesis, the crystalline structure and morphology of synthesized cellulose by enzymatic polymerization shows the relationship with the arrangement and the orientation of enzyme. It is succeeded to recreate event of biosynthesis that the characteristic of synthesized cellulose is dependent on the configuration of enzyme by *in vitro* system. Now, cellulose attracts tremendous attention as raw material for versatile

application, thus deep understanding of biosynthesis and cellulolysis is needed to utilize it efficiency. The author believes that these structured studies of enzymatic polymerization become clue to resolving the biosynthetic mechanism of cellulose.

List of Publications

Chapter 1 "Enzymatic Polymerization Behavior Using Cellulose-Binding Domain Deficient Endoglucanase II”
Nakamura, I; Yoneda, H.; Maeda, T.; Makino, A.; Ohmae, M.; Sugiyama, J.; Ueda, M.; Kobayashi, S.; Kimura, S.

Macromolecular Bioscience, **2005**, *5*, 623–628.

Chapter 2 "Enzymatic Activities of Novel Mutant Endoglucanases Carrying Sequential Active Sites”
Nakamura, I.; Makino, A.; Sugiyama, J.; Ohmae, M.; Kimura, S.

International Journal of Biological Macromolecules, **2008**, *43*, 226–231.

Chapter 3 "Immobilization of His-tagged Endoglucanase on Gold via Various Ni-NTA Self-Assembled Monolayers and Its Hydrolytic Activity"
Nakamura, I.; Makino, A.; Ohmae, M.; Kimura, S.

Macromolecular Bioscience, **2010**, *10*, 1265–1272.

Chapter 4 "Enzymatic Polymerization Catalyzed by Immobilized Endoglucanase on Gold"
Nakamura, I.; Horikawa, Y.; Makino, A.; Sugiyama, J.; Kimura, S.

Biomacromolecules, accepted.

Chapter 5 "Fibrous Cellulose Prepared by Enzymatic Polymerization Using Cross-linked Mutant Endoglucanase II"

Nakamura, I.; Makino, A.; Horikawa, Y.; Sugiyama, J.; Ohmae, M.; Kimura, S.

Organic & Biomolecular Chemistry, submitted.

Acknowledgement

The present research was carried out under the direction of Professor Shunsaku Kimura at Department of Material Chemistry, Graduate School of Engineering, Kyoto University from 2003 to 2011.

The author would like to express her sincerest gratitude to Professor Shunsaku Kimura for his continuous guidance, suggestion and encouragement throughout the course of this work. The author is deeply grateful to Dr. Masashi Ohmae, Dr. Akira Makino and Dr. Tomoyuki Morita, for their constant advices, useful comments and valuable discussions throughout this work.

The author would like to express her gratitude to Professor Toshikazu Takigawa at Department of Material Chemistry, Graduate School of Engineering, Kyoto University, for his valuable comments and discussion. The author would like to express her gratitude to Professor Haruyuki Atomi at Department of Synthetic Chemistry and Biological Chemistry, Graduate School of Engineering, Kyoto University, for invaluable guidance and comments.

The author would like to thank Mr. Takatoshi Terada, Dr. Futoshi Fujimura, and Mr. Shotaro Uchizawa, for their stern and kindly teaching and valuable guidance and Mr. Makoto Fukuda, for his technical support. The author also would like to thank all the members of Professor Kimura's group for their encouragement and treasured memories.

Furthermore, the author wishes to thank Professor Junji Sugiyama, Dr. Thi Thi Nge and Dr. Yoshiki Horikawa at Research Institute for Sustainable Humanosphere (RISH), Kyoto University, for permitting the use of the transmission electron microscopy and the scanning electron microscopy, and for their technical supports and encouragements. The author also would like to thank Emeritus Professor Tadayuki Imanaka, Kyoto University for permitting the use of DNA sequencer.

The author is grateful to the Japan Society for the Promotion of Science for financial support.

Finally, the author expresses her deep appreciation her friends and family, especially her father, Mr. Osamu Nakamura, and her mother Mrs. Miyako Nakamura, for their continuous support and deep affection, and her sister, Ms. Natsuko Nakamura, for her useful discussion and encouragement throughout the course.

January, 2011

Itsuko Nakamura